
Electronic Thesis and Dissertation Repository

8-30-2018 1:30 PM

Exploring the Chemistry of Asymmetric Phosphines & Phosphinidene Sulfides

Taylor E. Pritchard, *The University of Western Ontario*

Supervisor: Ragogna, P. J., *The University of Western Ontario*

A thesis submitted in partial fulfillment of the requirements for the Master of Science degree in Chemistry

© Taylor E. Pritchard 2018

Follow this and additional works at: <https://ir.lib.uwo.ca/etd>



Part of the [Inorganic Chemistry Commons](#)

Recommended Citation

Pritchard, Taylor E., "Exploring the Chemistry of Asymmetric Phosphines & Phosphinidene Sulfides" (2018). *Electronic Thesis and Dissertation Repository*. 5664.
<https://ir.lib.uwo.ca/etd/5664>

This Dissertation/Thesis is brought to you for free and open access by Scholarship@Western. It has been accepted for inclusion in Electronic Thesis and Dissertation Repository by an authorized administrator of Scholarship@Western. For more information, please contact wlsadmin@uwo.ca.

Abstract

The field of low-coordinate main group chemistry has seen huge development in the last 30 years, with novel compounds that demonstrate unique structures and reactivity. Isolation of these species has relied on thoughtfully designed ligands normally containing substructure steric bulk. The area of phosphinidene chalcogenide isolation and transfer remains poorly understood by comparison. In this context, the major focus of thesis was on the development of a room-temperature method for the transfer of $RP=S$ moieties with and without sterically demanding substituents. The preparation and complete characterization of new asymmetric phosphines with *m*-terphenyl substituents was also reported. In Chapter 2, the characterization of secondary and tertiary phosphines which have the general formula $TerPhPR_1R_2$ ($TerPh = 2,6-Mes_2C_6H_3$, $Mes = 2,4,6-(CH_3)_3C_6H_2$) is reported. In Chapter 3, the utility of the condensation method developed by the Ragona group for the generation of $RP=S$ *in situ* for compounds with and without steric bulk was demonstrated and included the characterization of a number of [1+2], [2+2], [1+4], and [2+4] P,S-heterocycles. The stoichiometric generation and subsequent transfer of $RP=S$ without bulky ligands or norbornadiene scaffolds was unprecedented in literature and two different mechanistic pathways were hypothesized.

Keywords

Phosphorus – Sulfur – Phosphinidene Sulfide – Structure and Bonding – Low-coordinate main group chemistry – Heterocycles- Cycloadditions – Transfer Reactions

Co-Authorship Statement

This thesis includes work which has been submitted to various journals for publication in chapters two and three. The data presented in Chapter 2 corresponds to a manuscript co-authored by T. E. Pritchard, C. M. E. Graham, D. Thakur, and P. J. Ragona. DT was responsible for the preparation of two asymmetric phosphines under the direct supervision of CMEG as part of her fourth year thesis project (2.7, 2.8). CMEG was responsible for the collection and refinement of all X-ray diffraction data, he also aided with some components of the synthesis. The large majority of synthesis and characterization was performed by TEP, who also assembled the manuscript. PJR and CMEG both edited the manuscript.

The work described in chapter three was co-authored by T. E. Pritchard, C. M. E. Graham, P. D. Boyle, and P. J. Ragona. TEP was responsible for the synthesis and characterization of all compounds reported. CMEG aided with some aspects in the development of the condensation method, as well as one case where he collected X-ray diffraction data collection and did subsequent refinements. PDB was responsible for the collection and refinement of the majority of X-ray diffraction data. PJR edited the manuscript.

Acknowledgments

I would like to thank my supervisor Paul Ragona for his unwavering support throughout the duration of my MSc. He has undoubtedly improved my research and technical skills, pushed me to break bad habits of thought, and enforced critical thinking. Not only was Paul always present for lab questions and ideas, but I could count on him to be there personally for me as well when life got really stressful and I cannot thank him enough for that. Without his continued support, guidance, and belief in me as a person and a scientist, I would not be the person I am today. His enthusiasm for research motivated me to push myself while working on our projects. Paul has helped me develop throughout my degree both personally and professionally, for which I'll be forever grateful.

I have to thank all of the graduate students of the Ragona Group that I have been able to work with: Ryan, Tyler, Cam, Ben, Vanessa, Matt, Tristan, Soheil, and Kaijie. We have shared some pretty great memories together, had a few laughs (over a beer or a pig, perhaps), and created a group dynamic where I genuinely looked forward to coming in to lab every day. I especially have to thank Cam, my main partner in crime, who constantly answered my questions, shared numerous heartfelt conversations, and helped me learn how to think "like a grad student."

I also have to thank the talented and hardworking staff who made a large portion of this thesis possible. I thank Paul Boyle for his valuable training in X-ray crystallography and answering my many questions. Thanks to Mat Wilans and Aneta Borecki for their work with the NMR facilities and Doug Hairsine for help with Mass Spectrometry. Big thanks to John and Jon for their help with glovebox maintenance and MaryLou, Monica, Yuhua, and Sherry at Chembiostores.

Finally, I need to thank my friends and family for their unwavering support. Lauren, Sarah, and Taylor, thank you for being there for me and helping take my mind off science from time to time. A very special thank you goes to my boyfriend, Tom, who has kept me grounded throughout this degree, I could not have asked for any more support than what you have provided me.

Table of Contents

Abstract.....	i
Co-Authorship Statement.....	ii
Acknowledgements	iii
Table of Contents.....	iv
List of Tables	ix
List of Figures	x
List of Schemes	xv
List of Appendices	xvii
List of Abbreviations	xviii
List of Novel Compounds Reported	xxii
Chapter 1.....	1
1 Introduction.....	1
1.1 Fundamental Main Group Chemistry.....	1
1.2 Asymmetric Phosphines.....	2
1.3 Bulky Ligands & Low Coordinate Main Group Chemistry.....	4
1.4 Phosphinidenes – The Phosphorus Analogue of Carbenes.....	7
1.5 Phosphinidene Chalcogenides	11
1.5.1 Generating $RP=S$ <i>in situ</i> in the presence of trapping reagents.....	14
1.5.2 Stabilizing $RP=S$ with Creative Ligand Design.....	17

1.5.3 Developments in Transition Metal Stabilization of $RP=S$	19
1.6 Preparation of Small $(cRPCh)_n$ Heterocycles.....	21
1.7 Scope of Thesis.....	22
1.8 References.....	24
Chapter 2.....	30
2 Synthesis & Characterization of Asymmetric Phosphines.....	30
2.1 Introduction.....	30
2.2 Results & Discussion	33
2.2.1 Preparation of Asymmetric Phosphines.....	33
2.2.2 X-ray Crystallography	38
2.3 Conclusions	41
2.4 Experimental Section.....	42
2.4.1 Synthesis of 2.2	42
2.4.2 Synthesis of 2.3	43
2.4.3 Synthesis of 2.4	44
2.4.4 Synthesis of 2.6	45
2.4.5 Synthesis of 2.7	46
2.4.6 Synthesis of 2.8	47
2.5 References	48
Chapter 3.....	51

3	Probing the Reactivity of RP=S <i>via</i> Thermolysis & Condensation Pathways	51
	3.1 Introduction	51
	3.2 Results & Discussion	56
	3.2.1 Cycloaddition <i>via</i> Thermolysis	56
	3.2.2 Cycloaddition <i>via</i> Condensation – A More Selective Route	63
	3.2.3 RP=S Transfer Without Steric Bulk	64
	3.2.4 Structural Confirmation of Cycloadducts by X-ray Diffraction.....	76
	3.3 Conclusions	78
	3.4 Experimental Section	79
	3.4.1 Synthesis of 3.3 ^{1Fc}	79
	3.4.2 Synthesis of 3.3 ^{bisPh}	80
	3.4.3 Synthesis of 3.4 ^{1Fc}	81
	3.4.4 Synthesis of 3.4 ^{bisPh}	81
	3.4.5 Synthesis of 3.6 ^{Fc}	82
	3.4.6 Synthesis of 3.6 ^{FPh}	83
	3.4.7 Synthesis of 3.6 ^{Ph}	84
	3.4.8 Synthesis of 3.7	84
	3.4.9 Synthesis of 3.6 ^{Cl}	85
	3.4.10 Synthesis of 3.8 ^{Au}	85
	3.4.11 Synthesis of 3.8 ^S	86

3.4.12 Synthesis of 3.9	86
3.4.13 Special Considerations for X-ray Crystallography	87
3.5 References	88
Chapter 4	91
4 Conclusions and Future Outlook	91
4.1 Conclusions	91
4.2 Comprehensive Future Work	93
4.2.1 Additional Work Pertaining to Chapter 3	93
4.2.2 Bulky Ligands to Stabilize RP=S	95
4.2.3 Cycloaddition Chemistry: Expanding the scope of trapping reagents...	98
4.2.4 Cycloaddition Chemistry: Alkynes with β -Hydrogens	100
4.2.5 The Condensation Method: Can we transfer other RP=E?	101
4.3 Synthesis of 4.1	102
4.4 References	103
Chapter 5	104
5 Appendices	104
5.1 Experimental Methods	104
5.1.1 General Experimental Details	104
5.1.2 General Instrumentation	104
5.1.3 General Crystallographic Methods	105

5.2 Supplementary Information for Chapter 2	105
5.3 Supplementary Information for Chapter 3	106
Curriculum Vitae	107

List of Tables

Table 2-1: Summary of X-ray diffraction, collection, and refinement details for the compounds reported in Chapter 2.....	47
Table 3-1: Summary of X-ray diffraction, collection, and refinement details for the compounds reported in Chapter 3.....	87

List of Figures

Figure 1-1: Select examples of asymmetric phosphines used in transition metal and organo-catalysis.....	3
Figure 1-2: Asymmetric phosphines possessing central chirality, which are used as ligands, organocatalysts or stoichiometric reagents	3
Figure 1-3: Early low-coordinate examples with main group elements, with the majority featuring bulky aryl substituents	5
Figure 1-4: Significant discoveries in the area of main group chemistry. Top: carbodiphosphorane resonance forms	6
Figure 1-5: Left: cyanonitrene (1.19) and generic phosphinidene structure (1.20). Right: singlet and triplet phosphinidene ground electronic spin states	7
Figure 1-6: Examples of a nucleophilic phosphinidene complex (1.21), an electrophilic phosphinidene source (1.22), and a nucleophilic phosphinidene source (1.23)	8
Figure 1-7: Sequence of energies of the σ , π , and π^* orbitals obtained from <i>ab initio</i> STO/3G calculations for phosphalkene, iminophosphane, and oxaphosphane	12
Figure 1-8: Molecular orbitals calculated for $\text{MeP}=\text{S}$. ⁷⁷ Bottom left: olefinic reactivity mode for $\text{RP}=\text{S}$. Bottom right: carbenic reactivity mode for $\text{RP}=\text{S}$	13
Figure 1-9: Reaction of $\text{RP}=\text{S}$ generated <i>in situ</i> with alcohols (1.24), diethylsulfide (1.25), benzil (1.26), and dmbd (1.27 , 1.28). R = alkyl, aryl.	15
Figure 1-10: Thermolysis or photolysis of strained P,S-heterocycles for $\text{RP}=\text{S}$ generation <i>in situ</i>	17
Figure 1-11: Octamethylxylidene ligand stabilization of $\text{RP}=\text{Ch}$ (Ch = Se, 1.30 ; Ch = S, 1.31). Top: decomposition products of 1.30	18

Figure 1-12: Right: resonance forms for ylidic stabilization of P=Ch. Left: an example of its reactivity	19
Figure 1-13: Select examples of transition metal-stabilized phosphinidene sulfides (1.35-1.42)	20
Figure 1-14: Reported examples of 4-8-membered P,S-heterocycles	22
Figure 2-1: Select examples of secondary and tertiary asymmetric phosphines	31
Figure 2-2: Examples of compounds prepared using bulky aryl ligands (H-J) and the structure of targeted diphosphanylchalcogenanes (K)	32
Figure 2-3: Stacked $^{31}\text{P}\{^1\text{H}\}$ NMR spectra of purified 2.2 (top), 2.3 (middle), and 2.4 (bottom) with inset ^{31}P expansions included where splitting was observed	34
Figure 2-4: P-P single bond formation targeted through salt metathesis and dehydrohalogenative coupling using 2.1-2.4	35
Figure 2-5: $^{31}\text{P}\{^1\text{H}\}$ NMR spectrum of purified 2.6 with inset ^{31}P expansion highlighting a well-resolved AA'XX' spin system for the <i>meso</i> isomer and an unresolved AA'XX' spin system for the <i>rac</i> isomer	37
Figure 2-6: Solid-state structures for compounds confirmed by X-ray crystallography. Thermal ellipsoids are drawn at the 50% probability level. H atoms are omitted for clarity unless directly bound to phosphorus. Pertinent bond lengths [Å] and angles [°] are as follows: 2.2: P(1)-C(1) 1.861(3), P(1)-N(1) 1.663(3), P(1)-Cl(1) 2.2165(11), N(1)-P(1)-C(1) 101.67(3), N(1)-P(1)-Cl(1) 103.16(12). 2.3: P(1)-C(1) 1.854(3), P(1)-H(1) 1.29(3), P(1)-N(1) 1.684(3), N(1)-P(1)-C(1) 106.46(14), N(1)-P(1)-H(1) 100.7(14). 2.4: P(1)-C(1) 1.854(2), P(1)-H(1) 1.38(3), P(1)-Si(1) 2.2696(14), C(1)-P(1)-H(1) 96.5(12), Si(1)-P(1)-H(1) 94.2(12). 2.6: P(1)-C(1) 1.8409(17), P(1)-H(1) 1.35(3), P(1)-P(1) ¹ 2.2392(12), P(1)-P(1) ¹ -H(1) 91.4(11), C(1)-P(1)-H(1) 97.5(11) °. 2.7: P(1)-S(1) 2.1412(8), P(1)-C(1) 1.865(2), S(1)-Si(1) 2.1456(10), P-N _{avg} 1.6949(18), P(1)-S(1)-Si(1) 99.18(3), C(1)-P(1)-S(1) 105.75(6). 2.8: P-Se _{avg} 2.3073(14), P(1)-C(1) 1.862(5), P-N _{avg} 1.669(4), P(1)-Se(1)-P(2) 88.17(5), C(1)-P(1)-Se(1) 105.27(16).	39
Figure 3-1: Various known strategies for phosphinidene transfer. a) Visual representation of donor atom effect when adjacent to a phosphinidene center. b) RP=N transfer from norbornene scaffold, where RP=N exhibited carbenic reactivity. c) RP=S transfer from 7-	

phosphanorbornadiene, where $\text{RP}=\text{S}$ exhibited olefinic reactivity. d) $(\text{CO})_5\text{W-PR}$ transfer from norbornadiene, where $(\text{CO})_5\text{W-PR}$ exhibited carbenic reactivity)	52
Figure 3-2: Recent developments in the Ragona Group surrounding P,S-heterocycles and phosphinidene sulfide transfer. a) Synthesis of 3.2 by the condensation of 3.1 and $\text{S}(\text{TMS})_2$ b) [2+4] adduct (A) prepared by the thermolysis of 3.2 in dmbd c) Thermolysis of 3.2 in the presence of substituted acetylenes resulted in the formation of novel thiaphosphetene (C) and phosphirene sulfides (D1 , D2)	53
Figure 3-3: Top: Wittig olefination of carbonyls proceeding through an oxaphosphetane intermediate. Bottom: Metal-stabilized oxaphosphetane (E), P(V) oxaphosphetane (F), P(V) thiaphosphetanes (G , H), and a thiaphosphetene stabilized by the Martin ligand (I)	54
Figure 3-4: Mechanism of $\text{RP}=\text{S}$ transfer by the condensation method. i) Elimination of 2 TMSCl to yield free $\text{RP}=\text{S}$ as the reactive intermediate. ii) Stepwise elimination of TMSCl , where cyclization occurs from the phosphonium intermediate	55
Figure 3-5: Stacked $^{31}\text{P}\{^1\text{H}\}$ NMR spectra of prepared phosphirene sulfides and thiaphosphetenes. Structures for each derivative are included for clarity	58
Figure 3-6: Stacked ^1H NMR spectra of 3.3 ^{IFc} (top) and 3.4 ^{IFc} (bottom) with inset ^{31}P NMR expansions. Coupling between the olefinic proton and phosphorus is indicated by a star....	60
Figure 3-7: Stacked ^1H NMR spectra of 3.4 ^{bisPh} (top) and 3.3 ^{bisPh} (bottom) with inset expansions of the ^{31}P NMR spectrum. Coupling between the olefinic proton and phosphorus is denoted with a star.....	62
Figure 3-8: ^1H NMR spectrum of 3.6 ^{Fc} with expansion of $^{31}\text{P}\{^1\text{H}\}$ and ^{31}P NMR spectra included. Ring protons have been assigned star labels.....	66
Figure 3-9: ^1H NMR spectrum of 3.6 ^{FPh} with inset $^{19}\text{F}\{^1\text{H}\}$ and $^{31}\text{P}\{^1\text{H}\}$ NMR spectra expansions included. Proton assignment is denoted by coloured stars, whereas fluorine atom assignments are indicated by coloured circles. The unlabeled peak near 0 ppm corresponds to unreacted $\text{S}(\text{TMS})_2$	67
Figure 3-10: Stacked $^{31}\text{P}\{^1\text{H}\}$ NMR spectra. a) Crude reaction mixture in neat dmbd at 30 mg/mL. b) Crude reaction mixture in 5:1 toluene:dmbd ratio, resulting in primarily olefinic reactivity. Purified $^{31}\text{P}\{^1\text{H}\}$ NMR spectra of 3.6 ^{Ph} and 3.7 have also been included.....	69
Figure 3-11: ^1H NMR spectrum of 3.8 ^{Au} , where ring protons have been assigned with coloured star labels. An expansion of the $^{31}\text{P}\{^1\text{H}\}$ NMR spectrum has also been included ..	71

Figure 3-12: Stacked $^{31}\text{P}\{^1\text{H}\}$ NMR spectra for the reaction of PCl_3 and $\text{S}(\text{TMS})_2$ in neat dmbd at 4 h (top), 3 days (middle), and after washing crude oil with *n*-pentane (bottom) to yield **3.6^{Cl}**73

Figure 3-13: Stacked $^{31}\text{P}\{^1\text{H}\}$ NMR spectra taken from the reaction of $^{\text{F}}\text{PhPCl}_2$ with $\text{S}(\text{TMS})_2$ in neat dmbd. Conversion from the signal corresponding to **3.9** to -4.7 ppm (**3.6^{FPh}**) was observed. The formation of compound **3.9** was quite rapid, especially in contrast to the formation of **3.6^{FPh}**75

Figure 3-14: Solid state structures of **3.4^{IFc}** (top left), **3.3^{bisPh}** (top right), **3.6^{FPh}** (bottom left) and **3.8** (bottom right) with thermal ellipsoids drawn at 50 % probability. Hydrogen atoms have been omitted for clarity. Selected bond lengths [Å] and angles [°]: **3.4^{IFc}**: P(1)-S(1) 2.1729(11), P(1)-C(1) 1.823(2), P(1)-C(13) 1.850(2), S(1)-C(2) 1.781(2), C(1)-C(2) 1.350(3), C(1)-H(1) 0.9500, C(1)-P(1)-C(13) 105.37(10), C(1)-P(1)-S(1) 77.69(8), C(13)-P(1)-S(1) 102.41(8), C(2)-C(1)-P(1) 100.02(17), C(2)-S(1)-P(1) 75.84(8), C(2)-C(1)-H(1) 130.0, P(1)-C(1)-H(1) 130.0, C(1)-C(2)-S(1) 106.39(17). **3.3^{bisPh}**: P(1)-S(1) 1.9371(8), P(1)-C(1) 1.746(2), P(1)-C(2) 1.752(2), P(1)-C(11) 1.809(2), C(1)-C(2) 1.320(3), C(1)-H(1) 0.99(3), C(2)-C(3) 1.460(3), C(1)-P(1)-C(2) 44.36(10), C(1)-P(1)-C(11) 112.26(10), C(2)-P(1)-C(11) 115.68(10), C(1)-P(1)-S(1) 126.68(8), C(2)-P(1)-S(1) 123.69(8), C(11)-P(1)-S(1) 115.52(7), C(2)-C(1)-P(1) 68.06(14), C(2)-C(1)-H(1) 141.0(14), P(1)-C(1)-H(1) 149.2(14). **3.6^{FPh}**: P(1)-S(1) 2.0879(7), P(1)-C(1) 1.8705(18), P(1)-C(7) 1.8693(17), S(1)-C(10) 1.8613(18), C(7)-P(1)-C(1) 97.83(8), C(7)-P(1)-S(1) 98.26(5), C(10)-S(1)-P(1) 103.09(5), C(2)-C(1)-P(1) 114.39(12).77

Figure 4-1: Reaction of TripPCl_2 with $\text{S}(\text{TMS})_2$ to form $\text{RP}=\text{S}$ dimer, **4.1**. Stacked $^{31}\text{P}\{^1\text{H}\}$ NMR spectra taken at various time points are included to show the hypothesized formation of free $\text{RP}=\text{S}$ (denoted with a star) at 438 ppm. Dimer **4.1** had a phosphorus chemical shift of 143 ppm.....96

Figure 4-2: Solid state structure of **4.1** as determined by X-ray diffraction. The crystal contains two molecules in the asymmetric unit, although only one has been shown here for clarity. Pertinent bond lengths (Å) and angles (°) are as follows: S(1A)-P(1A) 2.1388(14), S(1A)-P(1A)¹ 2.1460(12), P(1A)-C(1A) 1.845(3), P(1A)-S(1A)-P(1A)¹ 90.58(5), C(1A)-P(1A)-S(1A)¹ 103.72(10), C(1A)-P(1A)-S(1A) 107.23(11), S(1A)-P(1A)-S(1A)¹ 89.42(5), C(2A)-C(1A)-P(1A) 119.0(3), C(6A)-C(1A)-P(1A) 123.7(2).97

Figure 4-3: Stacked $^{31}\text{P}\{^1\text{H}\}$ NMR spectra which show the crude reaction mixture following the thermolysis of **3.2** in a saturated toluene solution of ferrocenecarboxaldehyde (top) and the pentane insoluble portion (bottom)99

List of Schemes

Scheme 1-1: Rearomatization of norbornene releasing electrophilic complex. a) Reaction with 1,2-diphenylethylene to form a phosphirane-tungsten metal complex with retention of stereochemistry (left) and with an asymmetric alkyne to yield a phosphirene-tungsten metal complex (right). b) Reaction of aminophosphinidene complex to yield a phosphirene-cobalt metal complex upon reaction with diphenylacetylene.....	9
Scheme 1-2: Generation of a stable phosphinophosphinidene with examples of demonstrated reactivity	10
Scheme 1-3: Aromatization of 7-phosphanorbornadiene upon addition of heat or light to result in RP=S extrusion	14
Scheme 1-4: Dehalogenation of phenylthiophosphanoic dichloride to yield [2+4] cycloadducts analogous to those isolated by Mathey, and the corresponding crystalline product.....	16
Scheme 2-1: Synthesis of asymmetric phosphines from dichloroterphenylphosphine	33
Scheme 2-2: Preparation of terphenyldiphosphane (2.6) from 2.1	36
Scheme 2-3: Synthesis of 2.7 and 2.8 from the condensation reaction of 2.2 with Ch(TMS) ₂ (Ch = S, Se)	38
Scheme 3-1: Thermolysis of 3.2 in the presence of substituted alkynes lead to the formation of novel phosphirene sulfides (3.3ⁿ) and thiaphosphetenes (3.4ⁿ). Ring expansion to compound 3.5 was observed as a minor product formed during the thermolysis reaction.....	56
Scheme 3-2: The nature of the alkynes affected observed reactivity. Top: ethynylferrocene resulted in only olefinic reactivity. Bottom: 1,4-ethynylbenzene resulted in only carbenic reactivity. % yield is shown to the right for each case.....	64
Scheme 3-3: The condensation of various dichlorophosphines with S(TMS) ₂ in neat dmbd to yield RP=S cycloaddition products (3.6^R and 3.7)	64
Scheme 3-4: Preparation of 3.8^S by the addition of elemental sulfur to a mixture of 3.6^{Ph} and 3.7	72
Scheme 4-1: Hypothesized reaction between an NHC-based dichlorophosphine and S(TMS) ₂ to yield an isolable phosphinidene sulfide	98

Scheme 4-2: Proposed $RP=NR_1$ reaction with phenylacetylene or dmbd upon condensation of a dichlorophosphine with $R_1N(TMS)_2$ to yield 4- and 6-membered rings, respectively. R is an alkyl or aryl group for each case.....102

List of Appendices

Appendix 5.1: Experimental Methods	107
Appendix 5.2: Supplementary Information for Chapter 2.....	108
Appendix 5.3: Supplementary Information for Chapter 3.....	109

List of Abbreviations

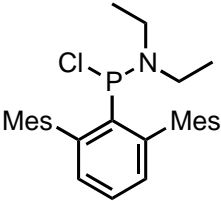
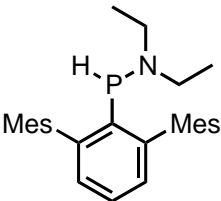
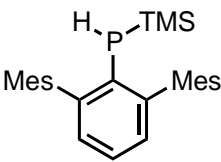
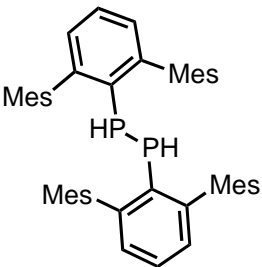
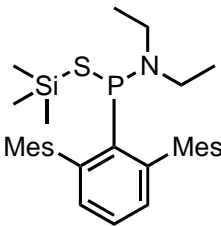
Ar	Aryl
Avg	average
BCF	Tris(pentafluorophenyl)borane, B(C ₆ F ₅) ₃
br	Broad
Bu	Butyl (-CH ₂ CH ₂ CH ₂ CH ₃)
CCDC	Cambridge Crystallographic Data Centre
Ch	Chalcogen; Group 16 element (O, S, Se, Te)
Cp	Cyclopentadienyl
Cp*	Pentamethylcyclopentadienyl
Cy	Cyclohexyl group (-C ₆ H ₁₁)
d	Doublet (for NMR), day (when used in Scheme)
dd	Doublet of doublets
dq	Doublet of quartets
ddq	Doublet of doublet of quartets
dt	Doublet of triplets
DBU	1,8-diazabicyclo[5.4.0]undec-7-ene
DCM	Dichloromethane (CH ₂ Cl ₂)
DFT	Density Functional theory
Dipp	2,6-diisopropylphenyl
DMAP	4-Dimethylaminopyridine
dmbd	2,3-dimethyl-1,3-butadiene
E	element
EA	Elemental analysis
e.g.	<i>Exemplie gratia</i> (for example)

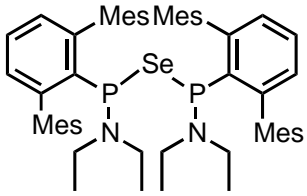
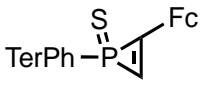
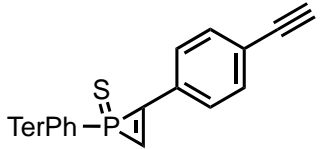
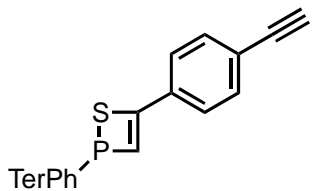
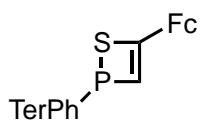
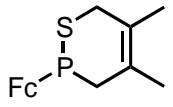
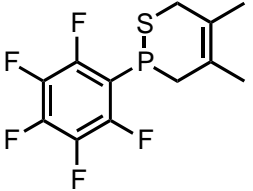
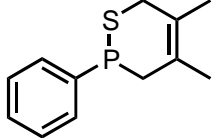
EPR	Electron paramagnetic resonance
Eq.	equivalents
ESI-MS	Electro-spray ionization mass spectrometry
Et	Ethyl, (-CH ₂ CH ₃)
<i>et al.</i>	<i>Et alii</i> (and others)
Et ₂ O	diethylether
Fc	Ferrocenyl (-C ₁₀ H ₉ Fe)
^F Ph	Pentafluorophenyl group (-C ₆ F ₅)
FT	Fourier transform
g	gram
GOF	Goodness of Fit
h	hour
HMBC	Heteronuclear multiple bond correlation
HMDSO	Hexamethyldisiloxane
HOMO	Highest occupied molecular orbital
<i>hν</i>	UV-light
Hz	Hertz
<i>In vacuo</i>	Under vacuum
<i>i</i> Pr	Isopropyl group (-CH(CH ₃) ₂)
IR	infrared
<i>J</i>	Coupling constant
K	Kelvin
kJ	Kilojoule
LUMO	Lowest unoccupied molecular orbital
M	metal

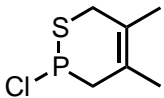
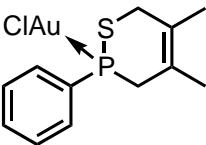
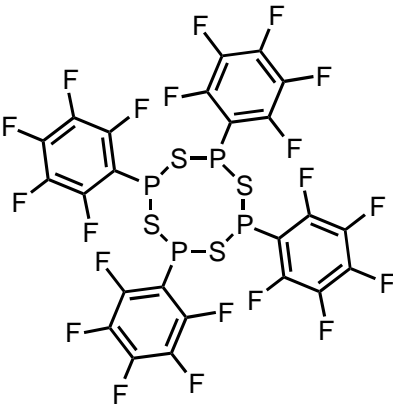
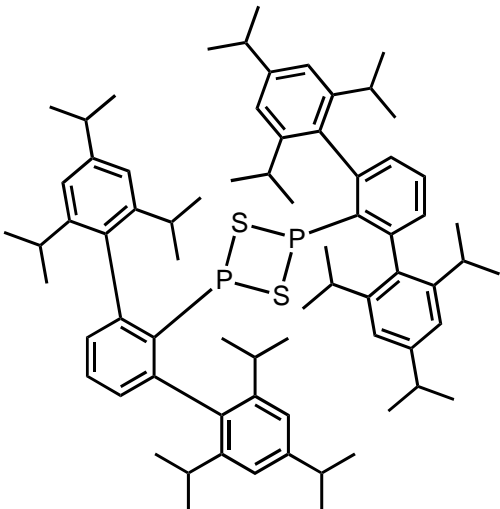
<i>m</i> -	meta
m	multiplet
<i>m/z</i>	Mass:charge ratio
m.p.	Melting point
Me	Methyl group (-CH ₃)
MeCN	Acetonitrile (CH ₃ CN)
Mes	Mesityl, 2,4,6-(CH ₃) ₃ C ₆ H ₂
Mes*	Supermesityl, 2,4,6-(<i>t</i> Bu) ₃ C ₆ H ₂
mg	milligram
MHz	megahertz
min	Minute(s)
mL	millilitre
mmHg	Millimeter of mercury, 1 mmHg = 1 torr
mmol	millimole
MO	Molecular orbital
mol	mole
MW	Molecular weight
<i>n</i> -	normal
NBO	Natural bond order
NHC	<i>N</i> -heterocyclic carbene
NMR	Nuclear magnetic resonance
Ph	Phenyl group (-C ₆ H ₅)
ppm	Parts per million
R	Alkyl or aryl group
RT	Room temperature

s	singlet
sept	septet
t	triplet
<i>t</i> Bu	<i>Tertiary</i> butyl (-C(CH ₃) ₃)
TerPh	Terphenyl, -2,6(Mes) ₂ C ₆ H ₃
THF	Tetrahydrofuran (C ₄ H ₈ O)
THT	Tetrahydrothiophene (C ₄ H ₈ S)
TMS	Trimethylsilyl group (-Si(CH ₃) ₃)
Trip	Triisopropylphenyl, 2,4,6-(<i>i</i> Pr) ₃ C ₆ H ₂
UV	Ultraviolet
v/v	Volume:volume ratio
xs	excess
Å	Angstrom (10 ⁻¹⁰ metre)
Δ	Delta
δ _H	Hydrogen chemical shift (ppm)
δ _C	Carbon chemical shift (ppm)
δ _P	Phosphorus chemical shift (ppm)
δ _F	Fluorine chemical shift (ppm)
{ ¹ H}	Proton decoupled
°	degrees
°C	Degrees Celsius
ν	Frequency
ρ	Density
λ	Wavelength

List of Novel Compounds Reported

Structure	Compound Number	Synthetic Details Page number
	2.2	43
	2.3	44
	2.4	44
	2.6	45
	2.7	46

	<p>2.8</p>	<p>47</p>
	<p>3.3^{IFc}</p>	<p>82</p>
	<p>3.3^{bisPh}</p>	<p>83</p>
	<p>3.4^{bisPh}</p>	<p>84</p>
	<p>3.4^{IFc}</p>	<p>84</p>
	<p>3.6^{Fc}</p>	<p>85</p>
	<p>3.6^{FPh}</p>	<p>86</p>
	<p>3.6^{Ph}</p>	<p>87</p>

	3.6^{Cl}	88
	3.8^{Au}	88
	3.9	89
	4.1	106

Chapter 1

1 Introduction

1.1 Fundamental Main Group Chemistry

The underlying theme of modern fundamental main group chemistry has focused on developing an understanding of the influence of structure and bonding on reactivity. This has been achieved through comprehensive analysis of the structure and bonding between main group elements. The chemistry of most main group elements found in the *s*- and *p*-blocks of the Periodic Table, has been explored and have displayed a wide variety of bonding motifs. Despite the fundamental nature of this research, numerous high impact discoveries have paved the way for new and innovative applications, including flame-retardant polyphosphazanes and the wide-spread utility of siloxane polymers.^{1,2} Main group researchers have also been awarded Nobel prizes for their contributions to the scientific community.

One of the first Nobel prizes was awarded to Victor Grignard in 1912 to for the development of “Grignard reagents”, which have had a lasting impact in organic synthesis.³ Another Nobel prize was awarded to Fritz Haber in 1918 for the production of ammonia (NH₃) from the combination of its gaseous constituents, N₂ and H₂.⁴ In 1963, the work of Karl Ziegler and Giulio Natta was recognized and received a Nobel prize for organotitanium/aluminum catalysts which facilitated the polymerization of terminal alkenes.⁵ Directly incorporating *p*-block elements, the work of Herbert C. Brown and Georg Wittig was recognized for its contribution to organic synthesis in 1979 with a Nobel prize for new phosphorus and boron reagents.⁶ More recently, in 2005, Yves Chauvin, Robert H. Grubbs, and Richard R. Schrock were awarded the Nobel prize for the development of metathesis methods in organic synthesis using carbenes as ligands on transition metal catalysts.⁷

Industrially and academically relevant knowledge has been gained from high impact discoveries focused on main group elements. The development of easily prepared siloxane polymers, which consist of repeating Si-O linkages, have been used as

hydrophobic coatings, elastomers, and biocompatible materials, amongst many other applications.^{1,8} Polyphosphazanes contain repeating Cl_2PN units and these materials are used as high temperature elastomers, polyelectrolytes and in biomedical implants.^{2,9,10}

This brief overview of significant main group discoveries only scratches the surface of the impact that main group research has had on other fields of research. Without fundamental main group research, many key industrial and academic developments would not have been possible. It is critical to understand that main group chemistry has undergone significant changes in the past fifty years and its research outcomes will continue to have a lasting impact on fundamental and applied research in the years to come.

1.2 Asymmetric Phosphines

Phosphines have been used as ligands for transition metals for decades because they are excellent σ donors. The tunable steric and electronic properties of phosphine ligands are important to their widespread use in catalysis. In the early-to-mid 20th century, triphenylphosphine was a common ligand of choice for transition metal catalysis. In modern catalysis, phosphine ligands with increasingly elaborate functionality have been reported and used. For example, chiral phosphine ligands have seen increased use in asymmetric catalysis in the last twenty years. Monodentate chiral phosphine ligands are rarer than their bi- or tridentate counterparts and often possess a chiral substituent as opposed to central chirality (Figure 1-1, **1.1-1.5**).¹¹⁻¹⁵ DuPhos (**1.5**) has had a significant impact on the field of asymmetric catalysis, allowing for enantio- and regioselective hydrogenation of olefins, among many other functional groups. Compound **1.3** has also been used as an organocatalyst for the cycloaddition of allenolates with imines and electron deficient olefins.¹⁶

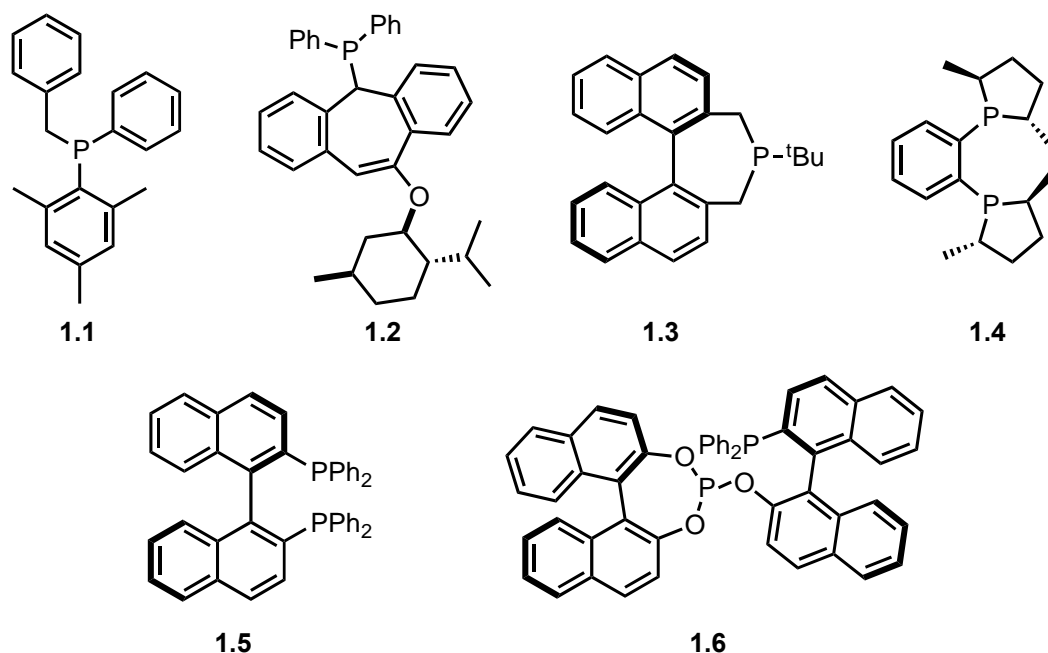


Figure 1-1. Select examples of asymmetric phosphines used in transition metal and organo-catalysis

In cases where multidentate phosphines do not perform well, monophosphine ligands possessing aryl and alkyl groups have been reported as excellent ligands for a wide variety of Pd-catalyzed C-C, C-N, and C-O bond forming reactions under mild conditions.¹⁷ The development of new phosphine ligands has since been centered around ease of preparation, a functional handle for derivitization, and those that contain central and/or axial chirality. A recent study by the Yang group demonstrated the potential utility of compounds **1.7** and **1.8** to catalyze C-H amination and cyclization in the absence of a transition metal catalyst (Figure 1-2).¹⁸

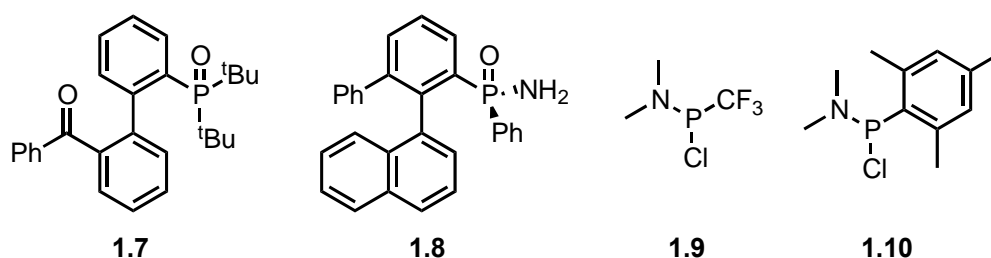


Figure 1-2. Examples of phosphines used as ligands, organocatalysts, and stoichiometric reagents. Compounds **1.8-1.10** possess chirality.

Phosphines are not only excellent ligands in the area of catalysis, but also play an important role in many stoichiometric transformations. Normally this reactivity stems from a reactive single bond to phosphorus, where P–Cl and P–H bonds have proven to be relatively simple to manipulate under mild, anaerobic conditions due to relatively low bond dissociation energy (P–Cl = 326 kJ mol⁻¹, P–H = 322 kJ mol⁻¹). Compounds **1.9** and **1.10** possess central chirality, which lends itself not only to a unique ligand for transition metal catalysis but also for selective stoichiometric reactivity with a number of other compounds (Figure 1-2).^{19–21} A number of different methods are reported for preparing these asymmetric phosphines possessing smaller aryl substituents; however, those with *m*-terphenyl ligands are less prevalent in literature.

1.3 Bulky Ligands & Low Coordinate Main Group Chemistry

The use of bulky aryl ligands has greatly aided in the establishment of main group centers with low coordination numbers. Over the last 30 years, there has been significant development in the variety and number of compounds containing main group elements that defy the double bond rule, a hallmark application for bulky ligands. The double bond rule states that atoms with a principle quantum number greater than or equal to 3 will not be able to form multiple bonds because their diffuse *p*-orbitals would result in poor orbital overlap and thus have much lower π -bond energies.²² Despite this, many compounds have been prepared that exhibit double or triple bonds between main group elements (*eg.* disilene (**1.11**); digermene (**1.12**); diphosphene (**1.13**); and phosphalkyne (**1.14**); Figure 1-3).^{23–26} Most of these compounds rely on bulky aryl ligands positioned at the main group element in order to stabilize the reactive main group center from reactions.²⁷ While these are not the only examples of low-coordinate main group compounds, their discovery has certainly shifted the focus towards isolating unique structures that challenge traditional rules of structure and bonding.

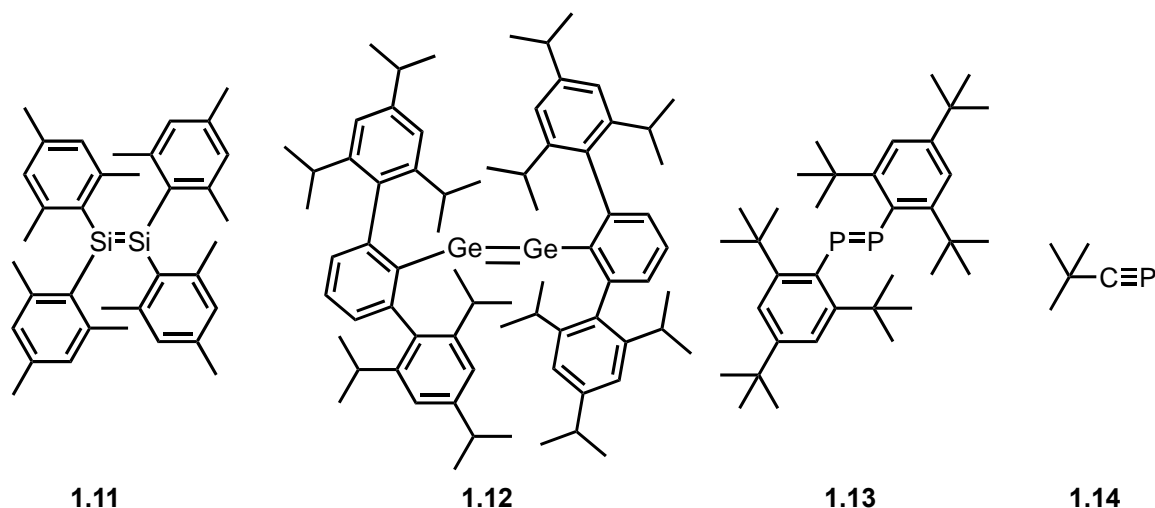


Figure 1-3. Early examples which feature multiple bonding between main group elements, with the majority featuring bulky aryl substituents

The chemistry of main group multiple bonds has been of interest because of differences in bonding between the light and heavy elements. West's disilene (**1.11**) displayed reactivity reminiscent to that of olefins, reacting readily at room temperature with hydrogen halides, alcohols, aldehydes, ketones, azides, oxygen, sulfur, and olefins.²⁶ The heightened reactivity observed can be attributed to the weaker π -bonding between Si atoms in comparison to their carbon counterparts.²³ An exciting discovery made by Power group found that digermene compounds were able to activate dihydrogen in the absence of a transition metal – the first reported example of a non-transition metal species activating H_2 .²⁴ Similar reactivity has been observed by *N*-heterocyclic carbenes (NHCs, Figure 1-4, **1.15**) with H_2 and NH_3 to afford addition products.²⁸ It has since been proven that digermene and distannylene (**1.16**, E = Sn) compounds are also promising candidates for C–H bond activation with cyclic olefins at room temperature (Figure 1-4).²⁹ The ability of main group compounds to mimic the reactivity of transition metal complexes has been a continued driving force in this research area.

Neutral bulky ligands have been used to stabilize many main group elements in their zero oxidation state, resulting in main group analogs of common homodiatom compounds (**1.16**).³⁰ The preparation of these main group analogs has been a popular area

of research since the realization that an acceptable Lewis structure for carbodiphosphoranes could be drawn as containing a central carbon atom doubly bound to two phosphorus atoms, leaving the central carbon with a formal oxidation state of zero (Figure 1-4).³¹ Main group analogs of naturally occurring diatomic species (*ie.* H₂, N₂, O₂) differ in that they possess lone pairs which serve as a handle for harnessing further reactivity. They have been demonstrated to act as donor atoms in Lewis type interactions, and see potential as synthetic building blocks for increasingly complex structures. The use of strong donors (*ie.* NHCs) to stabilize these allotropes has been expanded to a number of other *p*-block elements (Figure 1-4, **1.17**).

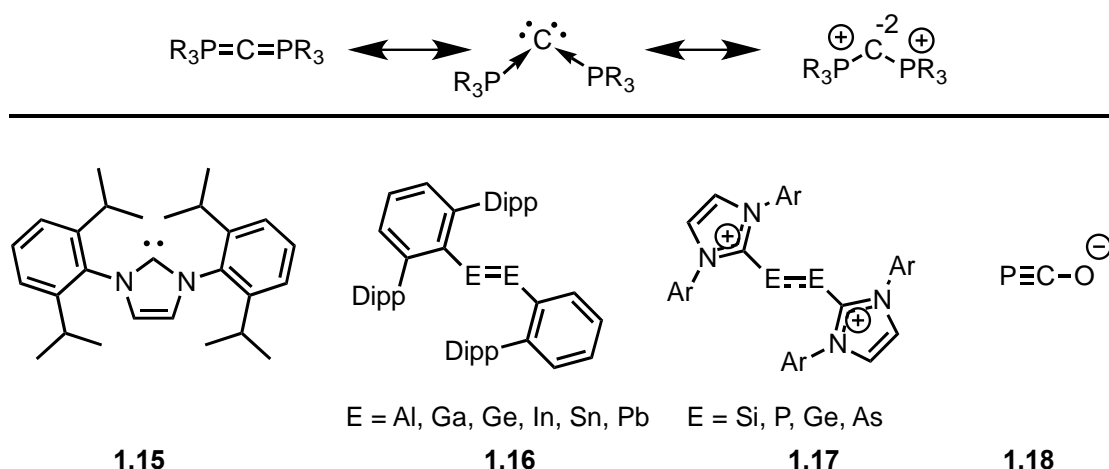


Figure 1-4. Significant discoveries in the area of main group chemistry. Top: carbodiphosphorane resonance forms.

Although NHC donors have aided in research surrounding the development of low-coordinate main group compounds with good solubility properties, they are not the only examples of synthetically useful low-coordinate compounds. The phosphorus analogue of the cyanate ion, 2-phosphaethynolate anion (**1.18**), has been used for the installation of [P]⁻ or [PCO]⁻ functionality, a precursor for P-heterocycles, and a synthon for phosphorus-containing small molecules.^{32,33} Difficulty in this area was previously limited by the challenges associated with the preparation of **1.18**; however, improvements by a number of researchers enabled scalable synthesis that facilitated the above reactivity studies.³⁴⁻³⁶ This example highlights that a fundamental main group species can have a dramatic impact in development of new reagents.

The high degree of success with compounds containing low-coordinate main group centers has bolstered efforts in the field to continue to push the boundaries of known structure and bonding motifs. Beyond the unusual structures they can display, these compounds often offer unique reactivity and are hypothesized to be useful outside their traditional role as ligands for catalysts. Potential applications include reactive synthons for more complex molecules and metal-free alternatives to activate a wide variety of different bonds.

1.4 Phosphinidenes – The Phosphorus Analogue of Carbenes

Phosphinidenes (phosphanylidenes) are elusive six electron species featuring a P(I) center. Their existence has been established by utilizing base stabilization, trapping reactions, or oligomerization and isolating the resulting products.^{33,37} These formally mono-coordinate species are exceedingly reactive in comparison to their carbene and nitrene counterparts (Figure 1-4, **1.15**; Figure 1-5, **1.19-1.20**). Like nitrenes and carbenes, phosphinidenes adopt either a singlet or triplet ground electronic state. In the singlet state there are two lone pairs of electrons on phosphorus and a low energy empty *p*-orbital. In the triplet state, one electron pair resides on phosphorus and two electrons with parallel spins occupy the other *p*-orbitals (Figure 1-5).³⁸

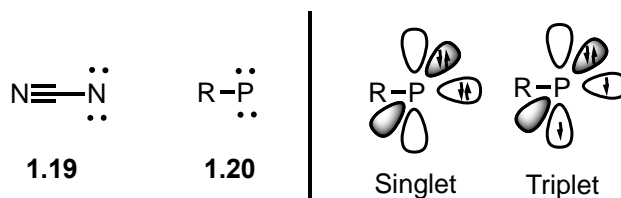


Figure 1-5. Left: cyanonitrene (**1.19**) and generic phosphinidene structure (**1.20**). Right: singlet and triplet phosphinidene ground electronic spin states

The area of phosphinidene research has seen an explosion since their detection by Gaspar *et al.*, who used electron paramagnetic resonance (EPR) spectroscopy to detect trapped triplet mesitylphosphinidene at 77 K after the photolysis of *trans*-2,3-dimethyl-1-mesitylphosphirane. The generated phosphinidene was subsequently trapped with 3-hexyne.³⁹ Experimental efforts since have resulted in phosphinidene fragments generated

in situ by retro-cycloadditions of phosphorus heterocycles, and the reduction of halophosphines under generally harsh conditions with triplet reactivity patterns observed as a result.^{40–44} The retrocyclization of 7-phosphanorbornenes driven by aromatization of the scaffold has proven to be a reliable method for the generation of numerous phosphinidene fragments, including those supported by metals, and π -donor atoms (*ie.* N, O, S, P).^{40,41,45–49} Most recently, an elegant study by the Cummins group demonstrated that aminophosphinidenes could be generated by thermally induced anthracene elimination from dibenzo-7-phosphanorbornadiene (**1.22**, Figure 1-6).⁴⁷ Their work covered an impressive range of R_2N -P- transfer reactions and document first order kinetics consistent with a singlet ground state mechanism being operative.⁵⁰ The thermal decomposition of norbornadiene scaffolds to release reactive phosphinidene fragments *in situ* has been an attractive strategy for many research groups to harness phosphinidene reactivity.^{32,43,51–53}

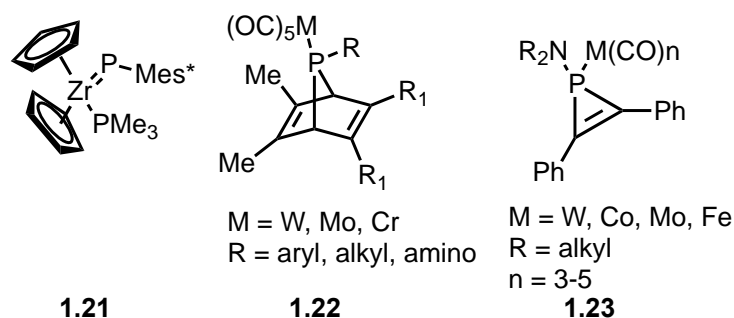
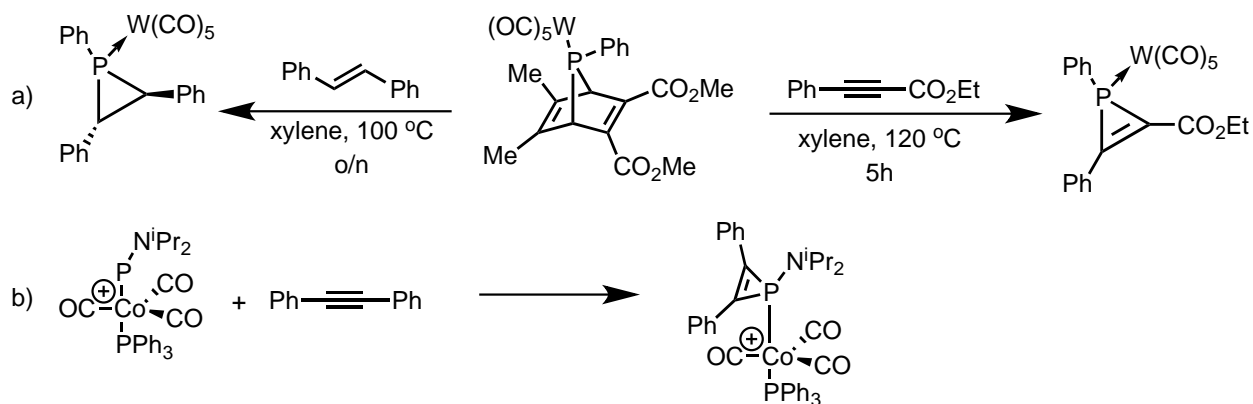


Figure 1-6. Examples of a nucleophilic phosphinidene complex (**1.21**), an electrophilic phosphinidene source (**1.22**) and an amino-substituted electrophilic phosphinidene source (**1.23**)

Carbenes in metal complexes are understood to possess either electrophilic (Fischer) or nucleophilic (Schrock) character, and phosphinidene-metal complexes demonstrate similar bonding profiles (**1.21-1.23**, Figure 1-6).⁵⁴ Nucleophilic phosphinidene complexes consist of a P=M double bond and studies have indicated that their reactivity resulted from triplet radical character at both the phosphorus and metal centers.⁴¹ These complexes were first discovered over 30 years ago, but new examples now cover a range of both early and late transition metals. Reactivity studies in all cases of nucleophilic phosphinidene complexes have demonstrated the reactivity stems from the P=M double bond.⁴⁵

Alternatively, electrophilic phosphinidene-metal complex reactivity stems from the phosphorus center in a carbenic fashion, or in combination with a donor atom in an olefinic fashion, to yield $[1+x]$ or $[2+x]$ cycloadducts, respectively ($x = 1$ or 2). The bond between the phosphorus and metal center was identified as a singlet dative interaction, which allowed for the phosphinidene transfer as identified by its products upon trapping with various reagents.⁵⁵ Electrophilic phosphinidene complexes ($[\text{RP-M}(\text{CO})_5]$, $\text{M} = \text{Cr}, \text{Mo}, \text{W}$; **1.22**) were first discovered by Mathey in the 1980s. $[1+2]$ cycloaddition chemistry was observed with alkenes and alkynes to yield phosphiranes and phosphirenes, respectively (Scheme 1-1, a).^{44,56-58} Most of these metal phosphinidene complexes are generated *in situ* by the aromatization of the norbornadiene scaffolds which release the reactive fragment and the metal carbonyl acts as a Lewis acid to stabilize the phosphinidene prior to trapping. Although the majority of electrophilic phosphinidene complexes are identified by reactions with various trapping agents, amino-substituted phosphinidene-metal complexes have been successfully isolated and characterized (**1.23**, Figure 1-6).⁵⁹ These isolable derivatives possessed analogous reactivity to their transient counterparts, which indicated that the presence of the donor

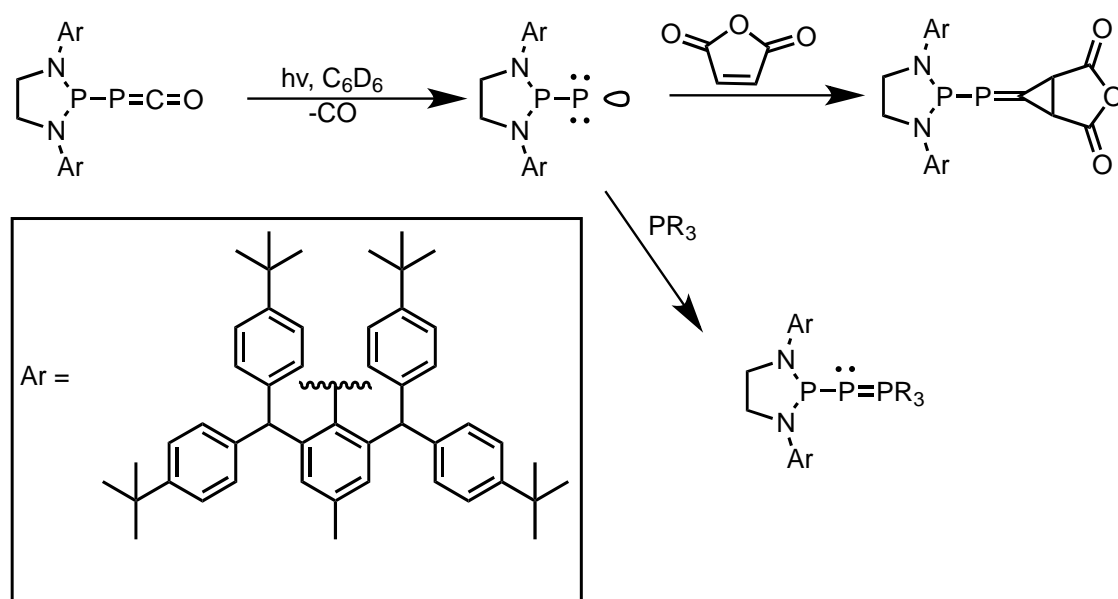


Scheme 1-1. Rearomatization of norbornene releasing electrophilic phosphinidene

complex. a) Left: reaction with 1,2-diphenylethylene to form a phosphirane-tungsten metal complex with retention of stereochemistry. Right: reaction with an asymmetrically substituted alkyne to yield a phosphirene-tungsten metal complex. b) Reaction of aminophosphinidene complex to yield a phosphirene-cobalt metal complex upon reaction with diphenylacetylene

atom did not impede the desired reaction from occurring (*ie.* [1+2] cycloaddition occurring at phosphorus, Scheme 1.1, b).⁴²

Research in this area has seen a substantial increase in the last three decades, and as a result, alternative routes to access phosphinidenes which do not require electronic stabilization by a metal center have been developed. The most successful donor atoms used to obtain singlet phosphinidene compounds with reactivity that can be harnessed are bulky NHCs^{60–63} and phosphine ligands.^{48,64,65} Most recently, the first “bottle-able” phosphinidene was prepared by Bertrand *et al.* by the photolysis of a phosphaketene protected by extremely bulky groups on the nitrogen atoms of the compound.^{48,65} This unique compound was found to have a terminal P-P double bond, where the terminal phosphorus possessed phosphinidene character. Versatile reactivity with CO, strong donors, or trapping agents stemming from the phosphorus center was observed (Scheme 1-2).^{48,65}



Scheme 1-2. Generation of stable phosphinophosphinidene with examples of demonstrated reactivity

A recurring theme for phosphinidene chemistry is unique ligand design, normally featuring large aryl substituents at the phosphorus center. The goal of this research is to develop reliable and reproducible synthetic methodologies for the preparation and

utilization of phosphinidenes as synthetic building blocks or ligands for transition metals and other potential applications (*eg.* polymerization).

1.5 Phosphinidene Chalcogenides

Phosphinochalcogoylidenes, known more commonly as phosphinidene chalcogenides, consist of a two-coordinate phosphorus center with a formal double bond between the phosphorus and chalcogen atom.²⁶ The isolation of these species as a “free” unit has been an ongoing struggle for main group synthetic chemists. The understanding of these compounds has been developed through their identification in the gas phase by mass spectrometry and infrared spectroscopy, as well as through their reactions with various trapping reagents.^{66–69} The development of $\text{RP}=\text{Ch}$ transfer chemistry would be greatly aided by a method which would allow for $\text{RP}=\text{Ch}$ to be accessed stoichiometrically under mild conditions.

Phosphinidene chalcogenides have been targets of synthetic chemists for a number of decades and differ from parent phosphinidenes in that they possess a singlet electronic ground state. Parent phosphinidenes ($\text{RP}:$) are known to possess triplet ground states through computational studies as well as EPR spectroscopy.⁷⁰ A level of ambiguity in the area of phosphinidene chalcogenide research still exists because a thorough understanding of their chemistry is lacking; however, calculations have aided in predicting the reactivity of these compounds. Phosphinidenes can be stabilized by the presence of a donor atom (*ie.* $\text{E} = \text{N}, \text{O}, \text{S}, \text{P}$) through the formation of a formal $\text{E}=\text{P}$ double bond.^{71,72} The presence of this double bond was verified computationally to bias reactivity towards a singlet ground state at phosphorus and have rendered $\text{RP}=\text{S}$ as isolobal with singlet carbenes and silylenes.^{71,73} An influential report by Niecke and Schoeller in 1982 played a large role in the early stages of this field, where they used theoretical chemistry to predict the reactivity of $\text{RP}=\text{E}$ systems with alkynes.⁷³ They found that weaker (p-p) π -bonds tend to undergo [2+2] dimerization reactions to yield 4-membered heterocycles (olefinic reactivity). Conversely, those with more polar (p-p) π -bonds tend to react *via* [1+2] cycloaddition pathways (carbenic reactivity). The tendency of $\text{RP}=\text{E}$ to undergo [1+2] *versus* [2+2] cycloaddition reactions depended on the identity

of E. Phosphaalkenes (RP=C), with a small electronegativity difference between C and P, tend towards cycloaddition mechanistic pathways, where oxaphosphanes (RP=O) and iminophosphanes (RP=N) prefer chelotropic reactivity pathways based on differences in their HOMO-LUMO energy gaps (Figure 1-7).⁷³

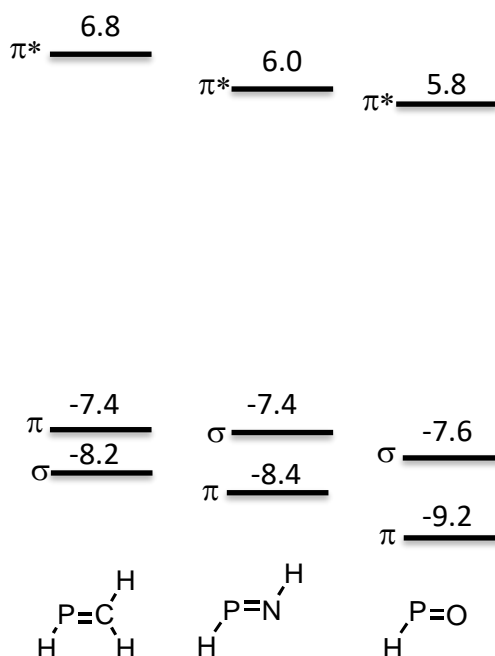


Figure 1-7. Sequence of energies of the σ , π , and π^* orbitals obtained from ab initio STO/3G calculations for phosphaaalkene, iminophosphane and oxaphosphane⁷³

The observation of this phenomenon is explained by orbital crossing of 2 HOMOs, where the HOMO in less electronegative RP=E systems (E = C) consists of a P=C π -orbital, and in more polarized systems (E = N, O) the HOMO is an orbital of σ symmetry corresponding to the lone pair on phosphorus. The LUMO for both cases is the π^* -orbital of the P=E double bond.⁷³ Tuning the R group on phosphorus to be π -donating or π -accepting can also inverse the energy of σ and π , and when E = S this could result in the observation of both olefinic and carbenic behaviour. In comparison to HP=O, theoretical findings predicted that reactivity should be analogous to singlet carbenes (σ HOMO, 1,1-

dipole). This prediction has since been confirmed experimentally by a number of different studies on the reactivity of phosphinidene oxides and sulfides.^{71,74–76}

Despite the sound theoretical and experimental evidence surrounding the chemistry of $\text{RP}=\text{O}$, the understanding of heavier Group 16 elements ($\text{RP}=\text{E}$, $\text{E} = \text{S}, \text{Se}, \text{Te}$) is far less developed from both computational and experimental standpoints. Based on Niecke and Schoeller's report, the decrease in electronegativity when using heavier chalcogens should cause a decrease in the dominant carbenic character to result in prominently olefinic reactivity.⁷³ Theoretical studies performed by the Mathey group on sulfur systems indicated a $\text{P}=\text{S}$ bond order of 1.93, indicative of a double bond between P and S atoms.⁷⁷ The HOMO was an in-plane orbital comprised of the $\sigma(\text{P}-\text{C})$ orbital, the lone pair on phosphorus, and the in-plane p -orbital of sulfur. The HOMO-1 consists of the $\text{P}=\text{S}$ π -orbital, which is a strong indication that both carbenic and olefinic reactivity could be observed when $\text{E} = \text{S}$ (Figure 1-8).⁷⁷

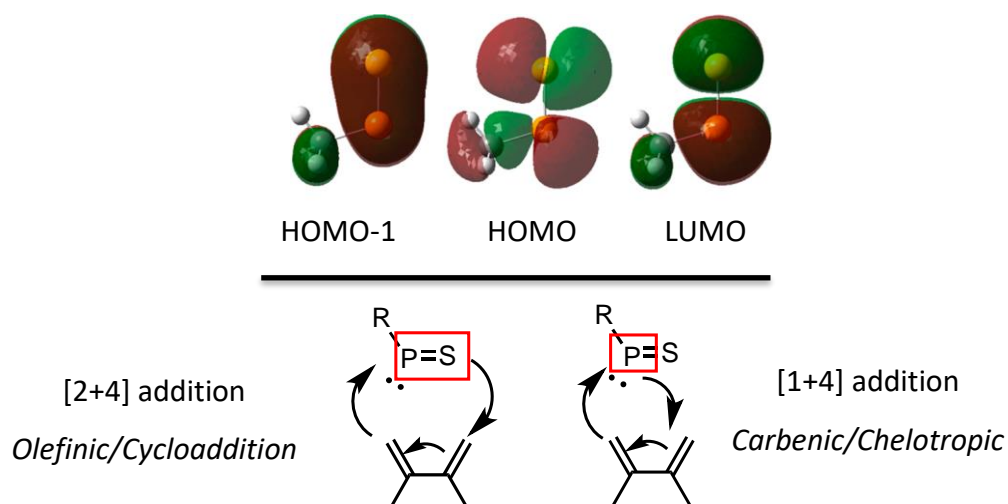
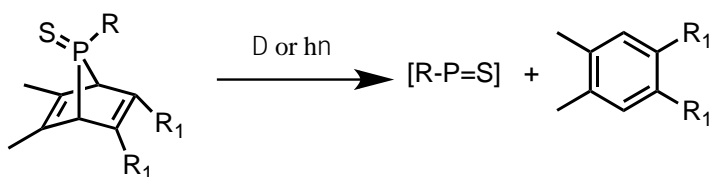


Figure 1-8. Molecular orbitals calculated for $\text{MeP}=\text{S}$.⁷⁷ Bottom left: olefinic reactivity mode for $\text{RP}=\text{S}$. Bottom right: Carbenic reactivity mode for $\text{RP}=\text{S}$.

1.5.1 Generating $\text{RP}=\text{S}$ *in situ* in the presence of trapping reagents

Since the early experiments which focused on phosphinidene sulfide transfer, there have been numerous methods developed which aim to generate $\text{RP}=\text{S}$ as a transient intermediate. *In situ* generation of $\text{RP}=\text{S}$ in the presence of a trapping reagent has inhibited self-reaction and polymerization to result in the formation of products which indicate $\text{RP}=\text{S}$ acted as a stoichiometric reactive unit. In most of these cases, “free” $\text{RP}=\text{S}$ cannot be isolated and characterized, so its existence is owed to the cycloadducts that are formed as a result of its reactivity. Other mechanisms which do not involve the production of $\text{RP}=\text{S}$ as a free reactive unit should be entertained. There have been ongoing efforts across the field working to ascertain the true nature of these transformations.

Similar to phosphinidene chemistry, the degradation of bicycles with a bridgehead $\text{RP}=\text{S}$ unit (bound through phosphorus) has been a reliable strategy for accessing phosphinidene sulfides *in situ*.⁵⁸ Most commonly, 7-phosphanorbornadiene precursors have been used and exposing the scaffolds to thermal or photolytic conditions in the presence of a trapping reagent lead to extrusion and subsequent trapping of the $\text{RP}=\text{S}$ bridgehead fragment (Scheme 1-3).^{43,50,52,78}



Scheme 1-3. Chelotropic elimination of $\text{RP}=\text{S}$ from 7-phosphanorbornadiene upon addition of heat or light

The earliest examples which showcase the transfer of $\text{RP}=\text{S}$ from norbornadiene precursors have displayed dominant 1,1-dipole reactivity for insertion reactions with various alcohols (**1.24**) and disulfides (**1.25**). For cycloaddition reactions with benzil (**1.26**) and 2,3-dimethylbutadiene (dmbd, **1.27**), [1+4] cycloadducts are common products (Figure 1-9).^{51,52,57,79,80} These results were indicative of carbene-like reactivity, analogous to what was observed for $\text{RP}=\text{O}$ derivatives. Many of these early transformations used

harsh reaction conditions (*ie.* high temperature) to drive conversion to the desired products; however, the Mathey group recently demonstrated the room temperature reaction of $\text{RP}=\text{S}$ with dmbd yielded a [2+4] cycloadduct and no carbenic reactivity was observed (**1.28**, Figure 1-9).⁷⁷ $\text{RP}=\text{S}$ in this example was released by the dehydrobromination of a 7-phosphanorbornadiene scaffold, which left the rearomatized aryl group and an ammonium bromide salt as byproducts of the room temperature process. Although compound **1.28** could not be directly isolated and structurally characterized due to oily nature of the low molecular weight material, its $\text{W}(\text{CO})_5$ derivative was successfully isolated and subsequently characterized. The types of reactions which can be performed using this method are versatile; however, triplet phosphinidene sulfide reactivity patterns which are not as straightforward as their oxaphosphane counterparts have been observed.

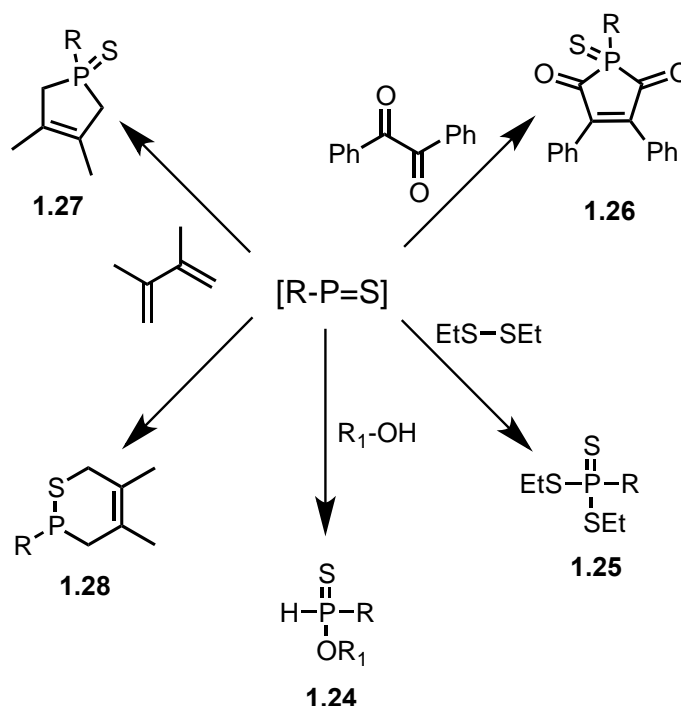
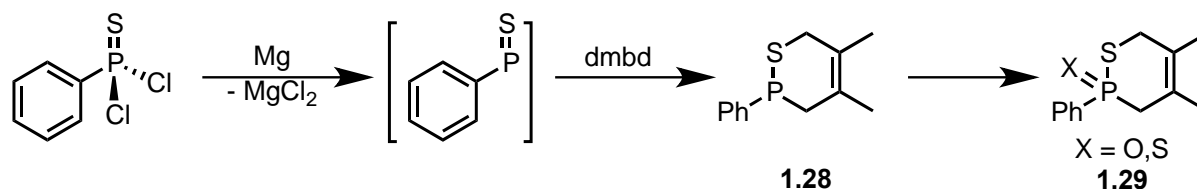


Figure 1-9. Reactivity of $\text{RP}=\text{S}$ generated *in situ* with alcohols (**1.24**), diethylsulfide (**1.25**), benzil (**1.26**), and dmbd (**1.27**, **1.28**). R = alkyl, aryl.

Other early methods for *in situ* production of $\text{RP}=\text{S}$ were developed by Harwood and Crofts in the 1960s and improved upon later by Inamoto, involving the dehalogenation of thiophosphonic dihalides in the presence of trapping agents.^{81–85} The

results obtained by this method were consistent with those observed for norbornadiene scaffolds, where products featured RP=S insertion. When dmbd was added during the dechlorination step, [2+4] cycloaddition products were observed with structures analogous to those isolated by Mathey (**1.28**).^{86,87} Within the same reaction, they noted the formation of [1+4] adducts (**1.27**) which were also isolated and characterized. This result demonstrated that both olefinic and carbenic reactivity pathways are energetically accessible by this methodology (Scheme 1-4). In this case, the authors proposed that decomposition or oxidation of the [2+4] adduct occurred during the workup of the reaction and precluded its isolation; however, although no concrete evidence either way has been presented to date. Others have questioned the true nature of this mechanism with respect to the formation of free phosphinidene sulfide due to inconsistencies in results from Inamoto.⁸⁶ Nevertheless, the dehalogenation of thiophosphanoic dihalides has become one standard method for accessing RP=S *in situ* and has been used to generate new compounds in a variety of instances which are similar to those produced by 7-phosphanorbornadiene aromatization.^{84–88}



Scheme 1-4. Dehalogenation of phenylthiophosphanoic dichloride to yield [2+4] cycloadduct analogous to Mathey, and corresponding crystalline oxidation product

Strained heterocyclic compounds containing P and S functionality are also amenable to the liberation of RP=S, although there are fewer examples in literature. Primarily, phoshirane and phospholene sulfides have been subjected to heat (thermolysis) or light (photolysis) in the presence of alcohols, diethylsulfide and dmbd to result in products similar to those discussed previously (**1.24–1.27**, Figure 1-10; Figure 1-9).^{71,89,90} Gaspar and coworkers have shown that extrusion of RP=S from 2,6-dimethoxyphosphirane sulfide was accomplished both thermolytically and photolytically by a first order process. This was confirmed by the lack of change observed with substoichiometric or excess diethylsulfide.⁷¹ This was strong evidence for the formation

of “free” $\text{RP}=\text{S}$ using this methodology. Performing the thermolysis or photolysis of the phosphirane sulfide in the presence of dmbd resulted in both olefinic and carbenic products from *in situ* generated $\text{RP}=\text{S}$. The observation of both cycloaddition products likely arose from competing mechanistic pathways under the specified reaction conditions. Thiaphosphetenes and phosphirene sulfides have proven to be amenable to $\text{RP}=\text{S}$ liberation under photolytic conditions – resulting in the dimerization of $\text{RP}=\text{S}$ fragments to yield a P_2S_2 ring which has been previously reported by the Ragogna group (Figure 1-10).^{37,91}

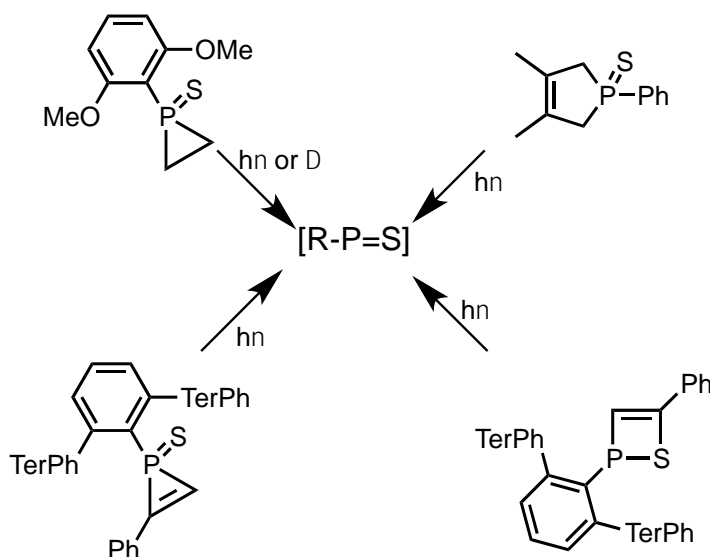


Figure 1-10. Thermolysis or photolysis of strained P,S-heterocycles for $\text{RP}=\text{S}$ generation *in situ*

1.5.2 Stabilizing $\text{RP}=\text{S}$ through Ligand Design

Despite the successes demonstrated by the $\text{RP}=\text{S}$ transfer reactions described above, formation of these products assumes the generation of a “free” phosphinidene sulfide in solution. It has been of interest over the last 30 years to obtain $\text{RP}=\text{S}$ as an isolable compound for further structural and electronic investigation to better understand this highly reactive species. Yoshifuji and coworkers demonstrate the first successful attempt at isolating a phosphinidene sulfide using an octamethylxylylene ligand (**1.31**).^{92–94} In comparison to the bulky, aryl auxiliary ligands that have been traditionally used to isolate low-coordinate main group compounds, the octamethylxylylene ligand is

reminiscent of the supermesityl functional group, where one of the *tert*-butyl groups is replaced with a dimethylamino substituent. As a consequence, the ligand not only offers stabilization by way of steric protection but also through donor participation from the nitrogen center. This strategy has been quite effective for the isolation of a number of phosphinidene chalcogenides, including a rare example of an $\text{RP}=\text{Se}$ (R = octamethylxylylidene) (Figure 1-11, **1.30**).⁹⁵ The selenium derivative was observed to be unstable despite the amino group (Figure 1-11). This has precluded the authors' ability to structurally characterize this compound, although NMR data supports their proposed structure with characteristic downfield shifts in the $^{31}\text{P}\{^1\text{H}\}$ NMR spectrum ($\delta_{\text{P}} = 399.0$).⁹² The sulfide derivative (**1.31**) was found to be more stable, allowing for the collection of mass spectrometric and elemental analysis data, which in combination with a downfield shift in the $^{31}\text{P}\{^1\text{H}\}$ NMR spectrum ($\delta_{\text{P}} = 382.0$) confirms their hypothesized structure.⁹⁶ Crystallographic data were not obtained for compound **1.31** so structural confirmation of the ligand-stabilized phosphinidene sulfide and the nature of the interaction between the $\text{P}=\text{S}$ double bond and the NMe_2 moiety is still unknown. No further work on this ligand framework has been reported since.

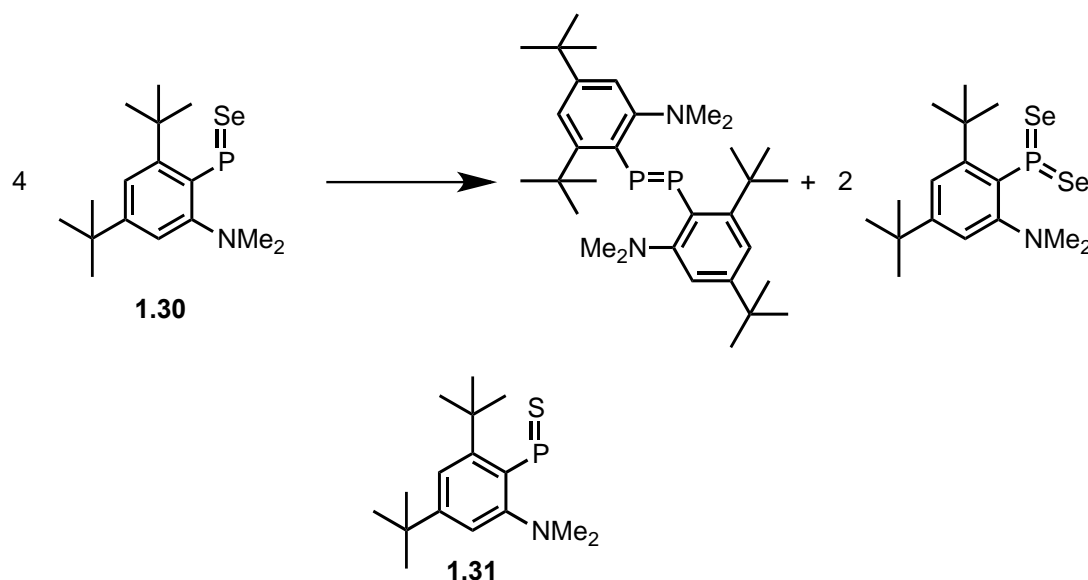


Figure 1-11. Octamethylxylylidene ligand stabilization of $\text{RP}=\text{Ch}$ ($\text{Ch} = \text{Se}$, **1.30**; $\text{Ch} = \text{S}$, **1.31**). Top: decomposition products of **1.30**

Ylidic stabilization of a terminal P=S unit has also been an attractive strategy to isolate “free” RP=S. Schmidpeter *et al.* reported the first examples of this method with a terminal P=S unit (Figure 1-12).⁹⁷ Because of the increased conjugation present in the ylidic molecule, the question remained as to whether a formal double bond was present between phosphorus and sulfur atoms (**1.32**) or if the charge-separated resonance form was dominant (**1.33**). Crystallographic analysis of these compounds indicate a P=S bond which is slightly elongated in comparison to the Pyykko and Atsumi bond length (1.96 Å), evidence that the charge-separated form is a better representation of the electronic nature of this compound.^{98,99} As further evidence for the charge separated species, reactivity of the ylid-stabilized P=S stems from the chalcogen atom (**1.34**, Figure 1-12).^{97,100} The ylidic stabilization does not allow for the observation of P=S double bond reactivity.

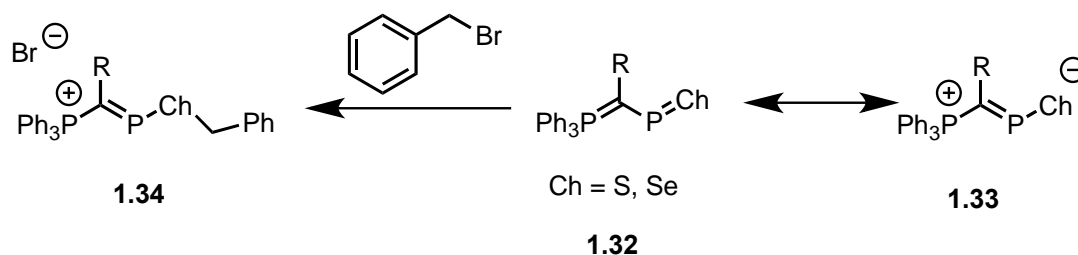


Figure 1-12. Resonance forms that represent ylidic stabilization of P=Ch (right) and an example of its reactivity (left)

1.5.3 Developments in Transition Metal Stabilization of RP=S

Phosphinidene-metal chemistry has been the subject of many reviews.^{26,41,42,44,49,59,61,86,101,102} The development of phosphinidene chalcogenide chemistry has been aided substantially by research on metal-phosphinidene complexes. The two main methods to prepare transition metal stabilized phosphinidene sulfides are: to generate naked RP=S fragments *via* transfer reactions, or by building the RP=S unit through direct bonding with metal centers.

The first successful example of transition metal stabilized RP=S was by Fawzi and coworkers in the 1980s. Their group reduced a phosphathioic dichloride in the

presence of $\text{Mn}_2(\text{CO})_{10}$ to yield a metallacycle containing a Mn-P-Mn^- bond where the anionic Mn is stabilized by a bond to a positively charged sulfur atom (**1.35**, Figure 1-13).⁸⁸ Attempts with 7-phosphanorbornadienes and $(\eta^5\text{-C}_5\text{H}_5)_2\text{Mo}_2(\text{CO})_6$ lead to the formation of multiple products. Two products with contrasting structures were isolated from the mixture: a binuclear complex with a Mo-Mo bond (**1.36**) and a binuclear complex where $\text{RP}=\text{S}$ has inserted into the Mo-Mo bond (**1.37**).¹⁰³ Performing the analogous reaction with Lawesson's reagent generated identical products.¹⁰⁴

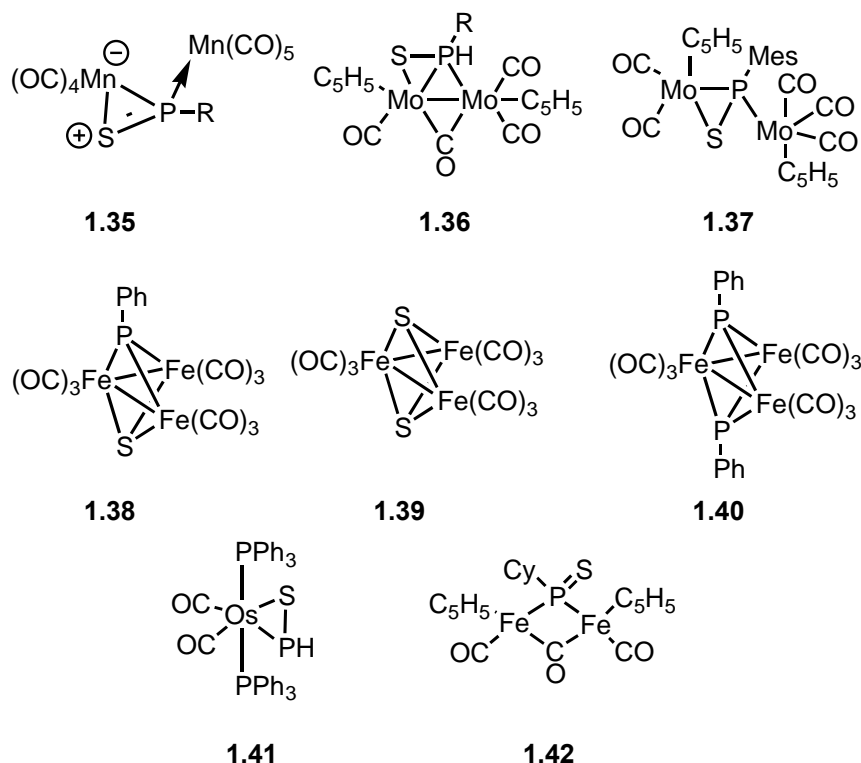


Figure 1-13. Select examples of transition metal stabilized phosphinidene sulfides (**1.35-1.42**)

In the 1980s, Seyferth and Withers reported the first generation of a “free” phosphinidene sulfide by a similar route involving the dehalogenation of phosphathioic dichlorides in the presence of $\text{Fe}_3(\text{CO})_{12}$.¹⁰⁵ While this did not yield the elusive metal-stabilized phosphinidene chalcogenides, a number of new products were formed that highlighted the breaking of the $\text{P}=\text{S}$ double bond to form trinuclear iron complexes containing phosphorus, sulfur, or a mixture of both elements as ligands (**1.38-1.40**, Figure

1-13). The Ruiz group have also demonstrated the ability to generate $\text{RP}=\text{S}$ units in the coordination sphere of a transition metal on a number of different occasions.^{106–109} While this strategy may not result in the formation of “free” $\text{RP}=\text{S}$ in solution, it has not inhibited the ability to use this method to generate stoichiometric $\text{RP}=\text{S}$ transfer reagents. Complexes developed by the Ruiz group display nucleophilic character stemming from phosphorus when exposed to elemental sulfur. This caused the $\text{RP}=\text{S}$ framework to be associated to transition metal coordination sphere (**1.41–1.42**, Figure 1-13).^{102,106,108–110}

1.6 Preparation of Small (c-RPCh)_n Heterocycles

Interesting P,S-heterocycles have been prepared by increasing steric demand at phosphorus and in the absence of trapping reagents,. The formation of cyclic oligomers are typically favoured, where rings with P_3S_3 or P_4S_4 cores are common for the condensation reaction of dichlorophosphines with reagents such as Na_2S , Li_2S , and $\text{S}(\text{TMS})_2$ (**1.43–1.44**, Figure 1-14).^{111–113} The formation of the 6- and 8-membered rings has been previously reported for a number of different reactions and is postulated to stem from the self-reaction of *in situ* generated $\text{RP}=\text{S}$ to form the trimer or tetramer, respectively.^{94,95,114–116} Derivatives of these rings containing other chalcogen atoms do exist; however, they were not completely characterized until recently.^{95,115}

Increasing the steric bulk substantially to a *m*-terphenyl ligand at phosphorus leads to the formation of $\text{RP}=\text{Ch}$ dimers (**1.45–1.46**, Figure 1-14).³⁷ The steric demand of the *m*-terphenyl ligand coupled with the strained 4-membered ring has allowed for solution-accessible monomeric $\text{RP}=\text{Ch}$ by thermal or photolytic methods. Interesting chemistry that resulted from the thermolysis of **1.45** has been reported, including the generation of a novel phosphirene sulfide and the first structurally characterized thiaphosphetene.⁹¹ Ring expansion has been observed in the presence of bases and Lewis acidic metals (*ie.* Cu, Ag) to yield compounds similar to **1.43**.¹¹⁷ The steric protection offered by the *m*-terphenyl ligand in combination with donation from a strong base (*ie.* NHCs) have also allowed for the isolation and structural characterization of the first base stabilized phosphinidene sulfide.³⁷

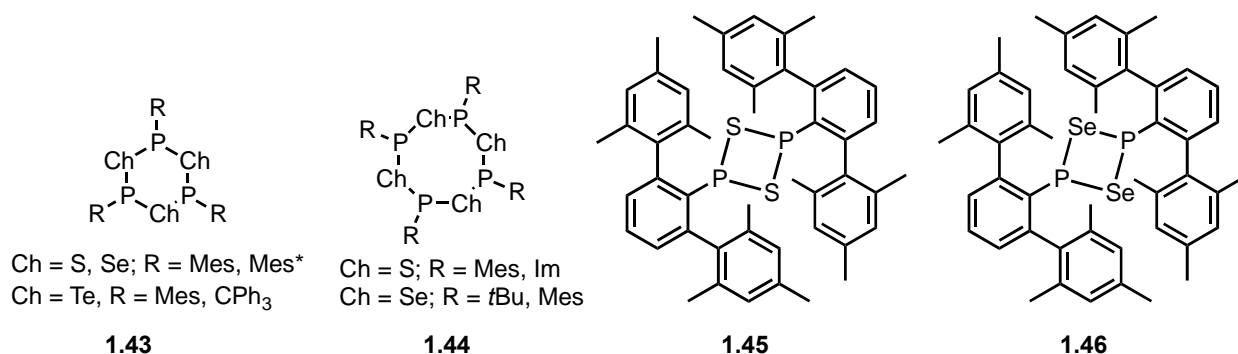


Figure 1-14. Reported examples of 4-8-membered P,S-heterocycles

1.7 Scope of Thesis

This thesis has two main components: 1) the gram-scale synthesis of novel asymmetric phosphines possessing sterically demanding ligands and 2) the development of methods to access RP=S under mild conditions for a variety of R groups on the phosphorus center. Novel P,S-heterocycles were reported resulting from reactions of *in situ* generated RP=S with a variety of trapping reagents (Section 1-6). Many of the described methods for phosphinidene or RP=S transfer rely on the degradation of heterocycles or the presence of transition metals to stabilize the reactive fragment. While these have proven to be successful routes for accessing phosphinidene sulfides, the development of a synthetic protocol to access RP=S, where removal of the metal and scaffold from the resulting products is not necessary, is certainly desirable. In order to use RP=S transfer in synthetic applications, the method of production must be tolerant of a wide variety of R groups bound to phosphorus. The development of a simple synthetic protocol will allow for researchers to access a variety of novel heterocycles upon reactions with a number of trapping reagents.

The generation of transient RP=S in this thesis was accomplished by thermolysis, or by condensation. The starting material required for the thermolysis method (**1.45**) was prepared by the condensation of *m*-terphenyl dichlorophosphine and S(TMS)₂ at room temperature on a gram scale. From here, RP=S can be accessed by gently heating a solution of **1.45** in the presence of trapping agents to yield novel P,S-heterocycles (Scheme 1-5). Interestingly, RP=S can also be generated and trapped *in situ* from the

condensation of a number of dichlorophosphines (with and without sterically demanding ligands) and $\text{S}(\text{TMS})_2$, and was thus coined the condensation method.

Chapter 2 focuses on the development of synthetic procedures for the preparation of various P-stereogenic phosphines possessing *m*-terphenyl ligands. The development of asymmetric phosphines possessing different reactivity handles for use as stoichiometric reagents or ligands for transition metals has been an ongoing area of research. The reported compounds represent an addition to the library of known asymmetric phosphines.

Chapter 3 focuses on further developing the transfer chemistry of phosphinidene sulfides and building a library of cycloaddition products to gain an understanding of phosphinidene sulfide reactivity patterns. Thermolysis of **1.45** in the presence of various substituted alkynes resulted in the formation of new P,S-heterocycles which represented products of both olefinic and carbenic reactivity pathways, in one pot. The ratio of resulting products was tunable based on the temperature and concentration that the thermolysis is performed under. Alternatively, the condensation method offers a room temperature protocol to access $\text{RP}=\text{S}$ in solution to generate structures analogous to those by the thermolysis method, but with greater selectivity. This selectivity stems from the operation of only one of carbenic **or** olefinic mechanistic pathways, dependent on the electron density of the trapping reagent used. The condensation method also allows for $\text{RP}=\text{S}$ to be generated and trapped when R was not sterically demanding, a first for the field. Electron-donating, electron-withdrawing and aryl R groups on dichlorophosphines have proven to be suitable reagents for the generation $\text{RP}=\text{S}$ *in situ* and have resulted in novel P,S-heterocycles when the reaction is performed in the presence of dmbd. In cases where R is not sterically demanding, it is possible to access products of both olefinic and carbenic reactivity pathways within the same reaction mixture and again, the ratio of these products is heavily dependent on reaction concentration.

As a general note, lone pairs have been included in Figures where bonding and/or singlet-triplet electronic ground states is the main focus for the compound being shown. Lone pairs have not been included for all P(III) species. Another note is the use of “ $\text{RP}=\text{Ch}$ ”, which is in place of phosphinidene chalcogenides ($\text{Ch} = \text{S}, \text{Se}$).

1.8 References

- (1) Schmid, H.; Michel, B. *Macromolecules*. **2000**, *33*, 3042–3049.
- (2) Jaeger, R. D.; Gleria, M. *Prog. Polym. Sci.* 1998, *23*, 179–276.
- (3) Nobel Prize Media AB. Press Release: The 1912 Nobel Prize in Chemistry. https://www.nobelprize.org/nobel_prizes/chemistry/laureates/1912/ (Accessed June 15, 2018).
- (4) Nobel Prize Media AB. Press Release: The 1918 Nobel Prize in Chemistry. https://www.nobelprize.org/nobel_prizes/chemistry/laureates/1918/ (Accessed June 15, 2018).
- (5) Nobel Prize Media AB. Press Release: The 1963 Nobel Prize in Chemistry. https://www.nobelprize.org/nobel_prizes/chemistry/laureates/1963/ (Accessed June 15, 2018).
- (6) Nobel Prize Media AB. Press Release: The 1979 Nobel Prize in Chemistry. https://www.nobelprize.org/nobel_prizes/chemistry/laureates/1979/ (Accessed June 15, 2018).
- (7) Nobel Prize Media AB. Press Release: The 2005 Nobel Prize in Chemistry. https://www.nobelprize.org/nobel_prizes/chemistry/laureates/2005/ (Accessed June 15, 2018).
- (8) Mark, J. E.; Allcock, H. R.; West, R. *Inorganic polymers*; Oxford University Press, 2005.
- (9) Guo, Q. H.; Pintauro, P. N.; Tang, H.; O'Connor, S. *J. Memb. Sci.* **1999**, *154*, 175–181.
- (10) Neilson, R. H.; Wisian-Neilson, P. *Chem. Rev.* **1988**, *88*, 541–562.
- (11) Bayardon, J.; Jugé, S. *Phosphorus(III) Ligands Homog. Catal. Des. Synth.* **2012**, *10*, 355–389.
- (12) Shintani, R.; Duan, W. L.; Nagano, T.; Okada, A.; Hayashi, T. *Angew. Chemie - Int. Ed.* **2005**, *44*, 4611–4614.
- (13) Schmitz, C.; Holthusen, K.; Leitner, W.; Franciò, G. *Eur. J. Org. Chem.* **2017**, *2017*, 21, 4111–4116.
- (14) Nozaki, K.; Sato, N.; Tonomura, Y.; Yasutomi, M.; Takaya, H.; Hiyama, T.; Matsubara, T.; Koga, N. *J. Am. Chem. Soc.* **1997**, *119*, 12779–12795.
- (15) Burk, M. J.; Feaster, J. E.; Nugent, W. A.; Harlow, R. L. *J. Am. Chem. Soc.* **1993**,

115, 10125–10138.

- (16) Zhao, Q.-Y.; Lian, Z.; Wei, Y.; Shi, M. *Chem. Commun.* **2012**, 48, 1724–1732.
- (17) Old, D. W.; Wolfe, J. P.; Buchwald, S. L. *J. Am. Chem. Soc.* **1998**, 120, 9722–9723.
- (18) Ma, Y. N.; Li, S. X.; Yang, S. D. *Acc. Chem. Res.* **2017**, 50, 1480–1492.
- (19) Dutartre, M.; Bayardon, J.; Jugé, S. *Chem. Soc. Rev.* **2016**, 45, 5771–5794.
- (20) Anagnostis, J.; Turnbull, M. M. *Polyhedron*. **2004**, 23, 125–133.
- (21) Allefeld, N.; Grasse, M.; Ignat'ev, N.; Hoge, B. *Chem. Eur. J.* **2014**, 20, 8615–8620.
- (22) Power, P. P. *Chem. Rev.* **1999**, 99, 3463–3504.
- (23) West, R.; Fink, M. J.; Michl, J. *Science*. **1981**, 214, 1343–1344.
- (24) Power, P. P. *Chem. Rec.* **2012**, 12, 238–255.
- (25) Cowley, A. H.; Kilduff, J. E.; Newman, T. H.; Pakulski, M. *J. Am. Chem. Soc.* **1982**, 104, 5820–5821.
- (26) Regitz, M. *Chem. Rev.* **1990**, 90, 191–213.
- (27) Power, P. P. *J. Organomet. Chem.* **2004**, 689, 3904–3919.
- (28) Perry, A. L.; Low, P. J.; Ellis, J. R.; Reynolds, J. D. *Science*. **2017**, 308, 1912–1915.
- (29) Summerscales, O. T.; Fettingner, J. C.; Power, P. P. *J. Am. Chem. Soc.* **2011**, 133, 11960–11963.
- (30) Toyota, K.; Matsushita, Y.; Shinohara, N. *Heteroat. Chem.* **2001**, 12, 418–423.
- (31) Tonner, R.; Öxler, F.; Neumüller, B.; Petz, W.; Frenking, G. *Angew. Chemie - Int. Ed.* **2006**, 45, 8038–8042.
- (32) Allen, D. W. *Organophosphorus Chem.* **2015**, 44, 1–55.
- (33) Müller, C. *Eur. J. Inorg. Chem.* **2016**, 569–571.
- (34) Jupp, A. R.; Goicoechea, J. M. *Angew. Chem. - Int. Ed.* **2013**, 52, 10064–10067.
- (35) Krummenacher, I.; Cummins, C. C. *Polyhedron*. **2012**, 32, 10–13.
- (36) Puschmann, F. F.; Stein, D.; Heift, D.; Hendriksen, C.; Gal, Z. A.; Grützmacher, H. F.; Grützmacher, H. *Angew. Chem. - Int. Ed.* **2011**, 50, 8420–8423.
- (37) Graham, C. M. E.; Pritchard, T. E.; Boyle, P. D.; Valjus, J.; Tuononen, H. M.; Ragogna, P. J. *Angew. Chem. - Int. Ed.* **2017**, 129, 6332–6336.

- (38) Belloli, R. *J. Chem. Ed.* **1971**, 48, 422–426.
- (39) Li, X.; Weissman, S. I.; Lin, T. S.; Gaspar, P. P.; Cowley, A. H.; Smirnov, A. I. *J. Am. Chem. Soc.* **1994**, 116, 7899–7900.
- (40) Lammertsma, K. *Top. Curr. Chem.* **2003**, 229, 95–119.
- (41) Aktaş, H.; Chris Slootweg, J.; Lammertsma, K. *Angew. Chem. - Int. Ed.* **2010**, 49, 2102–2113.
- (42) Mathey, F. *Dalt. Trans.* **2007**, 1861–1868.
- (43) Van Eis, M. J.; Zappey, H.; De Kanter, F. J. J.; De Wolf, W. H.; Lammertsma, K.; Bickelhaupt, F. J. *Am. Chem. Soc.* **2000**, 122, 3386–3390.
- (44) Mathey, F. *Angew. Chem. - Int. Ed.* **1987**, 26, 275–286.
- (45) Ehlers, A. W.; Baerends, E. J.; Lammertsma, K. *J. Am. Chem. Soc.* **2002**, 124, 2831–2838.
- (46) Wit, J. B. M.; Eijkel, G. T. Van; Franciscus, J. J.; Kanter, D.; Schakel, M.; Ehlers, A. W.; Spek, A. L.; Lammertsma, K. *Angew. Chem. - Int. Ed.* **1999**, 2, 2596–2599.
- (47) Li, X.; Lei, D.; Chiang, M. Y.; Gaspar, P. P. *J. Am. Chem. Soc.* **1992**, 114, 8526–8531.
- (48) Waterman, R. *Chem.* **2016**, 1, 27–29.
- (49) Mathey, F. *Angew. Chem. - Int. Ed.* **2003**, 42, 1578–1604.
- (50) Transue, W. J.; Velian, A.; Nava, M.; Garc, C.; Temprado, M.; Cummins, C. C. *J. Am. Chem. Soc.* **2017**, 139, 10822–10831.
- (51) Quin, L. D.; Szewczyk, J. *J. Chem. Soc., Chem. Comm.* **1986**, 844–846.
- (52) Compain, C.; Donnadieu, B.; Mathey, F. *Organometallics*. **2005**, 24 (7), 1762–1765.
- (53) Tran Huy, N. H.; Ricard, L.; Mathey, F. *Angew. Chem. - Int. Ed.* **2001**, 40, 1253–1255.
- (54) Montgomery, C. D. *J. Chem. Ed.* **2015**, 92 (10), 1653–1660.
- (55) Mathey, F.; Hoa, N.; Huy, T.; Marinetti, A. *Helv. Chim. Act.* **2001**, 84, 2938–2957.
- (56) Fischer, J.; Marinetti, A.; Charrier, C.; Mathey, F. *Organometallics*. **1985**, 4, 2134–2138.
- (57) Santini, C. C.; Fischer, J.; Mathey, F.; Mitschler, A. *J. Am. Chem. Soc.* **1980**, 102, 5809–5815.

- (58) Marinetti, A.; Mathey, F.; Fischer, J.; Mitschler, A. *J. Am. Chem. Soc.* **1982**, *104*, 4484–4485.
- (59) Mercier, F.; Deschamps, B.; Mathey, F. *J. Am. Chem. Soc.* **1989**, *111*, 9098–9100.
- (60) Pal, K.; Hemming, O. B.; Day, B. M.; Pugh, T.; Evans, D. J.; Layfield, R. A. *Angew. Chem. - Int. Ed.* **2016**, *55*, 1690–1693.
- (61) Aktas, H.; Slootweg, J. C.; Ehlers, A. W.; Lutz, M.; Spek, A. L.; Lammertsma, K. *Organometallics*. **2009**, *28*, 5166–5172.
- (62) Wang, Y.; Xie, Y.; Abraham, M. Y.; Gilliard, R. J.; Wei, P.; Schaefer, H. F.; Schleyer, P. R.; Robinson, G. H. *Organometallics*. **2010**, *2004*, 9751–9753.
- (63) Wang, Y.; Robinson, G. H. *Inorg. Chem.* **2011**, *50*, 12326–12327.
- (64) Olkowska-oetzel, J.; Pikies, J. *Appl. Organomet. Chem.* **2003**, *17*, 28–35.
- (65) Liu, L.; Ruiz, D. A.; Munz, D.; Bertrand, G. *Chem* **2016**, *1*, 147–153.
- (66) Binnewies, M.; Borrmann, H. *Zeitschrift für Anorg. und Allg. Chem.* **1983**, *552*, 147–154.
- (67) Schnöckel, H.; Schunck, S. *Zeitschrift für Anorg. und Allg. Chem.* **1983**, *552*, 163–170.
- (68) Schnöckel, H.; Schunck, S. *Zeitschrift für Anorg. und Allg. Chem.* **1987**, *552*, 155–162.
- (69) Schnöckel, H.; Lakenbrink, M. *Zeitschrift für Anorg. und Allg. Chem.* **1989**, *507*, 70–76.
- (70) Li, X.; Weissman, S. I.; Lin, T.; Gaspar, P. P.; Louis, S.; Cowley, A. H.; Smirnov, A. I. *J. Am. Chem. Soc.* **1994**, *112*, 7899–7900.
- (71) Gaspar, P. P.; Qian, H.; Beatty, A. M.; André D’Avignon, D.; Kao, J. L. F.; Watt, J. C.; Rath, N. P. *Tetrahedron*. **2000**, *56*, 105–119.
- (72) Nixon, J. F. *Chem. Rev.* **1988**, *88*, 1327–1362.
- (73) Schoeller, W. W.; Niecke, E. *Chem. Comm.* **1982**, *49*, 569–570.
- (74) Kyri, A. W.; Schnakenburg, G.; Streubel, R. *Chem. Comm.* **2016**, *52*, 8593–8595.
- (75) Cowley, A. H.; Gabbañ, F. P.; Corbelin, S.; Decken, A. *Inorg. Chem.* **1995**, *34*, 5931–5932.
- (76) Yamamoto, Y.; Soc, J. A. C.; Robinson, S. D.; Acta, I. C.; Joshi, K. K.; Mills, S.; Pauson, P. L. *Angew. Chem. - Int. Ed.* **1978**, *17*, 867–868.

- (77) Wang, L.; Ganguly, R. *Organometallics*. **2014**, 14–17.
- (78) Foreman, M. R. S. J.; Slawin, A. M. Z.; Woollins, J. D. *J. Chem. Soc. Dalton Trans.* **1999**, 3, 1175–1184.
- (79) Hussong, R.; Heydt, H.; Regitz, M. *Z. Naturforsch.* **1986**, 41, 915–921.
- (80) Kashman, Y.; Wagenstein, I.; Rudi, A. *Tetrahedron*. **1976**, 32, 2427–2431.
- (81) Harwood, H. J.; Pollart, K. A. *J. Org. Chem.* **1963**, 28, 3430–3433.
- (82) Crofts, P. C.; Fox, I. S. *J. Chem. Soc. B* **1968**, 1416–1420.
- (83) Nakayama, S.; Yoshifuji, M.; Okazaki, R.; Inamoto, N. *Chem. Comm.* **1971**, 1186–1187.
- (84) Nakayama, S.; Yoshifuji, M.; Okazaki, R.; Inamoto, N. *Bull. Chem. Soc. Jpn.* **1975**, 48, 3733–3737.
- (85) Nakayama, S.; Yoshifuji, M.; Okazaki, R.; Inamoto, N. *Chem. Comm.* **1971**, 113, 1186–1187.
- (86) Schmidt, U. *Angew. Chem. - Int. Ed.* **1975**, 14, 523–528.
- (87) Nakayama, S.; Yoshifuji, M.; Okazaki, R.; Inamoto, N. *J. Chem. Soc. Perkin I.* **1973**, 1969–1974.
- (88) Lindner, E.; Auch, K.; Hiller, W.; Fawzi, R. *Angew. Chem. - Int. Ed.* **1984**, 23, 320–320.
- (89) Holand, S.; Mathey, F. *J. Org. Chem.* **1981**, 46 (22), 4386–4389.
- (90) Tomioka, H.; Kato, Y.; Izawa, Y. *J. Chem. Soc. Perkin II.* **1980**, 1017–1021.
- (91) Ragogna, P. J.; Graham, C.; Macdonald, C.; Boyle, P.; Wisner, J. *Chem. Eur. J.* **2017**.
- (92) Yoshifuji, M.; Hirano, M.; Toyota, K. *Tetrahedron Lett.* **1993**, 34, 1043–1046.
- (93) Yoshifuji, M.; Sangu, S.; Hirano, M.; Toyota, K. *Chem. Lett.* **1993**, 1715–1718.
- (94) Kamijo, K.; Toyota, K.; Yoshifuji, M. *Chem. Lett.* **1999**, 567–568.
- (95) An, D. L.; Toyota, K.; Yasunami, M.; Yoshifuji, M. *Chem. Lett.* **1994**, 199–200.
- (96) Rivière, F.; Ito, S.; Yoshifuji, M. *Tetrahedron Lett.* **2002**, 43, 119–121.
- (97) Jochem, G.; Nöth, H.; Schmidpeter, A. *Angew. Chem. - Int. Ed.* **1993**, 32, 1089–1091.
- (98) Pyykkö, P.; Atsumi, M. *Chem. Eur. J.* **2009**, 15, 12770–12779.
- (99) Pyykkö, P.; Atsumi, M. *Chem. Eur. J.* **2009**, 15, 186–197.

- (100) Wilker, S.; Laurent, C.; Sarter, C.; Puke, C.; Erker, G. *J. Am. Chem. Soc.* **1995**, *117*, 7293–7294.
- (101) Waterman, R. *Dalt. Trans.* **2009**, 9226, 18–26.
- (102) Sterenberg, B. T.; Udachin, K. A.; Carty, A. J. *Organometallics*. **2001**, *20*, 4463–4465.
- (103) Rita, H.; Heinrich, H.; Gerhard, M.; Manfred, R. *Chem. Ber.* **1987**, *120*, 1263–1267.
- (104) Alper, H.; Petrignani, J. F.; Einstein, F. W. B.; Willis, A. C. *Organometallics*. **1983**, *2*, 1422–1426.
- (105) Seyferth, D.; Withers, H. P. *Organometallics*. **1982**, *1*, 1294–1299.
- (106) Alvarez, M. A.; Amor, I.; Garc, M. E.; Garc, D.; Ruiz, M. A. *Inorg. Chem.* **2012**, *51*, 7810–7824.
- (107) Alvarez, B.; Angeles Alvarez, M.; Amor, I.; García, M. E.; Ruiz, M. A. *Inorg. Chem.* **2011**, *50*, 10561–10563.
- (108) Alvarez, C. M.; Alvarez, M. A.; García, M. E.; González, R.; Ruiz, M. A.; Hamidov, H.; Jeffery, J. C. *Organometallics*. **2005**, *24*, 5503–5505.
- (109) Albuerne, I. G.; Alvarez, M. A.; García, M. E.; García-Vivó, D.; Ruiz, M. A. *Inorg. Chem.* **2015**, *54*, 9810–9820.
- (110) Hirth, U.; Malisch, W. *J. Org. Chem.* **1992**, *439*, 5–8.
- (111) Yogendra, S.; Chitnis, S. S.; Hennersdorf, F.; Bodensteiner, M.; Fischer, R.; Burford, N.; Weigand, J. J. *Inorg. Chem.* **2016**, *55*, 1854–1860.
- (112) Henne, F. D.; Watt, F. A.; Schwedtmann, K.; Hennersdorf, F.; Kokoschka, M.; Weigand, J. J. *Chem. Comm.* **2016**, *52*, 2023–2026.
- (113) Lensch, C.; Sheldrick, G. M. *J. Chem. Soc. Dalt. Trans.* **1984**, *1*, 2855–2857.
- (114) Cetinkaya, B. *J. Chem. Soc. Chem. Commun.* **1982**, 691–693.
- (115) Nordheider, A.; Chivers, T.; Schçn, O.; Karaghiosoff, K.; Arachchige, K. S. A.; Slawin, A. M. Z.; Woollins, J. D. *Chem. Eur. J.* **2014**, *20*, 704–712.
- (116) M. Yoshifuji, K. Toyota, K. Ando. *J. Chem. Inf. Model.* **2013**, *53*, 1689–1699.
- (117) Graham, C. M. E.; Valjus, J.; Pritchard, T. E.; Boyle, P. D.; Tuononen, H. M.; Ragogna, P. J. *Inorg. Chem.* **2017**, *56*, 13500–13509.

Chapter 2

2 Synthesis & Characterization of Asymmetric Phosphines

2.1 Introduction

The importance of asymmetric phosphine ligands in transition metal chemistry, catalysis, and organic synthesis cannot be overstated.¹⁻¹¹ The ability to modify the steric and electronic properties of both mono- and diphosphines has facilitated the development of metal phosphine-based catalysis across a wide range of applications.¹²⁻¹⁴ Asymmetric phosphines have been used as ligands for transition metals to perform catalytic reactions with high enantioselectivity for various C–X (X= H, C, N, B) bond forming reactions.^{15,16} While there have been extensive studies on asymmetric phosphines in the literature, many examples utilize smaller aryl substituents as one of the ligands. Dialkylaminochlorophosphines (**A-D**, Figure 2-1), for example, present an opportunity to bias reactivity at the phosphorus center towards the P–N or P–Cl bond. This strategy has been widely used for the synthesis of unique cage complexes,¹⁷ new organophosphorus compounds,¹⁸ and also in the development of ligands for transition metal complexes.^{15,16,19} Secondary phosphines (**E**, Figure 2-1) are obtained from the deprotonation and subsequent quenching of the phosphide anion of their parent primary phosphines with TMSCl.²⁰ Amphiphilic phosphines have been useful synthetic tools since the late 1990s, particularly for the synthesis of bis[phosphine-ethyl] ethers for use as multi-dentate ligands for a variety of different transition metal complexes (**F**, Figure 2-1).²¹ Many compounds featuring the bonding environments shown in Figure 2-1 have been prepared featuring large aryl groups as well, with examples from the literature that include Mes (Mes = 2,4,6-trimethylphenyl), Mes* (Mes* = 2,4,6-tri-*tert*butylphenyl), and dipp (dipp = diisopropylphenylphosphine) substituents.

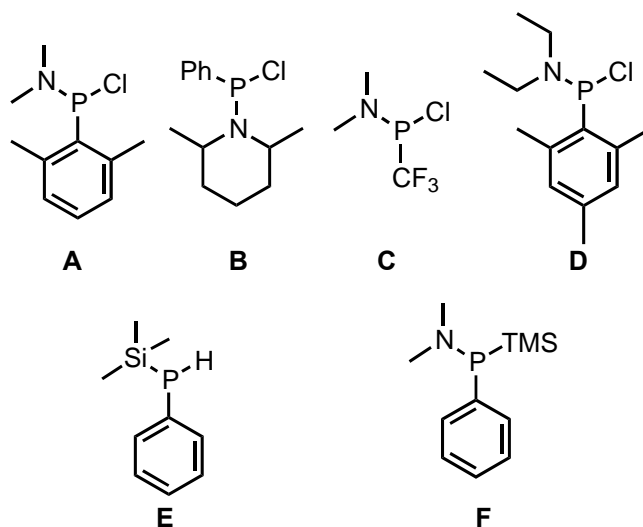


Figure 2-1. Select examples of secondary and tertiary asymmetric phosphines

Although phosphines of this nature have proven to be valuable reagents for the synthesis of bioactive compounds and as ligands in catalysis, there are fewer examples of asymmetric phosphines which possess *m*-terphenyl substituents.²² The incorporation of these bulky groups proved on numerous occasions to suppress reactivity of main group centres, and can offer kinetic stabilization for otherwise reactive units.²³ Incorporating bulky groups into asymmetrically substituted phosphorus compounds will add to the chemically diverse library of phosphine ligands.

Furthermore, the preparation of compounds with bonds to phosphorus have often relied heavily on the use of sterically encumbered substituents to aide in the prevention of undesirable side reactions and decomposition.²⁴ For example, the use of *m*-terphenyl ligands – which consist of a *meta*-substituted central benzene ring bound to two Mes or Mes* groups, for example – was instrumental in Yoshifuji *et al.*'s isolation of diphosphenes (**H**, Figure 2-2).^{25,26} The corresponding diphosphanes (**I**, Figure 2-2) have since been prepared through a number of different routes; however, they were first isolated as a byproduct of diphosphene synthesis.^{27,28} We have been exploiting the steric bulk of terphenyl ligands (TerPh = 2,6-MesC₆H₃) as kinetic stabilization for some time to prepare 4-membered phosphorus-chalcogen rings amenable to the liberation of phosphinidene chalcogenides. This achievement has not been demonstrated with smaller aryl substituents on phosphorus (**J**, Figure 2-2).^{29,30}

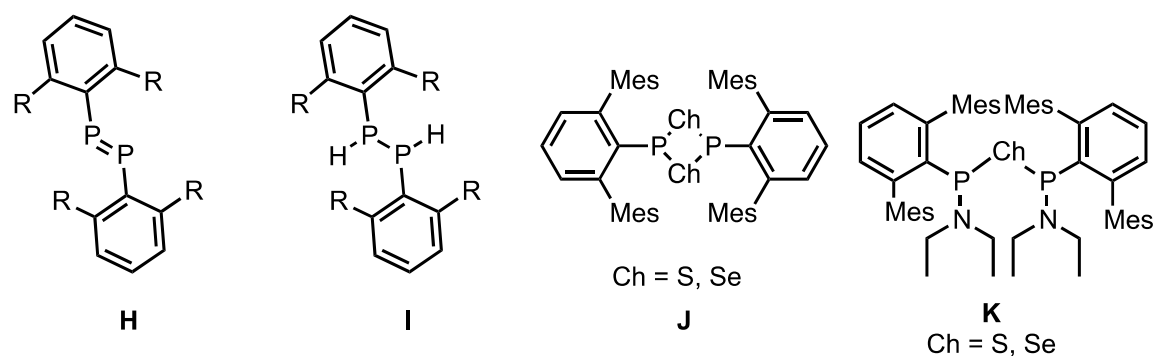


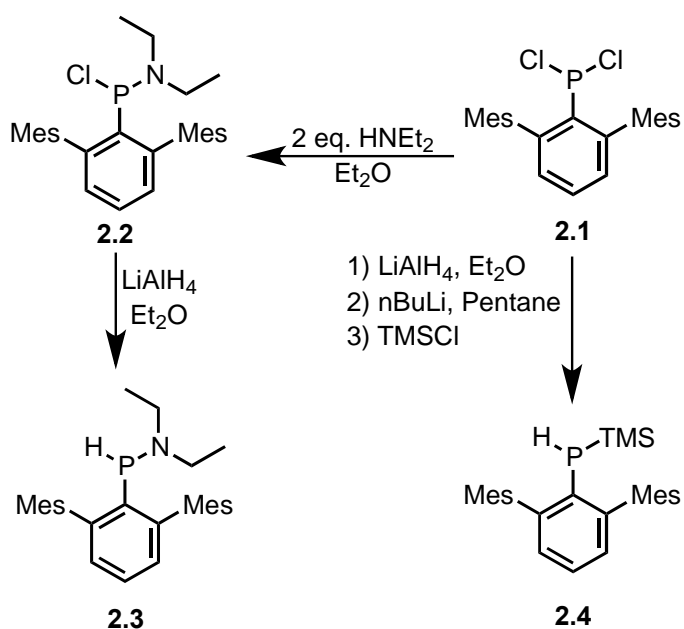
Figure 2-2. Examples of compounds prepared using bulky aryl ligands (**H-J**) and targeted diphosphanylchalcogenane structure (**K**)

In this context we report on the synthesis and comprehensive characterization of various asymmetric phosphines with a TerPh ligand. We have been able to prepare phosphines possessing $-\text{Cl}$, $-\text{H}$, $-\text{NEt}_2$, and $-\text{Si}(\text{CH}_3)_3$ functionality in good yield on a gram scale. All prepared derivatives possess a bias for selective reactivity at a single bond to phosphorus, so a number of homocoupling reactions were carried out with the prepared asymmetric phosphines in attempts to generate a P-P single bond stoichiometrically *via* dehydrohalogenative coupling and salt metathesis. Diphosphane, **2.6** ($\text{R} = \text{Mes}$), has been previously been reported by the cleavage of Zr-P bonds of the complex $\text{Cp}^*_2\text{Zr}(\text{PMesPMes})$ in the presence of phenylacetylene; however, it has yet to be structurally characterized or prepared without the use of metals.²⁹ Our synthetic strategy involved the reduction of terphenyldiphosphene to terphenyldiphosphane, which proceeded in near quantitative yield and its complete structural characterization is detailed within. The kinetic stability offered by the steric bulk of the TerPh ligand may allow for novel reactivity; however, attempted reactions with sulfur monochloride and **2.6** resulted in inconsistent reactivity. Diphosphanylchalcogenanes (**K**) were targeted not only as interesting asymmetric phosphines derivatives, but as precursors for the synthesis of novel asymmetric P,Ch-heterocycles.

2.2 Results & Discussion

2.2.1 Preparation of Asymmetric Phosphines

Dichloroterphenylphosphine (**2.1**) was prepared using literature procedures and acted as the initial precursor for the prepared asymmetric phosphines.^{29,31,32} The addition of two stoichiometric equivalents of diethylamine to **2.1** resulted in the appearance of a new singlet in the $^{31}\text{P}\{^1\text{H}\}$ NMR spectrum after two hours ($\delta_{\text{P}} = 139.0$; Scheme 2-1, Figure 2-3). After removal of the resulting ammonium chloride salt *via* vacuum filtration through a glass frit, volatiles were removed *in vacuo* to give a white powder. Single crystals of X-ray diffraction quality were obtained by placing a concentrated solution of the resulting powder in *n*-pentane at $-35\text{ }^{\circ}\text{C}$ overnight. Subsequent structural analysis confirmed the structure of **2.2** (81% total yield). Redissolving single crystals of **2.2** in benzene- d_6 displayed the same singlet as the reaction mixture, along with a single set of TerPh resonances in the ^1H NMR spectrum. In the solid state, **2.2** was discovered to be quite sensitive to hydrolysis upon short exposure to the ambient environment.



Scheme 2-1. Synthesis of asymmetric phosphines from dichloroterphenylphosphine

Compound **2.2** was an ideal precursor for other asymmetric phosphines because it possessed one reactive P-Cl bond. This allowed for a high degree of control over reactivity at the phosphorus center. The corresponding secondary phosphine was obtained

from **2.2** by reduction with excess LiAlH_4 to yield compound **2.3**. Compound **2.2** was dissolved in THF and added to a suspension of 3 stoichiometric equivalents LiAlH_4 in THF. Excess LiAlH_4 was quenched with degassed water and the supernatant was filtered through Celite/ MgSO_4 (3:1 v/v) on a glass frit before removal of solvent *in vacuo* to give a white powder (65% yield; Scheme 2-1). Compound **2.3** appeared as a doublet in the ^{31}P spectrum at $\delta_{\text{P}} = 1.86$ with a coupling constant of 236.8 Hz (Figure 2-3). A single set of TerPh peaks and a doublet corresponding to P-H coupling ($^1J_{\text{HP}} = 236.8$ Hz) were present in the ^1H NMR spectrum confirmed the composition of **2.3**. Attempts to generate a P-P single bond by dehydrogenative coupling with **2.2**, **2.3** and a variety of bases (DBU, DMAP, NEt_3) were unsuccessful. The resultant ^{31}P NMR spectra showed that either no reaction had occurred or multiple products were formed which could not be isolated.

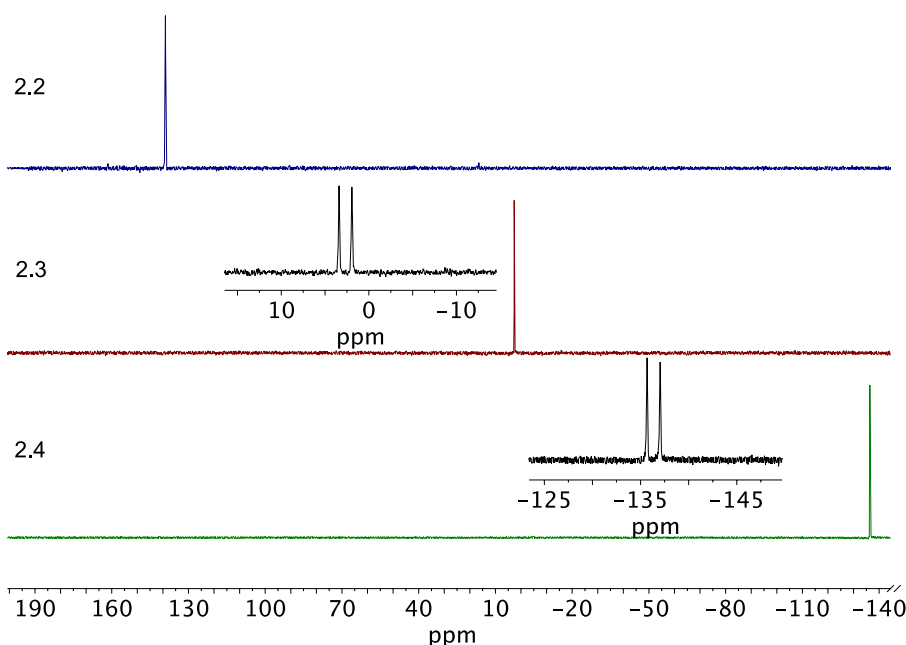


Figure 2-3. Stacked $^{31}\text{P}\{^1\text{H}\}$ NMR spectra of purified **2.2** (top), **2.3** (middle), and **2.4** (bottom) with inset ^{31}P NMR spectra expansions included where splitting was observed

Following reduction of **2.1** to terphenylphosphine with LiAlH_4 , the corresponding phosphide anion was generated using 5 equivalents of *n*-BuLi in coordinating solvent (Et_2O or THF) and removing volatiles *in vacuo* left a bright orange powder.²⁵ When redissolved in benzene- d_6 , a ^{31}P signal at -136.4 ppm was observed, this was shifted

upfield from Ar^*PH_2 ($\delta_{\text{P}} = -146.7$, $^1J_{\text{PH}} = 209.9$ Hz), with a coupling constant of 176.0 Hz, consistent with $^1J_{\text{PH}}$ coupling reported in literature for phosphide anions.²⁵ Excess *n*-BuLi was removed by washing the crude reaction mixture with hexanes, then the pink powder was dissolved in Et_2O and excess TMSCl was added at 0 °C (Scheme 2-1). A drastic colour change from a dark pink solution to colourless occurred almost instantaneously. Compound **2.4** was isolated as a white powder in 26% yield after removal of solvent *in vacuo*. The doublet in the ^{31}P NMR spectrum persisted at -136.4 ppm with a P-H coupling constant of 220.0 Hz (Figure 2-3). The ^1H NMR spectrum contained diagnostic signals which supported the formation of **2.4**, with a doublet at 3.10 ppm ($^1J_{\text{HP}} = 220.0$ Hz) and the presence of a doublet at $\delta_{\text{H}} = -0.20$, corresponding to 9 TMS protons coupled to phosphorus ($^2J_{\text{HP}} = 4.8$ Hz). The formation of a P-P single bond was targeted again by dehydrohalogenative coupling with **2.4** and **2.2** using a variety of bases, but due to the complexity of the resulting NMR spectra, this route was not pursued. We hypothesized that the steric bulk of the terphenyl ligand inhibited the reactive components from being accessible to each other. A summary of the stoichiometric reaction attempts to form single P-P bonds are shown in Figure 2-4 (not shown are solvent, temperature and concentration variations).

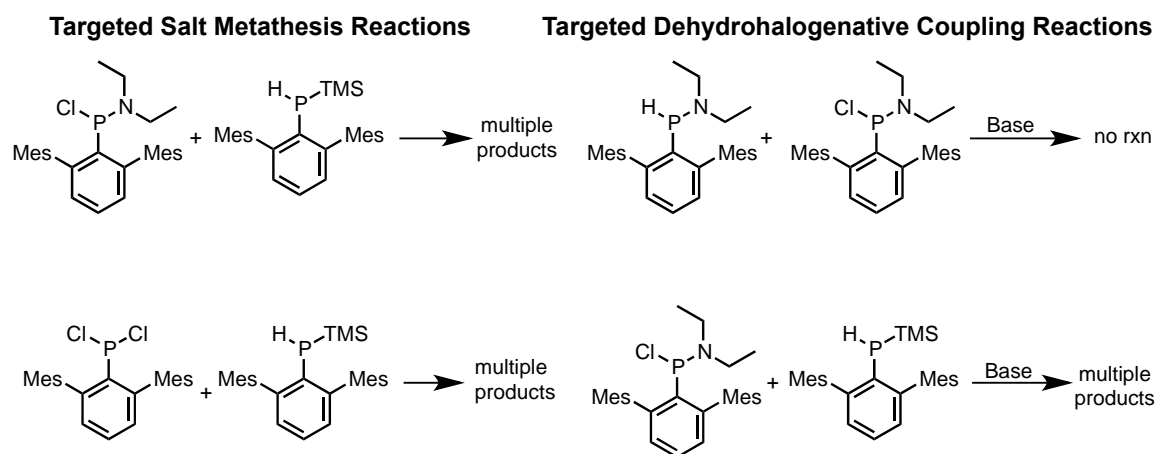
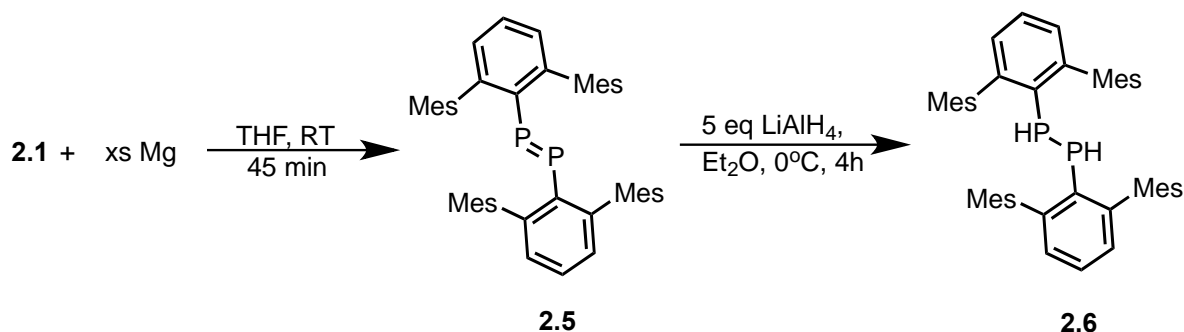


Figure 2-4. Targeted P-P single bond formation strategies, salt metathesis and dehydrohalogenative coupling, using **2.1-2.4**

A method reported by Protasiewicz *et al.* for the synthesis of P=P double bonds was used to prepare terphenyldiphosphene (**2.5**).^{26,33,34} Following recrystallization from a

concentrated solution of pentane at $-35\text{ }^{\circ}\text{C}$, compound **2.5** corresponded to a singlet at $\delta_{\text{P}} = 493.2$, consistent with previous literature reports.³³ Compound **2.5** was only obtained when Mg turnings were activated with naphthalene (Rieke Mg), other attempts when Mg turnings were activated with I_2 or dibromoethane did not yield the desired product. Compound **2.5** was redissolved in THF and added to a suspension of 5 stoichiometric equivalents of LiAlH_4 in THF which had been cooled to $0\text{ }^{\circ}\text{C}$. The solution became a deep red colour within 5 minutes and was allowed to warm to room temperature over the course of 4 hours. Using a five-fold excess of LiAlH_4 , only an 8% of terphenylphosphine was generated by integration of the ^{31}P NMR spectrum (TerPhPH_2 , $\delta_{\text{P}} = -146.7$). The $^{31}\text{P}\{^1\text{H}\}$ NMR spectrum also contained signals corresponding to the diphosphane product (**2.6**) observed at chemical shifts of -100.9 and -110.2 ppm in a 9:1 ratio, respectively (Scheme 2-2).



Scheme 2-2. Preparation of terphenyldiphosphane (**2.6**) from **2.1**

Both TerPhPH_2 and **2.6** were highly soluble in ethereal and hydrocarbon solvents, but were readily separated by crystallization at $-35\text{ }^{\circ}\text{C}$ overnight from a solution of pentane:hexamethyldisiloxane (1:2), in which **2.6** was highly insoluble. Washing crude reaction mixtures 3-5 times with 2 mL of HMDSO also yielded sufficiently pure bulk material. The coupled ^{31}P NMR spectrum displayed an $\text{AA}'\text{XX}'$ spin system for $\delta_{\text{P}} = -100.9$ and what initially appeared to be a doublet of doublets for $\delta_{\text{P}} = -110.2$, but was in fact a second unresolved $\text{AA}'\text{XX}'$ spin system (Figure 2-5). Other diphosphanes reported by Clegg *et al.* show the formation of 2 products with a similar coupling pattern to **2.6**.³⁵ Using this information, the two different peaks could be assigned as the *rac* and *meso*

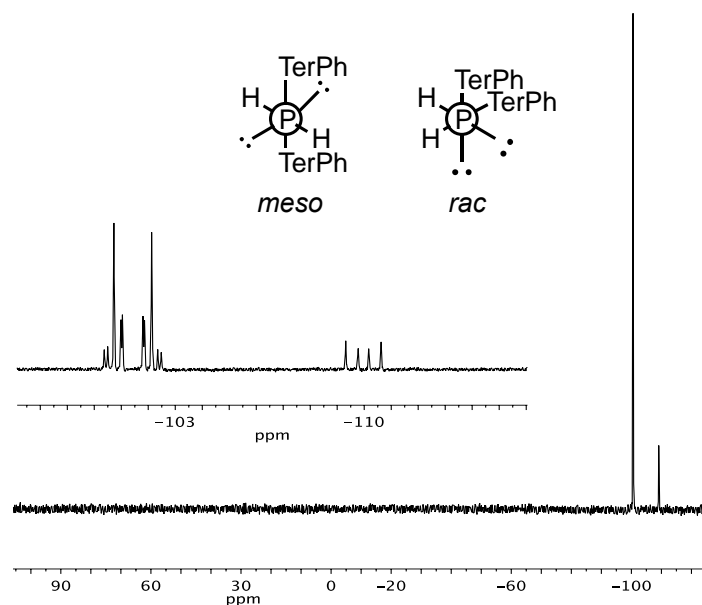
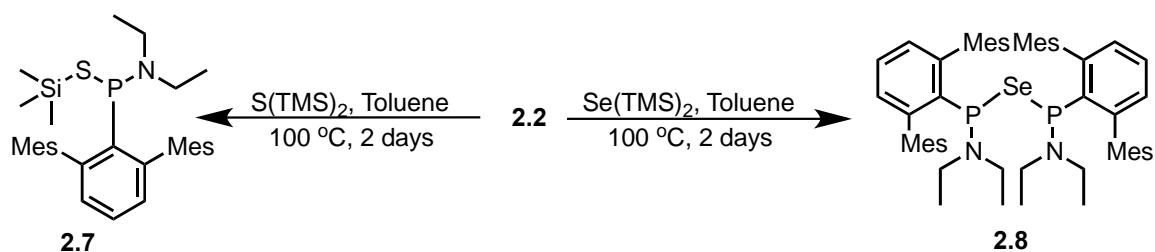


Figure 2-5. $^{31}\text{P}\{^1\text{H}\}$ NMR spectrum of purified **2.6** with inset ^{31}P expansion highlighting half of a well-resolved AA'XX' spin system for the *meso* isomer and an unresolved AA'XX' spin system for the *rac* isomer.

diastereomers of **2.6**, where the *meso* isomer is favoured ($\delta_{\text{P}} = -100.9$) due to the steric bulk imposed by the TerPh ligand. The *rac* isomer also possesses an AA'XX' spin system which cannot be deduced due to a lack of peak intensity. Attempts to separate the *rac* and *meso* isomers were not successful. In the ^1H NMR spectrum, complex multiplets which corresponded to P-H coupling from both diastereomers were overlapping in several instances. There were also two sets of peaks corresponding to mesityl methyl protons in the aliphatic region in a 9:1 ratio, which was indicative of the presence of both diastereomers. Having obtained a P-P single bond, dehydrohalogenative coupling with S_2Cl_2 and base was targeted. Attempts with DBU and DMAP generally lead to a complex mixture of products in the $^{31}\text{P}\{^1\text{H}\}$ NMR spectrum with poor reproducibility. The steric bulk imposed by the TerPh ligands likely inhibited the desired reaction from occurring cleanly.

The synthesis of diphosphanylchalcogenanes (Ch = S, Se) were also targeted as precursors for asymmetric phosphorus chalcogen rings. Upon addition of excess $\text{S}(\text{TMS})_2$ to a solution of **2.2**, the appearance of two signals was observed by $^{31}\text{P}\{^1\text{H}\}$ NMR spectroscopy ($\delta_{\text{P}} = 34.0, 83.0$). The exclusive formation of monophosphanylsulfane (**2.7**,

$\delta_P = 83.0$) was favoured by allowing the reaction to proceed at 100 °C for 48 hours. After removal of all solvent *in vacuo*, the yellow residue was purified by crystallization at the interface of a pentane and MeCN solution overnight at -35 °C (Scheme 2-3). The ^1H NMR spectrum of the yellow powder contained one set of TerPh peaks, as well as a singlet corresponding to the $-\text{SiMe}_3$ protons at $\delta_H = 0.20$. Even when the reaction was performed with a substoichiometric amount of $\text{S}(\text{TMS})_2$, only monophosphanylsulfane (**2.7**) was obtained. Despite difficulties in achieving the diphosphanylsulfane, the diphosphanylselane (**2.8**) was readily prepared *via* a similar procedure with one stoichiometric equivalent of $\text{Se}(\text{TMS})_2$ ($\delta_P = 99.1$, Scheme 2-3). The $^{31}\text{P}\{^1\text{H}\}$ NMR spectrum confirmed the presence of the P-Se bond, with $^{77}\text{Se}-^{31}\text{P}$ coupling at a magnitude of 221.2 Hz. The corresponding ^1H NMR spectrum contained one set of Ar* resonances as well as two sets of complex multiplets corresponding to the $-\text{NEt}_2$ groups.



Scheme 2-3. Synthesis of **2.7** and **2.8** from the condensation reaction of **2.2** with $\text{Ch}(\text{TMS})_2$ (Ch = S, Se)

2.2.2 X-Ray Crystallography

Images of the solid-state structures for the prepared asymmetric phosphines are shown in Figure 2-6.

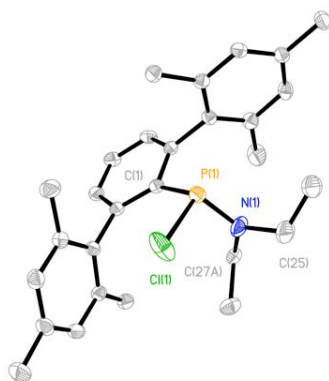
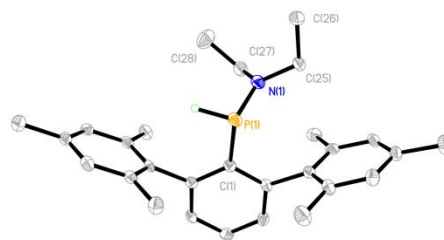
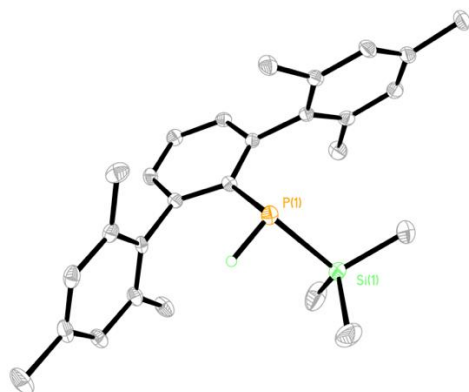
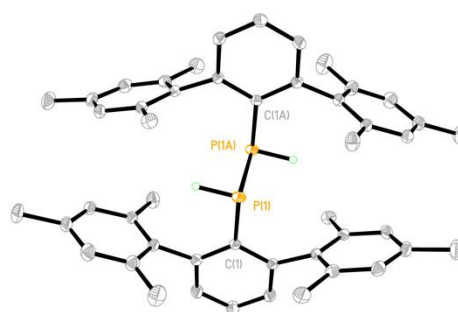
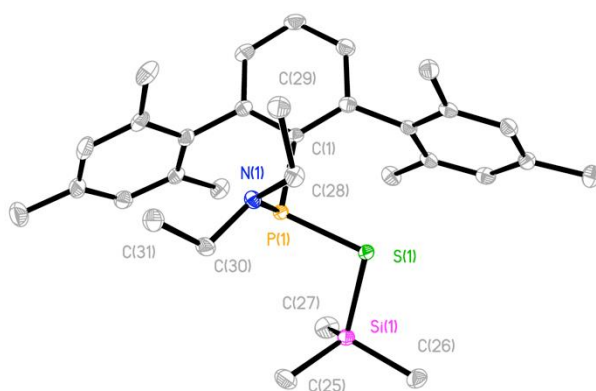
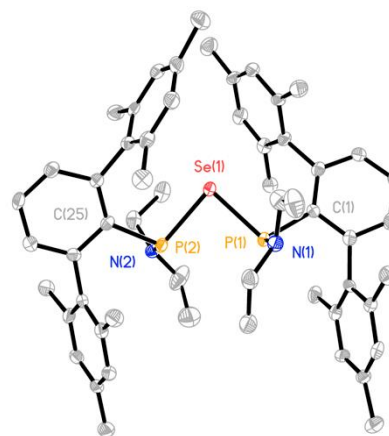
**2.2****2.3****2.4****2.6****2.7****2.8**

Figure 2-6. Solid-state structures for compounds confirmed by X-ray crystallography. Thermal ellipsoids are drawn at the 50% probability level. H atoms are omitted for clarity unless directly bound to phosphorus. Pertinent bond lengths [\AA] and angles [$^\circ$] are as follows: **2.2**: P(1)-C(1) 1.861(3), P(1)-N(1) 1.693(3), P(1)-Cl(1) 2.2165(11), N(1)-P(1)-C(1) 101.67(3), N(1)-P(1)-Cl(1) 103.16(12). **2.3**: P(1)-C(1) 1.854(3), P(1)-H(1) 1.29(3), P(1)-N(1) 1.684(3), N(1)-P(1)-C(1)

106.46(14), N(1)-P(1)-H(1) 100.7(14). **2.4**: P(1)-C(1) 1.845(2), P(1)-H(1) 1.38(3), P(1)-Si(1) 2.2696(14), C(1)-P(1)-H(1) 96.5(12), Si(1)-P(1)-H(1) 94.2(12). **2.6**: P(1)-C(1) 1.8409(17), P(1)-H(1) 1.35(3), P(1)-P(1)¹ 2.2392(12), P(1)-P(1)¹-H(1) 91.4(11), C(1)-P(1)-H(1) 97.5(11) °. **2.7**: P(1)-S(1) 2.1412(8), P(1)-C(1) 1.865(2), S(1)-Si(1) 2.1456(10), P-N_{avg} 1.6949(18), P(1)-S(1)-Si(1) 99.18(3), C(1)-P(1)-S(1) 105.75(6). **2.8**: P-Se_{avg} 2.3073(14), P(1)-C(1) 1.862(5), P-N_{avg} 1.669(4), P(1)-Se(1)-P(2) 88.17(5), C(1)-P(1)-Se(1) 105.27(16).

Single crystals of compound **2.2** were obtained at -35 °C from a concentrated solution of pentane overnight (Figure 2-6). Normal P-N, P-Cl and P-C bond lengths were observed.³⁶ Crystals of **2.3** suitable for X-ray crystallography were grown by placing a concentrated solution of **2.3** in pentane at -35 °C for two days, and confirmed the proposed structure (Figure 2-6). A shorter P-N bond length was observed (P-N = 1.684(3) Å) in comparison to compounds **2.2**. This was a manifestation of the fact that Cl and N have lone pairs of electrons that are capable of donating electron density to the phosphorus center. For compound **2.2**, competition exists between the N and Cl atoms for donation into the phosphorus centre. Compound **2.3** does not have this competition because the H atom does not possess lone pairs and resulted in the contraction of the P-N bond. In fact, the P-N bond in compound **2.3** is approaching multiple bond character in comparison to P=N double bond containing compounds (P=N ~ 1.6 Å).³⁷ Normal P-H (1.29(3) Å) and P-C (1.854(3) Å) bond lengths were also observed.³⁶ For compound **2.4**, crystals suitable for X-ray crystallography were obtained from a concentrated solution of pentane left at -35 °C overnight (Figure 2-6). Normal P-H (1.38(3) Å) and P-C (1.845(2) Å) bonds are observed for **2.4**.³⁶ The P-Si bond length is 2.2696(14) Å, which was in alignment with other known P-Si single bonds.³⁸ Comparing the P-C bond lengths across compounds **2.2-2.4**, there was a significant decrease in bond length as the electron donating properties of the substituents on phosphorus increases. This was because of the same effect discussed for the contraction of the P-N bond, where the P-C bond in **2.4** is shortest because the Si atom has no lone pairs of electrons and **2.2** has the longest P-C bond as a result of both N and Cl atom lone pair donation into the phosphorus center.

Crystals of **2.6** suitable for X-ray diffraction were grown from a mixture of *rac* and *meso* isomers by placing a concentrated crude reaction mixture of **2.6** in pentane at -35 °C overnight. Compound **2.6** possessed a center of inversion in the center of the P-P bond, as expected for the *meso* isomer. The P-P bond had a length of 2.2392(12) Å, which fell

within the expected range for P-P single bonds.³⁶ The P-C (1.8409(17) Å) and P-H (1.35(3) Å) bonds also fall within the normal range. The solid state structure illustrated how the TerPh ligands formed a cage around the P-P bond with a pocket for further reactivity to potentially take place. The P-H bonds in **2.6** were longer than that seen for **2.3**, but were slightly shorter than the P-H bond in **2.4**. A bond angle of 91.4(11)° was measured for the P-P-H bond angle in **2.6**, with a smaller C-P-H bond angle (97.5(11)°) than seen for **2.2-2.4** for the analogous bond angle, likely caused by the imposed steric bulk of two terphenyl ligands.

In the case of compound **2.7**, a P-S single bond of 2.1412(8) Å and a P-S-Si bond angle of 99.18(3)° were measured and corresponded well with the only other known P-S-Si linkage in literature.³⁹ Typical P-C and P-N bond lengths (~1.84 Å and ~1.65 Å, respectively) were observed for **2.7**, although longer than those seen for compounds **2.2-2.4**. X-ray crystallographic analysis of compound **2.8** indicated a tight P-Se-P bond angle of 88.17(5)°, while P-Se bond lengths ($\text{P-Se}_{\text{avg}} = 2.3073(14)$ Å) were in typical range for P-Se single bonds and are similar to values reported by Weigand and colleagues for tetramesityldiphosphanylselane derivatives.⁴⁰

2.3 Conclusion

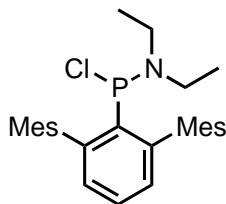
The synthesis and characterization of asymmetric phosphines, diphosphane and phosphanylchalcogenanes bearing a *m*-terphenyl functional group have been described. Dichloroterphenylphosphine (**2.1**) was the precursor for three new phosphines with 2 unique substituents, which were isolated and characterized in good yield. Reactivity was biased towards one substituent on the phosphorus center and a number of homocoupling reactions were attempted with compounds **2.2-2.4**. The reactions targeted dehydrohalogenative coupling and salt metathesis as a means to generate a P-P single bond stoichiometrically; however, no conclusive reactivity was observed between any of the prepared asymmetric phosphines. Terphenyldiphosphane, **2.6**, was prepared and completely structurally characterized. The kinetic stability provided by the steric bulk of the *m*-terphenyl ligands may allow for novel reactivity to be observed. Unfortunately, no reproducible results were obtained from reactions with **2.6** and S₂Cl₂. Overall, the development of asymmetric phosphorus compounds such as the ones reported are

promising candidates in catalysis as mono- or multi-dentate ligands for transition metals, and also the development of unique small molecules.

2.4 Experimental Section

For general experimental and crystallographic details, please see Chapter 5.

2.4.1 Synthesis of **2.2**



Two equivalents of diethylamine (1.59 mL, 15.4 mmol) were added dropwise to a solution of **2.1** (3.20 g, 7.70 mmol) in 180 mL of ether at room temperature. The slurry was filtered through a glass frit after stirring for 2 hours and then solvent was removed *in vacuo*. The crude white powder was redissolved in pentane and allowed to crystallize at -30 °C overnight, yielding crystals suitable for X-ray crystallography. Yield was increased by performing consecutive crystallizations by concentrating the pentane soluble portion *in vacuo*. Yield 5.65 g (81%).

³¹P NMR (Benzene-*d*₆, 161.8 MHz) δ: 139.0 (s).

¹H NMR (Benzene-*d*₆, 400 MHz) δ: 0.84 (t, ³*J*_{HH} = 7.2 Hz, 6H, NCH₂CH₃), 1.98 (s, 6H, Mes CH₃), 2.12 (s, 6H, Mes CH₃), 2.32 (s, 6H, Mes CH₃), 2.66 (dq, ³*J*_{HP} = 15.1 Hz, ³*J*_{HH} = 7.6 Hz, 2H, NCH₂CH₃), 2.85 (dq, ³*J*_{HH} = 7.2 Hz, ³*J*_{HP} = 14.4 Hz, 2H, NCH₂CH₃), 6.86-6.90 (s, 4H, Mes CH), 7.00 (dd, ³*J*_{HH} = 7.2 Hz, ⁴*J*_{HP} = 2.8 Hz, 2H, Ph CH), 7.44 (t, ³*J*_{HH} = 7.2 Hz, 1H, Ph CH).

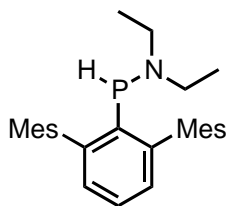
¹³C{¹H} NMR (CDCl₃, 150.8 MHz) δ: 13.6 (d, ³*J*_{CP} = 7.4 Hz), 21.1 (s), 21.2 (s), 21.6 (s), 44.5 (d, ²*J*_{CP} = 14.9 Hz), 128.0 (d, ¹*J*_{CP} = 20.7 Hz), 130.0 (s), 130.9 (s), 135.4 (d, ³*J*_{CP} = 2 Hz), 136.0 (s), 136.4 (s), 136.7 (s), 137.2 (s), 138.2 (d, ²*J*_{CP} = 4.5 Hz).

EA: calculated: 74.40 % C, 7.80 % H, 3.10 % N; found: 73.18 % C, 8.63 % H, 2.84 % N.

ESI-MS: 452.2 *m/z* C₂₈H₃₅PNCI [M]⁺

mp: 126 – 130 °C.

2.4.2 Synthesis of **2.3**



A solution of **2.2** (1.80 g, 3.98 mmol) in 15 mL of THF was added to a suspension of LiAlH_4 (0.151 g, 3.98 mmol) at 0 °C. The reaction was allowed to stir overnight and warm to room temperature. Unreacted LiAlH_4 was quenched with 3 mL degassed water at 0 °C.

The supernatant was decanted and filtered through a frit with a 1:1 ratio of celite and MgSO_4 and washed twice with 10 mL THF. Solvent was then removed *in vacuo*. Crystals suitable for X-ray crystallography were obtained from a concentrated pentane solution kept at -30 °C for two nights. Yield 1.1 g (65%).

^{31}P NMR (Benzene- d_6 , 161.8 MHz) δ : 1.86 (d, $^1J_{\text{PH}} = 236.8$ Hz).

^1H NMR (CDCl_3 , 400 MHz) δ : 0.69 (t, $^3J_{\text{HH}} = 4.8$ Hz, 6 H, NCH_2CH_3), 2.00 (s, 6H, Mes CH_3), 2.15 (s, 6H, Mes CH_3), 2.22 (dq, $^3J_{\text{HH}} = 4.8$ Hz, $^2J_{\text{HH}} = 9.2$ Hz, 2H, NCH_2CH_3), 2.35 (s, 6H, Mes CH_3), 2.46 (dq, $^3J_{\text{HH}} = 4.8$ Hz, $^2J_{\text{HH}} = 9.2$ Hz, 2H, NCH_2CH_3), 5.46 (d, $^1J_{\text{PH}} = 237.0$ Hz), 6.94 (s, 2H, Mes CH), 6.98 (s, 2H, Mes CH), 7.04-7.06 (dd, $^4J_{\text{PH}} = 1.2$ Hz, $^3J_{\text{HH}} = 5.2$ Hz, 2H, Ph CH), 7.38 (t, $^3J_{\text{HH}} = 5.2$ Hz, 1H, Ph *para*-CH).

$^{13}\text{C}\{^1\text{H}\}$ NMR (CDCl_3 , 150.8 MHz) δ : 14.5 (d, $^3J_{\text{CP}} = 6.0$ Hz), 20.7 (s), 20.8 (s), 20.9 (d, $^3J_{\text{CP}} = 4.4$ Hz), 21.1 (s), 48.4 (d, $^2J_{\text{CP}} = 20.2$ Hz), 127.9 (s), 128.3 (s), 128.8 (s), 134.8 (s), 136.3 (s), 137.0 (s), 137.5 (d, $^1J_{\text{CP}} = 26$ Hz), 139.1 (d, $^3J_{\text{CP}} = 2.4$ Hz), 145.1 (d, $^2J_{\text{CP}} = 18.2$ Hz).

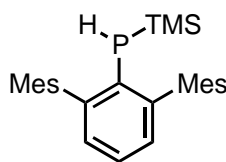
EA: calculated: 80.54 % C, 8.69 % H, 3.35 % N; found: 80.51 % C, 8.52 % H, 3.35 % N.

ESI-MS: 402.22 m/z [$\text{C}_{27}\text{H}_{33}\text{PN}$] $^+$ M- CH_3 .

ATR-IR (ranked intensity, cm^{-1}): 651 (11), 744.25 (3), 784.25 (8), 806.75 (7), 848 (4), 849 (2), 923.5 (9), 982 (6), 1035.25 (5), 1192.75 (1), 1447.25 (10), 2288.25 (12), 2958.5 (13), 2912.25 (14), 2851 (15).

mp: 118 – 120 °C

2.4.3 Synthesis of **2.4**



To a solution of terphenylphosphine (1.00 g, 2.89 mmol), 5 stoichiometric equivalents of *n*-BuLi (9.00 mL, 1.45 mmol) was added at 0 °C in 7 mL of ether. The resulting vibrant pink solution was allowed to come to room temperature (4 h) before solvent was

removed *in vacuo*. The orange-pink powder was washed twice with 3 mL of hexanes in the glovebox and any residual hexanes was removed *in vacuo*. The powder was redissolved in 5 mL ether and neat TMSCl was added dropwise until the bright pink solution changed to pale yellow (< 1 mL). At this point, all solvents were removed *in vacuo* and the white powder was washed with hexanes (3 x 3 mL). Crystals suitable for X-ray diffraction were grown by placing a concentrated solution of **2.4** in pentane at -30 °C for two days. Yield 190 mg (16 %).

³¹P NMR (Benzene-*d*₆, 161.8 MHz) δ: -136.4 (d, ¹J_{PH} = 220.0 Hz).

¹H NMR (Benzene-*d*₆, 400 MHz) δ: -0.20 (d, ³J_{HP} = 4.8 Hz, 9H, SiCH₃), 2.07-2.30 (s, 18H, Mes CH₃), 3.18 (d, ¹J_{HP} = 220.0 Hz, 1H, PH), 6.88-6.94 (6H, 4 Mes CH, 2 Ph CH), 7.08 (t, ³J_{HH} = 7.6 Hz).

¹³C{¹H} NMR (Benzene-*d*₆, 150.8 MHz) δ: 144.9 (d, ²J_{CP} = 15.5 Hz), 139.7 (d, ³J_{CP} = 3.8 Hz), 136.7 (s), 136.2 (s), 135.6 (s), 134.4 (s), 134.2 (s), 128.8 (s), 128.7 (s), 128.5 (s), 128.3 (s), 126.4 (s), 21.0 (d, ²J_{CP} = 22.4 Hz), 1.1 (d, ²J_{CP} = 17.6 Hz).

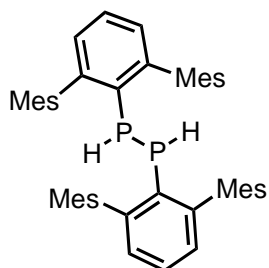
EA: calculated: 77.47 % C, 8.43 % H, 0.00 % N; found: 78.17 % C, 8.54 % H, 0.05 % N.

ESI-MS: 331.09 *m/z* [M-Si(CH₃)₃-CH₃+H]. M = C₂₇H₃₅PSi

ATR-IR (ranked intensity, cm⁻¹): 731.25 (3), 799 (2), 835.3 (13), 850 (1), 1068.75 (10), 1376 (6), 1098.25 (12), 1447.75 (4), 1612.75 (11), 2315 (7), 2850 (9), 2916.25 (5), 2957 (8).

m.p.: 89 – 91 °C.

2.4.4 Synthesis of **2.6**



A solution of **2.5** (250 mg, 0.363 mmol) in 10 mL THF was added to a suspension of LiAlH₄ (42.0 mg, 1.10 mmol) at 0 °C. Over the course of 4 h, the reaction was allowed to warm to room temperature. The bright red solution became colourless when quenched with excess degassed water. The supernatant was then removed and filtered through a frit with a 2:1 ratio of celite and MgSO₄, and finally washed twice with 5 mL THF. All solvents were removed *in vacuo* and the resulting crude material was purified by washing three times with 2 mL of

HMDSO. Crystals suitable for X-ray crystallography were obtained from a concentrated solution in ether at -30 °C for two nights. Yield 240 mg (95 %).

³¹P NMR (Benzene-*d*₆, 161.8 MHz) δ: -100.9 (dddd, ¹*J*_{PH} = 226.8 Hz, ¹*J*_{PH} = 215.1 Hz, ³*J*_{PH} = 22.2 Hz, ³*J*_{PH} = 29.0 Hz), -110.2 (m).

¹H NMR (Benzene-*d*₆, 400 MHz) δ: 1.83-2.23 (s, 18 H, Mes CH₃), 2.65-3.22 (m, 2H, P-H), 6.67-6.69 (s, 2H, Ph CH), 6.74-6.76 (s, 4H, Mes CH), 6.91 (t, ³*J*_{HH} = 8.0 Hz).

¹³C NMR (CDCl₃, 150.8 MHz) δ: 20.7 (d, ²*J*_{CP} = 14.6 Hz), 20.8 (d, ³*J*_{CP} = 7.2 Hz), 21.0 (s), 25.4 (s), 67.48 (s), 127.6 (s), 127.8 (s), 128.0 (s), 128.2 (s), 128.4 (d, ²*J*_{CP} = 18.4 Hz), 128.6 (s), 133.65 (dd, ¹*J*_{CP} = 15.4 Hz), 135.6 (s), 135.9 (s), 136.0 (s), 139.2 (s), 146.1 (dd, ²*J*_{CP} = 10.0 Hz).

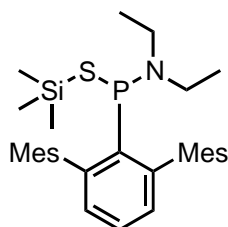
EA: calculated: 83.45 % C, 7.59 % H, 0.00 % N; found: 81.91 % C, 7.38 % H, 0.04 % N.

ESI-MS: 345.16 *m/z* [C₂₄H₂₆P]⁺.

FT-IR (ranked intensity, cm⁻¹): 742 (4), 802 (3), 849 (1), 1034 (6), 1180 (11), 1261 (13), 1373 (7), 1446 (2), 1564 (9), 1610 (5), 1724 (15), 1930 (16), 2328 (12), 2729 (14), 2852 (8), 2912 (3), 3033 (10).

mp: 122 – 123 °C.

2.4.5 Synthesis of **2.7**



S(TMS)₂ (0.112 mL, 0.531 mmol) was added to a solution of **2.2** (0.160 g, 0.354 mmol) in 2.5 mL toluene. The reaction was then heated to 100 °C for 48 h and all volatiles were removed *in vacuo*, giving rise to a yellow residue. The crude reaction mixture was purified by recrystallization in a solution of pentane and MeCN, yielding crystals suitable for X-ray crystallography. Yield 85 mg (47 %).

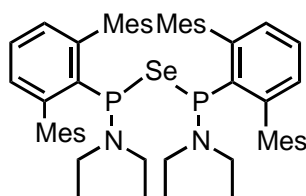
m.p. (nitrogen sealed capillary): 101-104 °C

³¹P NMR (Benzene-*d*₆, 161.8 MHz) δ: 83.0 (s)

¹H NMR (Benzene-*d*₆, 400 MHz) δ: 0.20 (s, 9H, SiCH₃), 0.85 (t, ³*J*_{HH} = 7.2 Hz, 6H, NCH₂CH₃), 2.20 (s, 6H, Mes CH₃), 2.25-2.26 (m, 12H, Mes CH₃), 2.53-2.59 (m, 2H, NCH₂CH₃), 2.76-2.83 (m, 2H, NCH₂CH₃), 6.86-6.89 (m, 6H, Mes CH), 7.11 (t, ³*J*_{HH} 7.2 Hz, 1H, Ph CH).

^{13}C NMR (CDCl_3 , 150.8 MHz) δ : 2.4 (d, $^1J_{\text{CSi}} = 7.1$ Hz), 21.2, 21.4 (d, $^2J_{\text{CP}} = 4.8$ Hz), 21.9 (d, $^3J_{\text{CP}} = 1.7$ Hz), 44.5 (d, $^1J_{\text{CP}} = 17.2$ Hz), 127.9 (s), 128.0 (s), 128.9 (s), 130.5 (s), 135.9 (s), 136.3 (s), 137.1 (s), 139.1 (s), 139.3 (s), 139.6 (d, $^2J_{\text{CP}} = 4.2$ Hz), 145.2 (d, $^1J_{\text{CP}} = 19.4$ Hz).

2.4.6 Synthesis of **2.8**



$\text{Se}(\text{TMS})_2$ (0.256 mL, 1.02 mmol) was added to a solution of **2.2** (0.519 g, 1.14 mmol) in 7 mL MeCN and allowed to reflux for 8 hours. The supernatant was removed *in vacuo* and the product was washed 3 times with MeCN to give yield an orange powder. X-ray quality crystals were obtained by dissolving the powder in a minimum amount of MeCN layered with pentane overnight at -35°C . Yield: 240 mg (46 %)

m.p. (nitrogen sealed capillary): $82\text{--}86^\circ\text{C}$

^{31}P NMR (Benzene- d_6 , 161.8 MHz, δ): 99.1 (s, $^1J_{\text{PSe}} = 546.8$ Hz)

^1H NMR (Benzene- d_6 , 400 MHz, δ): 0.86 (t, $^3J_{\text{HH}} = 7.2$ Hz, 12H, NCH_2CH_3), 2.10 (s, 12H, Mes CH_3), 2.18 (s, 12H, Mes CH_3), 2.23 (s, 12H, Mes CH_3), 2.50–2.58 (m, 4H, NCH_2CH_3), 2.72–2.80 (m, 4H, NCH_2CH_3), 6.79–6.82 (m, 12H, Mes CH), 7.04 (t, $^3J_{\text{HH}} = 7.6$ Hz, 2H, Ph CH)

^{13}C NMR (CDCl_3 , 150.8 MHz, δ): 13.7 (m), 21.2 (d, $^2J_{\text{CP}} = 2.4$ Hz), 21.3 (s), 22.0 (s), 45.7 (m), 128.1 (d, $^2J_{\text{CP}} = 5.9$ Hz), 128.5 (s), 130.5 (s), 135.7 (s), 135.9 (s), 137.3 (s), 139.8 (s), 145.5 (d, $^1J_{\text{CP}} = 17.0$ Hz).

2.4.7 Considerations for X-ray Crystallography

Table 2-1. Summary of X-ray diffraction collection and refinement details for the compounds reported in Chapter 2

	2.2	2.3	2.4	2.6	2.7	2.8
Formula	C ₂₈ H ₃₅ ClNP	C ₂₈ H ₃₆ NP	C ₂₇ H ₃₅ PSi	C ₄₈ H ₅₂ P ₂	C ₃₁ H ₄₄ NPSSi	C ₅₆ H ₇₀ N ₂ P ₂ Se
Formula weight (g mol⁻¹)	451.99	417.55	418.61	690.83	521.79	912.04
Crystal system	Monoclinic	Monoclinic	Monoclinic	Monoclinic	Monoclinic	Triclinic
Space group	P 2 ₁ /n	P2 ₁ /n	C 2/c	P 2 ₁ /n	P 2 ₁ /n	P -1
T (K)	110	110	110	110	110	110
a (Å)	8.7970(18)	8.156(5)	30.809(18)	8.377(3)	10.503(4)	11.475(2)
b (Å)	20.126(5)	24.494(16)	10.796(7)	21.380(8)	20.442(6)	12.731(2)
c (Å)	14.093(3)	12.123(7)	17.103(8)	11.642(5)	13.799(5)	18.611(3)
α (deg)	90	90	90	90	90	97.302(8)
β (deg)	90.189(6)	93.456(16)	120.930(12)	111.031(9)	92.241(15)	93.068(8)
γ (deg)	90	90	90	90	90	113.583(6)
V (Å³)	2469.7(10)	2418(2)	4880(5)	1942.6(13)	2960.4(17)	2455.3(7)
Z	4	4	8	2	4	2
F (000)	968	904	1808	740	1128	968
ρ (g cm⁻³)	1.216	1.147	1.140	1.181	1.171	1.234
λ (Å)	1.54178	0.71073	0.71073	0.71073	0.71073	1.54178
μ (cm⁻¹)	2.078	0.128	0.173	0.145	0.224	1.929
Measured fraction of data	0.994	0.999	0.998	0.999	0.999	0.991
R_{merge}	0.0369	0.0909	0.0555	0.0538	0.0512	0.0393
R_I, wR₂	0.0577, 0.1525	0.0684, 0.1677	0.0554, 0.1498	0.0584, 0.1669	0.0477, 0.1294	0.0576, 0.1440
R_I, wR₂ (all data)	0.610, 0.1555	0.1150, 0.1914	0.0759, 0.1640	0.0869, 0.1861	0.0624, 0.1392	0.0729, 0.1750
GOF	1.019	1.038	1.037	1.057	1.037	1.100

2.5 References

- (1) Allen, D. W. *Organophosphorus Chem.* **2015**, *44*, 1–55.
- (2) Benaglia, M.; Rossi, S. *Org. Biomol. Chem.* **2010**, *8*, 3824–3830.
- (3) Bohm, V. P. W.; Brookhart, M. *Angew. Chem. - Int. Ed.* **2001**, *40*, 4694–4696.
- (4) Dilworth, J. R.; Wheatley, N. *Coord. Chem. Rev.* **2000**, *199*, 89–158.
- (5) Evans, D. A.; Michael, F. E.; Tedrow, J. S.; Campos, K. R. *J. Am. Chem. Soc.* **2003**, *125*, 3534–3543.
- (6) Feng, J. J.; Chen, X. F.; Shi, M.; Duan, W. L. *J. Am. Chem. Soc.* **2010**, *132*, 5562–5563.
- (7) Kagan, H. B.; Sasaki, M. The chemistry of organophosphorus compounds. Wiley, **1990**.
- (8) King, R. B.; Sundaram, P. M. *J. Org. Chem.* **1984**, *49*, 1784–1789.
- (9) Roth, T.; Wadepohl, H.; Wright, D. S.; Gade, L. H. *Angew. Chem. - Int. Ed.* **2013**, 13823–13837.
- (10) Tang, W.; Zhang, X. *Chem. Rev.* **2003**, *103*, 3029–3070.
- (11) Wauters, I.; Debrouwer, W.; Stevens, C. V. *J. Org. Chem.* **2014**, *10*, 1064–1096.
- (12) Kolodyazhnyi, O. I.; Andrushko, N. V.; Grishkun, E. V. *Russ. J. Gen. Chem.* **2004**, *74*, 515–522.
- (13) Power, P. P. *J. Organomet. Chem.* **2004**, *689*, 3904–3919.
- (14) Kolodiazhnyi, O. I. *Tetrahedron Asymm.* **2012**, *23*, 1–46.
- (15) Bayardon, J.; Jugé, S. *Phosphorus(III) Ligands Homog. Catal. Des. Synth.* **2012**, *10*, 355–389.
- (16) Dutartre, M.; Bayardon, J.; Jugé, S. *Chem. Soc. Rev.* **2016**, *45*, 5771–5794.
- (17) Anagnostis, J.; Turnbull, M. M. *Polyhedron.* **2004**, *23*, 125–133.
- (18) Allefeld, N.; Grasse, M.; Ignat'ev, N.; Hoge, B. *Chem. Eur. J.* **2014**, *20*, 8615–8620.
- (19) Appel, R.; Geisler, K. *J. Organomet. Chem.* **1976**, *112*, 61–64.
- (20) Boéré, R. T.; Masuda, J. D. *Can. J. Chem.* **2002**, *80*, 1607–1617.
- (21) Buhling, A.; Kamer, P. C. J.; van Leeuwen, P. W. N. M.; Elgersma, J. W.;

- Goubitz, K.; Fraanje, J. *Organometallics*. **1997**, *16*, 3027–3037.
- (22) Buster, B.; Diaz, A. A.; Graham, T.; Khan, R.; Khan, M. A.; Powell, D. R.; Wehmschulte, R. J. *Inorganica Chim. Acta* **2009**, *362*, 3465–3474.
- (23) Clyburne, J. A. C.; McMullen, N. *Coord. Chem. Rev.* **2000**, *210*, 73–99.
- (24) Rivard, E.; Power, P. P. *Inorg. Chem.* **2007**, *46*, 10047–10064.
- (25) Urnezis, J. Protasiewicz, E. *Main Gr. Chem.* **1999**, *4*, 9–11.
- (26) Sasamori, T.; Takeda, N.; Tokitoh, N. *J. Phys. Org. Chem.* **2003**, *16*, 450–462.
- (27) Yoshifuji, M.; Shibayama, K.; Inamoto, N.; Matsushita, T.; Nishimoto, K. *J. Am. Chem. Soc.* **1983**, *105*, 2495–2497.
- (28) Yoshifuji, M.; Shima, I.; Inamoto, N.; Hirotsu, K.; Higuchi, T. *J. Am. Chem. Soc.* **1981**, *103*, 4587–4589.
- (29) Graham, C. M. E.; Pritchard, T. E.; Boyle, P. D.; Valjus, J.; Tuononen, H. M.; Ragona, P. J. *Angew. Chem. - Int. Ed.* **2017**, *129*, 6332–6336.
- (30) Graham, C. M. E.; Valjus, J.; Pritchard, T. E.; Boyle, P. D.; Tuononen, H. M.; Ragona, P. J. *Inorg. Chem.* **2017**, *15*, 13500–13510.
- (31) Lee, P. T. K.; McClintock, J.; Robertson, K. N.; Clyburne, J. A. C. *Main Gr. Chem.* **2011**, *10*, 187–204.
- (32) Nieger, M.; Niecke, E.; Overl, C.; Tirr, J.; Moser, C.; Spirk, S.; Pietschnig, R. **2007**, *3*, 46–48.
- (33) Protasiewicz, J. D.; Washington, M. P.; Gudimetla, V. B.; Payton, J. L.; Cather Simpson, M. *Inorg. Chim. Acta* **2010**, *364*, 39–45.
- (34) Smith, R. C.; Shah, S.; Protasiewicz, J. D. *J. Organomet. Chem.* **2002**, *646*, 255–261.
- (35) Blair, S.; Izod, K.; Taylor, R.; Clegg, W. *J. Organomet. Chem.* **2002**, *656*, 43–48.
- (36) Pyykkö, P.; Atsumi, M. *Chem. Eur. J.* **2009**, *15*, 186–197.
- (37) Pyykkö, P.; Atsumi, M. *Chem. Eur. J.* **2009**, *15*, 12770–12779.
- (38) Geib, D.; Arz, M. I.; Straumann, M.; Schnakenburg, G.; Filippou, A. C. *Angew. Chem. - Int. Ed.* **2015**, *54*, 2739–2744.
- (39) Sen, S. S.; Khan, S.; Roesky, H. W.; Kratzert, D.; Meindl, K.; Henn, J.; Stalke, D.; Demers, J. P.; Lange, A. *Angew. Chem. - Int. Ed.* **2011**, *50*, 2322–2325.
- (40) Yogendra, S.; Chitnis, S. S.; Hennesdorf, F.; Bodensteiner, M.; Fischer, R.;

Burford, N.; Weigand, J. J. *Inorg. Chem.* **2016**, *55*, 1854–1860.

Chapter 3

3 Probing the Reactivity of $RP=S$ *via* Thermolysis & Condensation Pathways

3.1 Introduction

There has been a long-standing interest among synthetic chemists in the synthesis and characterization of novel, unique heterocycles which incorporate heavier main group elements.^{1,2} This has led to a wealth of new compounds that have pushed the boundaries of known structural and bonding motifs in the main group. In particular, the synthetic and theoretical investigation of low-coordinate species, and their subsequent reactivity with unsaturated organic compounds, has become a remarkable and rapidly expanding field of main group chemistry over the last number of decades.^{3–11}

In contrast to the well established chemistry of carbenes, much less is known about the chemistry of the phosphorus analogue – phosphinidenes ($R-P:$). Phosphinidenes have two lone pairs of electrons which can adopt one of two ground spin states – singlet or triplet. Analogous to singlet carbenes, singlet phosphinidenes react *via* a concerted reaction mechanism, and thus, result in cleaner reactivity in comparison to their triplet counterparts, which participate *via* step-wise radical additions. Free phosphinidenes ($R-P:$) themselves are highly reactive and have only been isolated recently by Bertrand.¹⁴ A “free” phosphinidene refers to the existence of $RP:$, either transient or stable, without additional stabilizing groups. The more synthetically viable singlet ground state has been favoured in compounds which possess an adjacent donor atom (*ie.* N, P, S)^{3,9,10,12–17}, coordinating Lewis acid (*ie.* $W(CO)_5$)^{5–8,18–22} and/or a phosphanorbornadiene precursor^{4,15,23,24} (Figure 3-1, a). A number of new heterocycles were previously prepared through the cycloaddition chemistry of phosphinidene moieties generated *in situ* with unsaturated organic substrates – such as alkenes, dienes, and acetylenes. This strategy, along with the use of very bulky aryl ligands (*ie.* TerPh), has led to new classes of phosphorus containing heterocycles.

Reactivity from these two-coordinate phosphorus species has stemmed from one of two reactivity pathways – carbenic or olefinic. Carbenic reactivity is observed when

the reactivity originates from a HOMO on the phosphorus atom, generally yielding [1+4] and [1+2] cycloaddition products

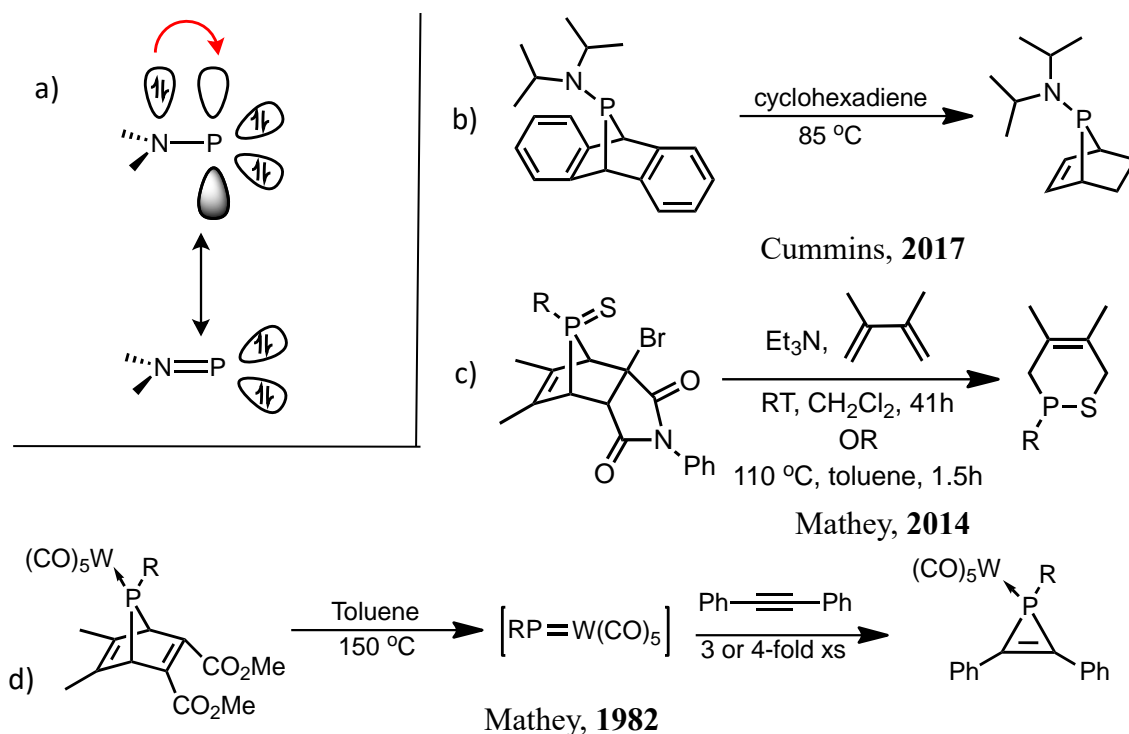


Figure 3-1. Various known strategies for phosphinidene transfer. a) Visual representation of donor atom effect when adjacent to a phosphinidene center. b) $\text{RP}=\text{N}$ transfer from norbornene scaffold, where $\text{RP}=\text{N}$ exhibits carbenic reactivity. c) $\text{RP}=\text{S}$ transfer from 7-phosphanorbornadiene, where $\text{RP}=\text{S}$ exhibits olefinic reactivity. d) $(\text{CO})_5\text{W}-\text{PR}$ transfer from norbornadiene, where $(\text{CO})_5\text{W}-\text{PR}$ exhibits carbenic reactivity.

upon exposure to dmbd or acetylenes.^{3,18,25,26} These have an exocyclic double bond from phosphorus to a second heteroatom, or the phosphorus is coordinated to a metal carbonyl. Olefinic type reactivity stems from the $\text{R}-\text{P}=\text{E}$ double bond, where both heteroatoms contribute to the HOMO ($\text{R} = \text{aryl, alkyl}$; $\text{E} = \text{NR, S, P, W}(\text{CO})_5$). These heterocyclic products tend to contain an even number of atoms. The majority of previously reported heterocycles have been prepared from the reaction of the two-coordinate $\text{RP}=\text{E}$ intermediate with C-C multiple bonds, only olefinic or carbenic behaviour is observed to result in the formation of just one cycloadduct.^{5,24,27–35} These methods rely on the thermolysis or base-induced degradation of a norbornadiene scaffold to produce the R-

P=E intermediate, which was determined to undergo a rapid cycloaddition with the trapping agent (Figure 3-1, b-d).^{3,18,26} While these methods have allowed for the cycloaddition to take place to result in the formation of novel heterocycles, the conditions often require heating at temperatures above 80 °C and extra purification steps to remove the rearomatized scaffold.

The Ragogna group has focused on developing an understanding of phosphinidene chalcogenide chemistry through the synthesis of strained heterocycles which exhibit novel bonding motifs. The added steric bulk provided by the TerPh ligand allowed for the identification of the P(III) derivative of a [2+4] cycloadduct with dmbd (**A**), previously only known for P(V)²⁷ or P-W(CO)₅^{36,37} adducts (Figure 3-2). Structural characterization of **A** required quaternization with MeI.³⁸ The steric bulk of the TerPh ligand also played a key role in the isolation of a rare NHC-stabilized phosphinidene sulfide (Figure 3-2, **B**),³⁹ although the isolation of a free phosphinidene sulfide remains an unsolved challenge. Compound **3.2** has served as an excellent precursor for investigating phosphinidene sulfide reactivity, relying only on heat to access monomeric R-P=S. When generated *in situ*, R-P=S undergoes relatively clean reactions with both

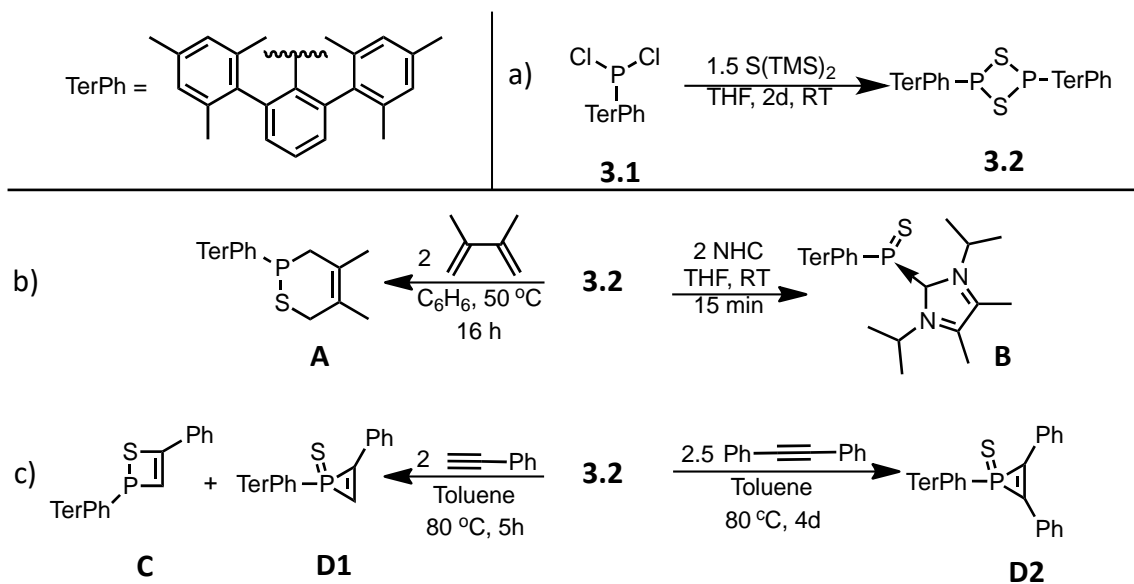


Figure 3-2. Recent developments in the Ragogna Group surrounding P,S-heterocycles and phosphinidene sulfide transfer. a) Synthesis of **3.2** by the condensation of **3.1** with S(TMS)₂. b) [2+4] adduct **A** prepared by thermolysis of **3.2** in dmbd. Upon the addition of NHC to **3.2**, base-stabilized phosphinidene sulfide **B** was isolated. c) Thermolysis of **3.2** in the presence of substituted acetylenes resulted in the formation of novel thiaphosphetene (**C**) and phosphirene sulfides (**D1**, **D2**).

terminal and internal alkynes (Figure 3-2, c). Computational work has shown this reaction likely passed through a phosphonium intermediate *via* stepwise elimination of TMSCl, although free $\text{RP}=\text{S}$ was energetically accessible under the same conditions. These two methods have lead to novel phosphirene sulfides (**D1**, **D2**) and a thiaphosphetene (**C**), which boasts a P(III) center, a structural motif absent in the literature.³⁶

Small inorganic ring systems containing a blend of main group elements and carbon have also remained key synthetic targets because, aside from addressing fundamental questions about structure and bonding, they play key roles as reaction intermediates and provide a means to solidify our understanding of important chemical transformations, particularly in organic synthesis. The most notable example of this is likely the 1,2-oxaphosphetane intermediate observed in the Wittig olefination of carbonyls (Figure 3-3).⁴⁰ Oxaphosphetanes have been studied since their isolation as pentavalent phosphorus species (**F**)^{41–43} or as P(III) compounds decorated with transition metals (**E**).^{31,44,45} Phosphetane rings containing heavier chalcogen atoms are scarce, likely due to the difficulty in controlling their transfer; however, examples of thiaphosphetanes containing P(V) centers (**G–H**) do exist in the literature.^{24,46–48} Prior to the synthesis of **C**, thiaphosphetenes were unknown except for a single report of a ring system containing a P(V) center stabilized by the Martin ligand (**I**).⁴⁹

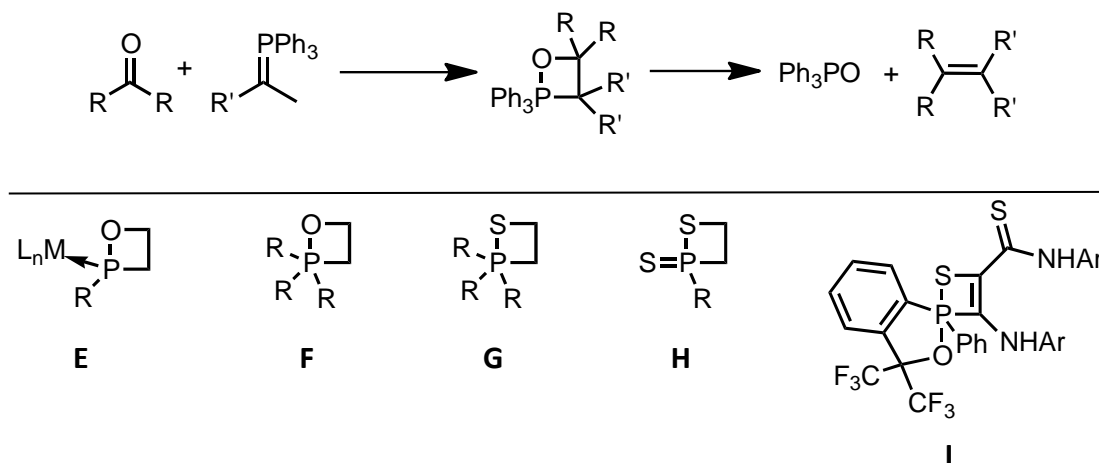


Figure 3-3. Top: Wittig olefination of carbonyls proceeding through an oxaphosphetane intermediate. Bottom: Metal-stabilized oxaphosphetane (**E**), P(V) oxaphosphetane (**F**), P(V) thiaphosphetane (**G**, **H**), and a thiaphosphetene stabilized by the Martin ligand (**I**)

This chapter highlights the preparation of a number of new cycloadducts – namely thiaphosphetenes, phosphirene sulfides and [4+2] cycloadducts – from R-P=S fragments that were generated *in situ* by one of two methods, without the harsh conditions or supportive bulky ligands as required previously. The thermolysis method relied on the gentle heating of **3.2** in the presence of excess alkyne, resulting in the formation of novel thiaphosphetenes and phosphirene sulfides. The condensation method involves the condensation reaction of dichlorophosphines and S(TMS)₂ in the presence of a large excess of trapping agent. The cycloaddition of R-P=S with the trapping agent occurred *via* a free R-P=S unit (i) or through a phosphonium intermediate (ii, Figure 3-4). Previous experiments utilizing the condensation methodology lead to a decreased number of products identified in the crude ³¹P{¹H} NMR spectra. Only the phosphirene sulfide derivatives were formed when the reaction was conducted in phenylacetylene which suggested that the phosphonium pathway was likely operative, and any R-P=S generated exhibited carbenic reactivity at phosphorus.³⁶

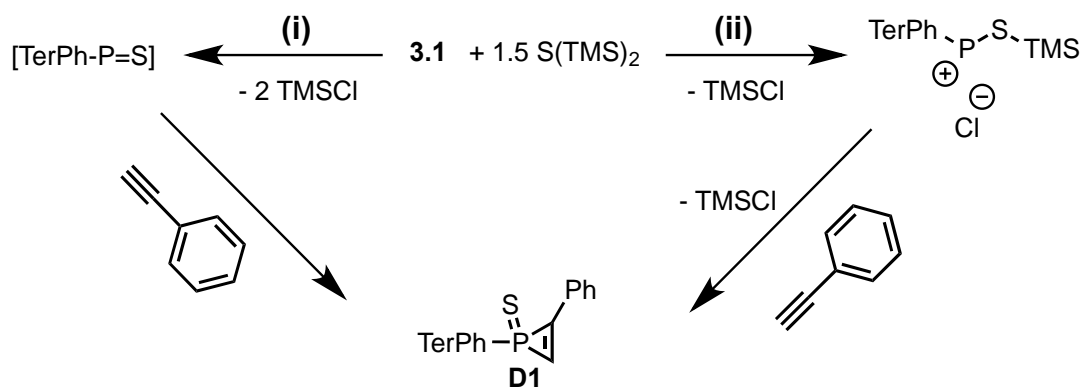


Figure 3-4. Mechanism of RP=S transfer by the condensation method. i) Elimination of 2 TMSCl to yield free RP=S as the reactive intermediate. ii) Stepwise elimination of TMSCl, where cyclization occurs from the phosphonium intermediate.

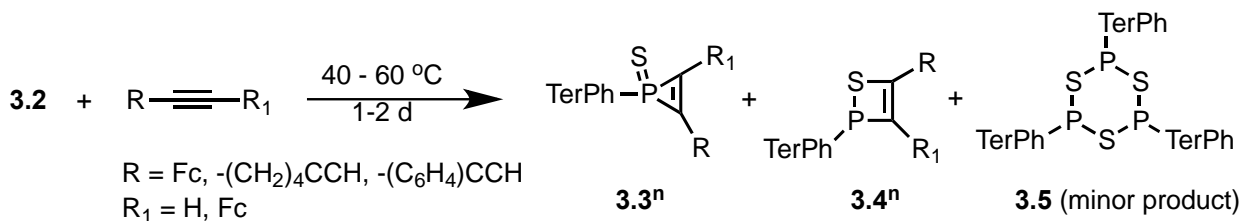
After demonstrating the success of the condensation method in our previous report, it was proposed that *in situ* generation of phosphinidene sulfide may not require the steric bulk offered by the TerPh ligand. To successfully prepare compound **3.2** – the starting material required for the thermolysis method – the steric bulk of TerPh ligands was necessary; however, if R-P=S could be generated without the need for bulky aryl ligands

it would immensely widen the scope of cycloaddition reactions that could be successfully performed. This chapter includes details that indicate phosphinidene sulfides can be generated from dichlorophosphines which do not possess steric bulk to generate [1+4] and [2+4] cycloadducts in neat or very concentrated dmbd solutions at room temperature.

3.2 Results & Discussion

3.2.1 Cycloaddition by Thermolysis – Novel Phosphirene Sulfides & Thiaphosphetenes

To develop an understanding of $RP=S$ transfer to alkynes by the thermolysis method, a reactivity study was performed with a number of mono- and di-substituted alkynes. Experiments were generally carried out as follows: a vial was charged with **3.2** and a five-fold stoichiometric excess of alkyne before dissolution in toluene. The resulting solution was transferred to a glass tube, at which point 1.2 stoichiometric equivalents of $S(TMS)_2$ was added, the tube was sealed and heated at 50 °C until no spectroscopic signal from **3.2** remained as indicated by $^{31}P\{^1H\}$ NMR spectroscopy (Scheme 3-1). An excess of $S(TMS)_2$ was required in order for the dichlorophosphine to be completely consumed during the reaction. This resulted in the formation of a number of phosphirene sulfides (**3.3ⁿ**) and thiaphosphetenes (**3.4ⁿ**), which were characterized structurally and spectroscopically.



Scheme 3-1. Thermolysis of **3.2** in the presence of substituted alkynes lead to the formation of novel phosphirene sulfides (**3.3ⁿ**) and thiaphosphetenes (**3.4ⁿ**). Ring expansion to compound **3.5** was observed as a minor product formed during the thermolysis reaction.

In the presence of neat mono- or bis-(trimethylsilyl)acetylene, the thermolysis of **3.2** did not result in conversion from the starting material over multiple days. This was an

indication that both terminal and internal alkynes which TMS functional groups were not amenable to [2+2] and [1+2] cycloadduct formation using this method. Other alkynes, such as bromoprop-3-yne and (trimethylsilyl)prop-3-yne, resulted in the appearance of a number of unidentified signals in the $^{31}\text{P}\{^1\text{H}\}$ NMR spectra which did not represent thiaphosphetenes or phosphirene sulfides based on their expected chemical shifts. When an electron-rich alkyne was used (*eg.* bis(ferrocenyl)acetylene) a new peak was present at -77.6 ppm in the $^{31}\text{P}\{^1\text{H}\}$ NMR spectrum. This was a similar chemical shift to those previously observed for phosphirene sulfides, and as such, **3.3**^{2Fc} has been the proposed structure (Figure 3-5). Compound **3.3**^{2Fc} was exceptionally sensitive and readily decomposed to compound **3.4**^{1Fc} and other ^{31}P -containing products in solution and the solid state. Crystallization was inhibited by the oily consistency of this product and difficulty associated with removing excess bis(ferrocenyl)acetylene in conjunction with decomposition issues. The steric strain imparted by two Fc ligands and the TerPh functional group likely contributed to the decomposition of the cycloadduct.

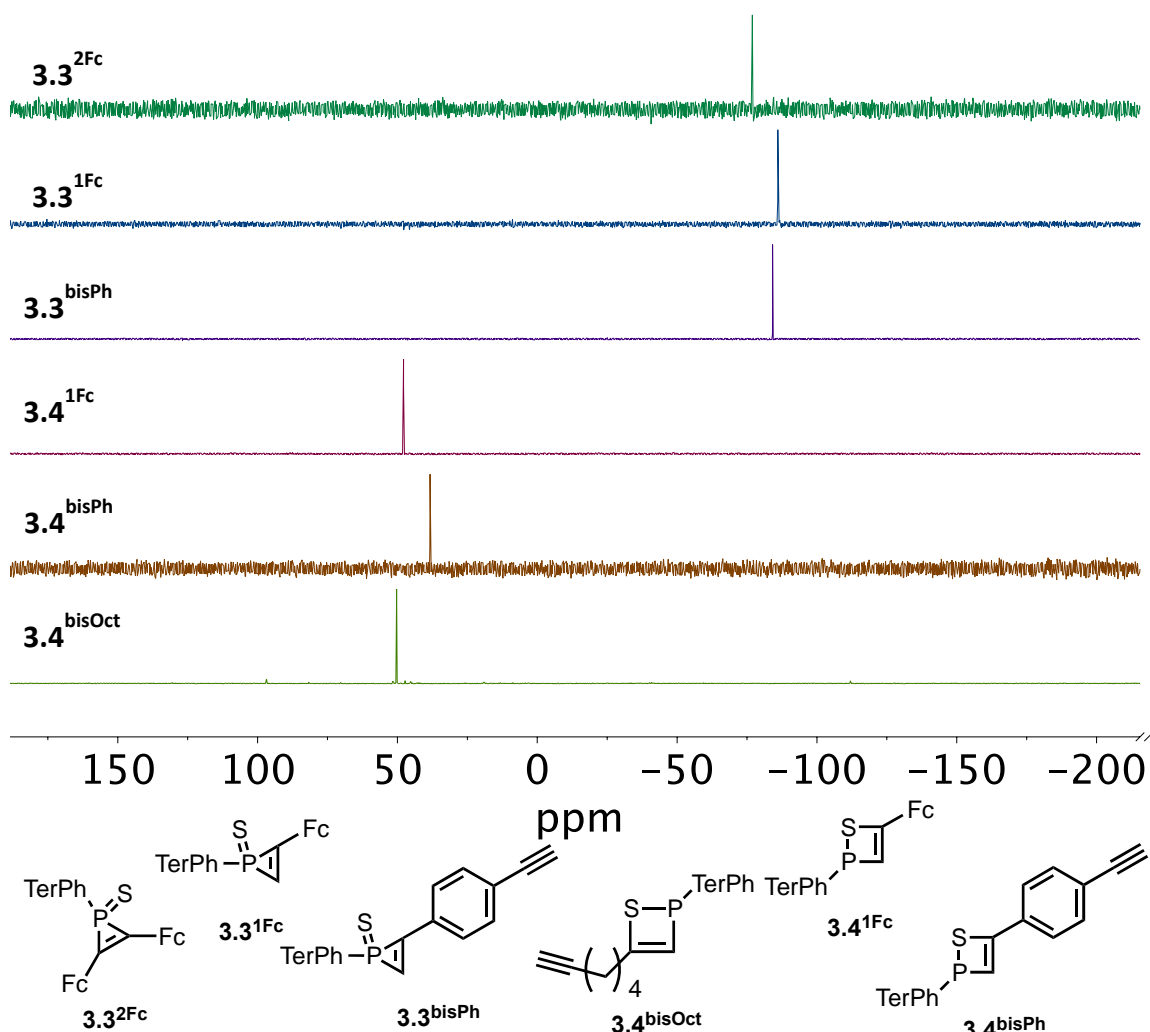


Figure 3-5. Stacked $^{31}\text{P}\{^1\text{H}\}$ NMR spectra of prepared phosphirene sulfides and thiaphosphetenes. Structures for each derivative are included for clarity.

When ethynylferrocene was used as a trapping agent, three new signals were observed in the $^{31}\text{P}\{^1\text{H}\}$ NMR spectrum ($\delta_{\text{P}} = 96.0, 47.8, -86.0$). The product at $\delta_{\text{P}} = 96$ was previously identified as the ring expansion product (**3.5**), consisting of a P_3S_3 core and flanking terphenyl ligands - formed by the insertion of one monomeric R-P=S unit into the P_2S_2 core of compound **3.2**.^{38,50} The formation of thiaphosphetene ($\delta_{\text{P}} = 47.8$, **3.4^{1Fc}**, Figure 3-5) was favoured when the alkyne was ethynylferrocene and the phosphirene sulfide ($\delta_{\text{P}} = -86.0$, **3.3^{1Fc}**) was formed as a minor product in a maximum

yield of 18 % (by integration). The reaction was concentration dependent, where at 5-15 mg/mL of **3.2** in toluene only **3.4^{IFc}** was observed by $^{31}\text{P}\{^1\text{H}\}$ NMR spectroscopy and at 20-30 mg/mL a mixture of **3.3^{IFc}**, **3.4^{IFc}**, and **3.5** was observed. Compound **3.4^{IFc}** was isolated as a bright orange, MeCN-insoluble powder which was as a doublet in the ^{31}P NMR spectrum ($^2J_{\text{PH}} = 21.7$ Hz; yield: 82 %). A corresponding doublet in the ^1H NMR spectrum was observed at 4.60 ppm with a coupling constant of 21.7 Hz. A single set of peaks was noted for *ortho*- and *para*- environments of the TerPh -CH₃ protons, evidence of a symmetrical structure (Figure 3-6). Washing the MeCN-soluble portion with pentane afforded compound **3.3^{IFc}** ($\delta_{\text{P}} = -86.0$), which was highly soluble in common organic solvents and persisted as a dark red oil upon isolation. Because of this, structural confirmation of **3.3^{IFc}** using X-ray diffraction was not possible. By comparison to a phosphirene sulfide recently characterized by the Ragogna group (**D1**, $\delta_{\text{P}} = -83.6$),³⁶ this product was identified as the corresponding [1+2] cycloadduct **3.3^{IFc}**. The ^{31}P NMR spectrum of **3.3^{IFc}** contained a poorly resolved multiplet, but P-H coupling was observed in the ^1H NMR spectrum ($\delta_{\text{H}} = 4.60$, $^2J_{\text{PH}} = 54.4$ Hz) along with a single set of TerPh and ferrocene resonances (Figure 3-6). The coupling constant between phosphorus and the olefinic ring hydrogen is much larger for compound **3.3^{IFc}** in comparison to **3.4^{IFc}**. The composition of **3.3^{IFc}** was confirmed by ESI-MS, which contained the molecular ion peak (586.2 *m/z*, [$\text{C}_{36}\text{H}_{35}\text{FePS}$]⁺). Compounds **3.3^{IFc}** and **3.4^{IFc}** were also found to be stable to decomposition upon short exposure to the ambient environment.

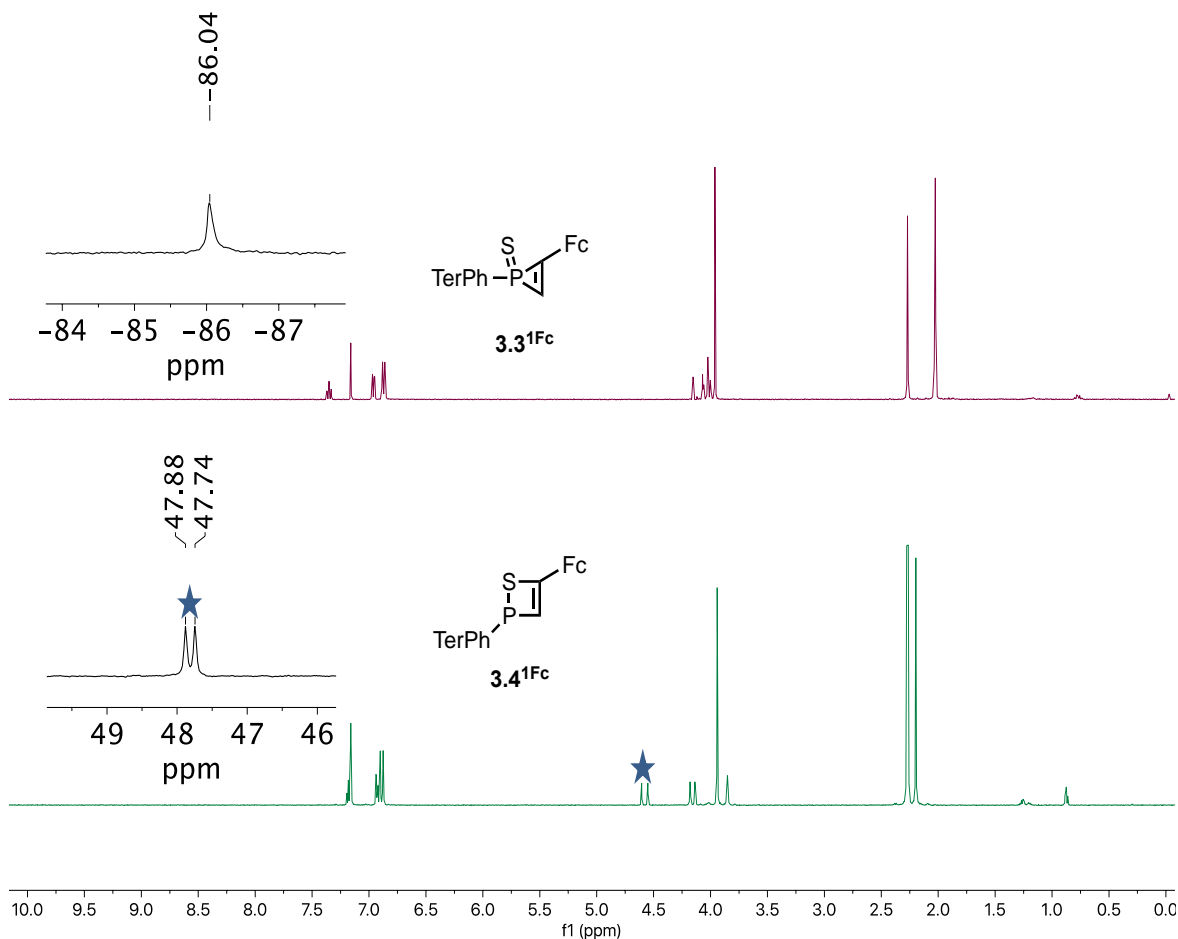


Figure 3-6. Stacked ^1H NMR spectra of **3.3**¹Fc (top) and **3.4**¹Fc (bottom) with inset ^{31}P NMR spectrum expansions. Coupling between the olefinic proton and phosphorus is indicated by a star

Interested in obtaining a compound functionalized with two thiaphosphetenes or phosphirene sulfides, attention was turned to performing the thermolysis reaction with diynes. Experiments consisted of heating a mixture of **3.2** and a stoichiometric excess of diyne in toluene for a minimum of 16 h, which resulted in the formation of both [2+2] and [1+2] cycloaddition products (**3.4**^{bisOct}, **3.3**^{bisPh}, **3.4**^{bisPh}). Compound **3.4**^{bisOct} was the hypothesized [2+2] cycloadduct obtained when 1,7-dioctyne is the trapping reagent because of the proximity of its chemical shift by $^{31}\text{P}\{^1\text{H}\}$ NMR spectroscopy in comparison to our other prepared derivatives ($\delta_{\text{p}} = 50.0$, $J_{\text{PH}} = 17$, 49.5 Hz, Section 5.4, Figure 5-2). It was likely that butyl chain contributed to the oily nature of **3.4**^{bisOct}, which

inhibited analysis by X-ray crystallography. In an effort to obtain crystalline powder, quaternization of the P(III) center was targeted with three stoichiometric equivalents of MeI. The resulting product was an oil, but a new peak at 72.3 ppm in the ^{31}P NMR spectrum which featured complex splitting was observed (Section 5.4, Figure 5-2). The ^1H NMR spectrum contained a number of peaks which could not be confidently assigned to the proposed structure (Section 5.4, Figure 5-3).

1,4-ethynylbenzene was used as the trapping agent to impart greater rigidity to the resulting cycloadducts. Compounds **3.5**, **3.3^{bisPh}** and **3.4^{bisPh}** were isolated ($\delta_{\text{P}} = 96.0$, 38.2, and -84.1, respectively). The product ratio is largely concentration dependent. High dilution (100 mg/50 mL toluene) favoured the formation of **3.4^{bisPh}** as the major product (60-80 % by integration) and minimized production of **3.5**. At higher concentrations (60 mg/5 mL toluene), there were 5 signals in the crude $^{31}\text{P}\{^1\text{H}\}$ NMR spectrum where compound **3.3^{bisPh}** was the major product (40-60 % by integration). ^{31}P NMR spectroscopic data obtained from crystals of **3.3^{bisPh}** redissolved in benzene- d_6 indicated that **3.3^{bisPh}** corresponded to the most upfield peak in the spectrum as a broad multiplet ($\delta_{\text{P}} = -84.1$, Figure 3-5). The ^1H NMR spectrum displayed long-range P-H coupling from the proton at the *para*- position of phenyl ring bound to phosphorus (Figure 3-7).³⁵ The ^1H NMR spectrum also contained 3 separate environments in the aliphatic region corresponding to the $-\text{CH}_3$ groups of the TerPh ligand. Coupling between the olefinic proton and phosphorus was observed significantly downfield in comparison to **3.3^{IFc}**, at 7.43 ppm in the ^1H NMR spectrum ($^2J_{\text{HP}} = 10.4$ Hz, Figure 3-7). Compound **3.3^{bisPh}** was also found to be stable to decomposition upon short exposure to the ambient environment.

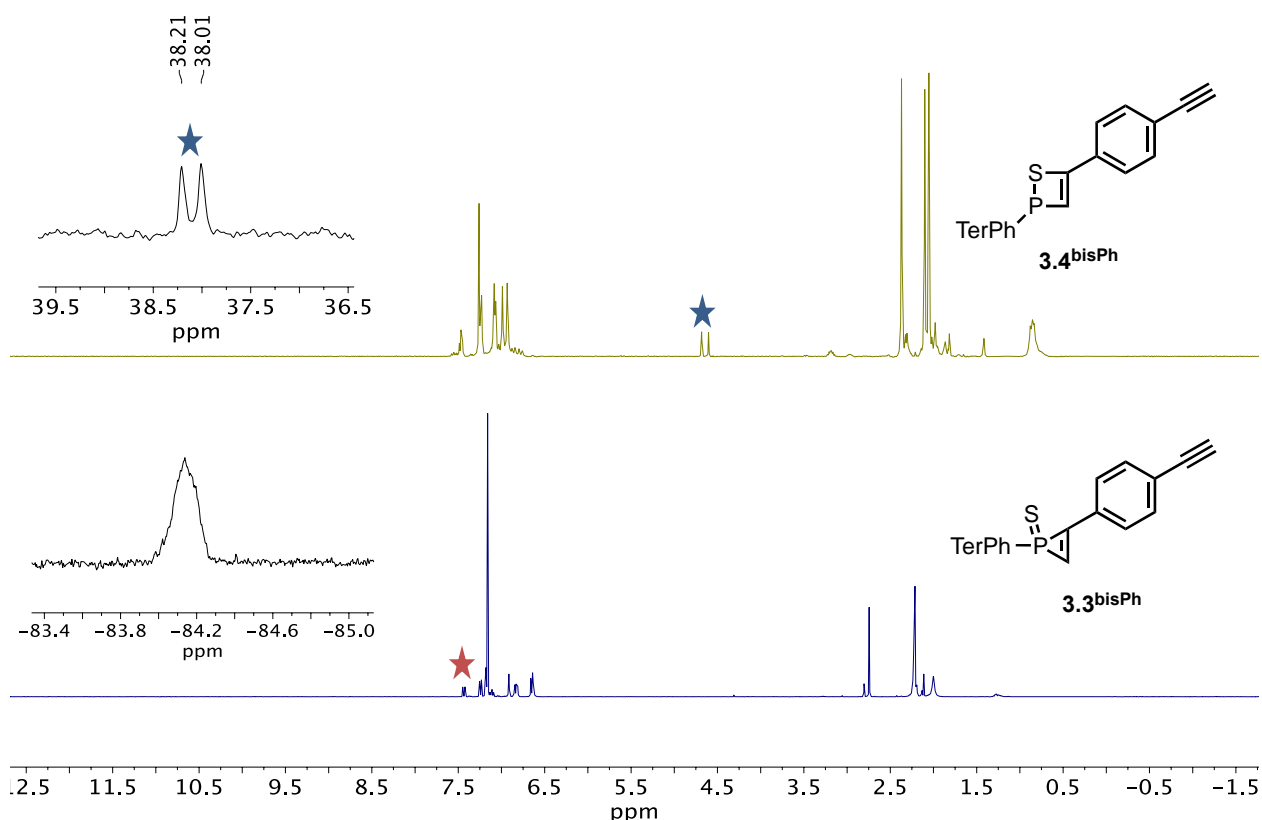


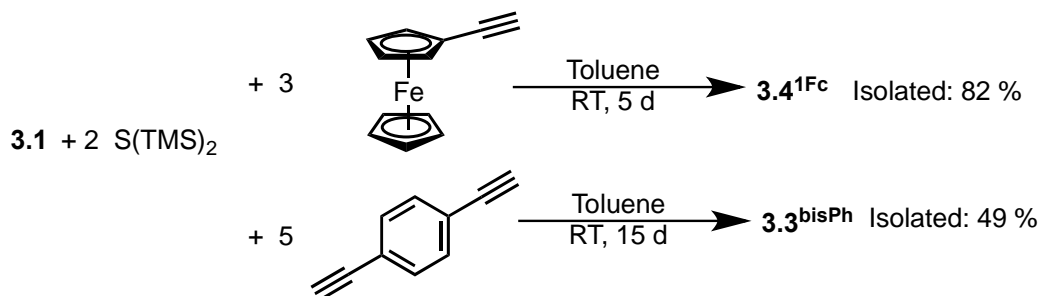
Figure 3-7. Stacked ^1H NMR spectra of **3.4bisPh** (top) and **3.3bisPh** (bottom) with respective expansions of the ^{31}P NMR spectrum inset. Coupling between the olefinic proton of the 3- or 4-membered ring and phosphorus is denoted with a star.

Obtaining analytically pure sample of **3.4bisPh** proved to be quite challenging because of the close structural similarity between **3.3bisPh** and **3.4bisPh**. The manipulation of the P(III) center in **3.4bisPh** offered a potential remedy to this issue. Unfortunately, while crude $^{31}\text{P}\{^1\text{H}\}$ NMR spectra obtained 1-8 h after exposure of a mixture of **3.3bisPh** and **3.4bisPh** to a variety of reaction partners (*eg.* $\text{W}(\text{CO})_5$, $\text{Mo}(\text{CO})_5$, $\text{AuCl}(\text{THT})$ and CuCl) indicated that a reaction had occurred ($\Delta\delta_{\text{P}(\text{avg})} = 42$ ppm), the resulting adducts were quite unstable and decomposed rapidly in the solid state and solution to multiple unidentified products. Quaternization of the P(III) center of **3.4bisPh** with MeI was also unsuccessful. Sulfurization of **3.4** was also attempted, but conversion was slow and lead to multiple, inseparable products. Nevertheless, after 12 consecutive crystallizations relying on the fact that **3.4bisPh** is only slightly less pentane soluble, compound **3.4bisPh**

was successfully isolated from **3.3^{bisPh}**, albeit in poor yield and purity (5.9 %). Compound **3.4^{bisPh}** persisted as a sticky oil, which has precluded single crystal growth thus far. The ^1H NMR spectrum of **3.4^{bisPh}** indicated an asymmetric structure, with 3 separate resonances corresponding to the $-\text{CH}_3$ groups of the TerPh ligand (Figure 3-7). Coupling to phosphorus was observed at higher field in comparison to **3.3^{bisPh}** ($\delta_{\text{H}} = 4.64$, $^2J_{\text{HP}} = 32.0$ Hz) and matched the coupling constant calculated from the doublet present in the ^{31}P NMR spectrum of **3.4^{bisPh}**. The signal corresponding to the proton of the terminal alkyne in both **3.3^{bisPh}** and **3.4^{bisPh}** was obscured by $-\text{CH}_3$ signals in the aliphatic region; however, a diagnostic chemical shift in the $^{13}\text{C}\{^1\text{H}\}$ NMR spectrum confirmed the alkyne was present (**3.3^{bisPh}**, $\delta_{\text{C}} = 79.1$; **3.4^{bisPh}**, $\delta_{\text{C}} = 77.2$).

3.2.2 Cycloaddition *via* Condensation – A More Selective Route

An alternative synthesis for compounds **3.4^{IFc}** and **3.3^{bisPh}** is the condensation reaction of **3.1** and $\text{S}(\text{TMS})_2$ in the presence of excess ethynylferrocene and 1,4-ethynylbenzene, respectively (Scheme 3-2). Stirring a toluene solution of **3.1**, ethynylferrocene (8 stoich. eq.), and 1.2 stoichiometric equivalents of $\text{S}(\text{TMS})_2$ at room temperature overnight lead to the formation of **3.4^{IFc}** as the sole product, indicated by a single doublet in the ^{31}P NMR spectrum. The prominent olefinic reactivity observed in this case was contradictory to the experimental results previously obtained by the Ragogna Group.³⁶ The analogous reaction performed in a solution of 8 stoichiometric equivalents of 1,4-ethynylbenzene resulted in solely carbenic reactivity and the formation of **3.3^{bisPh}**, as previously reported. Conversion to each of **3.4^{IFc}** and **3.3^{bisPh}** as the sole products was observed by $^{31}\text{P}\{^1\text{H}\}$ NMR spectroscopy. Isolated yields for both cases were improved from the thermolysis method described above (**3.4^{IFc}** yield: 82 %, **3.3^{bisPh}** yield: 49 %). Loss of yield in both cases was attributed to loss of product when removing excess trapping reagent and $\text{S}(\text{TMS})_2$.

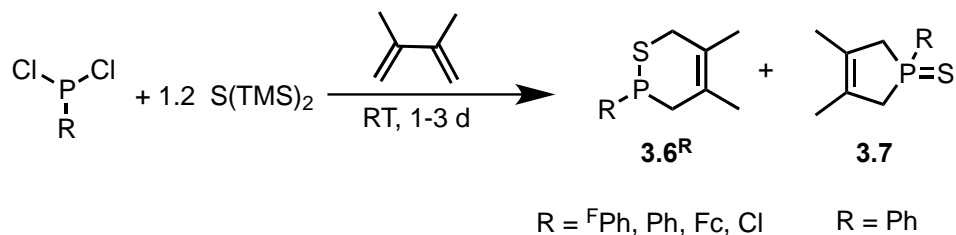


Scheme 3-2. The nature of the alkyne affects observed reactivity. With ethynylferrocene (top) olefinic reactivity is observed by the formation of **3.4^{1Fc}**. When 1,4-ethynylbenzene was used, carbenic reactivity resulted in the formation of **3.3^{bisPh}**. % yield is shown on the right for each case.

The increase in selectivity in product formation observed when using the condensation method was an indication that a different mechanism from the thermolysis method was operative. Previous computational studies have indicated that the lysis of the P_2S_2 ring present in **3.2** is enabled by association of the trapping agent to the dimer prior to the cycloaddition.⁵⁰ Conversely, the condensation method can proceed through a phosphonium intermediate or a “free” $\text{RP}=\text{S}$ intermediate, as previously discussed. While both mechanistic pathways were energetically accessible under our conditions, the phosphonium intermediate was slightly favoured energetically.^{38, 50} These mechanistic differences were attributed to the change in product distribution observed between the two protocols for accessing phosphinidene sulfides *in situ*.

3.2.3 Cycloaddition *via* Condensation – $\text{RP}=\text{S}$ Transfer Without Steric Bulk

The *in situ* generation of phosphinidene sulfide may mitigate the need for *m*-terphenyl substituents required for the preparation of the P_2S_2 ring (**3.2**). To test this hypothesis, 1.2 stoichiometric equivalents of S(TMS)_2 were added to a prepared solution of various dichlorophosphines in neat dmbd at room temperature and was stirred until the



Scheme 3-3. The condensation of various dichlorophosphines with S(TMS)_2 in neat dmbd to yield $\text{RP}=\text{S}$ transfer products (**3.6^R** and **3.7**)

signal corresponding to the starting material was not observed by $^{31}\text{P}\{^1\text{H}\}$ NMR spectroscopy. Alkyldichlorophosphines (*t*-BuPCl₂ and *s*-BuPCl₂) did not react. Electron-donating, electron-withdrawing and aryl- dichlorophosphines were all amenable to the formation of [2+4] cycloadducts (**3.6^R**) and, in one case, a [1+4] cycloadduct (**3.7**, Scheme 3-3). Performing these transformations with a different source of sulfide (*ie.* Na₂S, Li₂S) did not result in the transfer of the RP=S moiety.

When the reaction was performed with an electron-rich dichlorophosphine (FcPCl₂) resulted in the formation of a single product by $^{31}\text{P}\{^1\text{H}\}$ NMR spectroscopy (**3.6^{Fc}**, $\delta_{\text{P}} = -4.9$). The chemical shift suggested the formation of the [2+4] cycloadduct when compared to our previous results.³⁷ Removal of volatiles *in vacuo* left an orange, oily residue in the vial which could be extracted to give an orange powder. Upon removal of residual pentane *in vacuo*, the powder took on an oily consistency. The ^{31}P NMR spectrum revealed a broad triplet at $\delta_{\text{P}} = -4.9$. The corresponding ^1H NMR spectrum contained two resonances for each of the CH₃ groups from the diene portion of the cycloadduct and 4 different resonances for each of the methylene protons of the ring (Figure 3-8). The protons of the -CH₂ group adjacent to the chiral P(III) center were diastereotopic, and the protons of the -CH₂ group adjacent to sulfur were inequivalent because of their diastereotopicity. ESI-MS data confirmed the composition of **3.6^{Fc}** with a base peak corresponding to free gaseous phosphinidene sulfide, [C₁₀H₉FePS]⁺, dmbd, [C₆H₁₀]⁺, and a molecular ion peak at 330.05 *m/z*. Attempts thus far to obtain single crystals suitable for X-ray diffraction have not been successful at room temperature or -30 °C by vapor diffusion, reverse vapor diffusion, slow evaporation, and saturated solutions of **3.6^{Fc}**. Compound **3.6^{Fc}** was discovered to be quite unstable, and decomposed to a large number of unidentifiable signals in the $^{31}\text{P}\{^1\text{H}\}$ NMR spectrum over the course of one week.

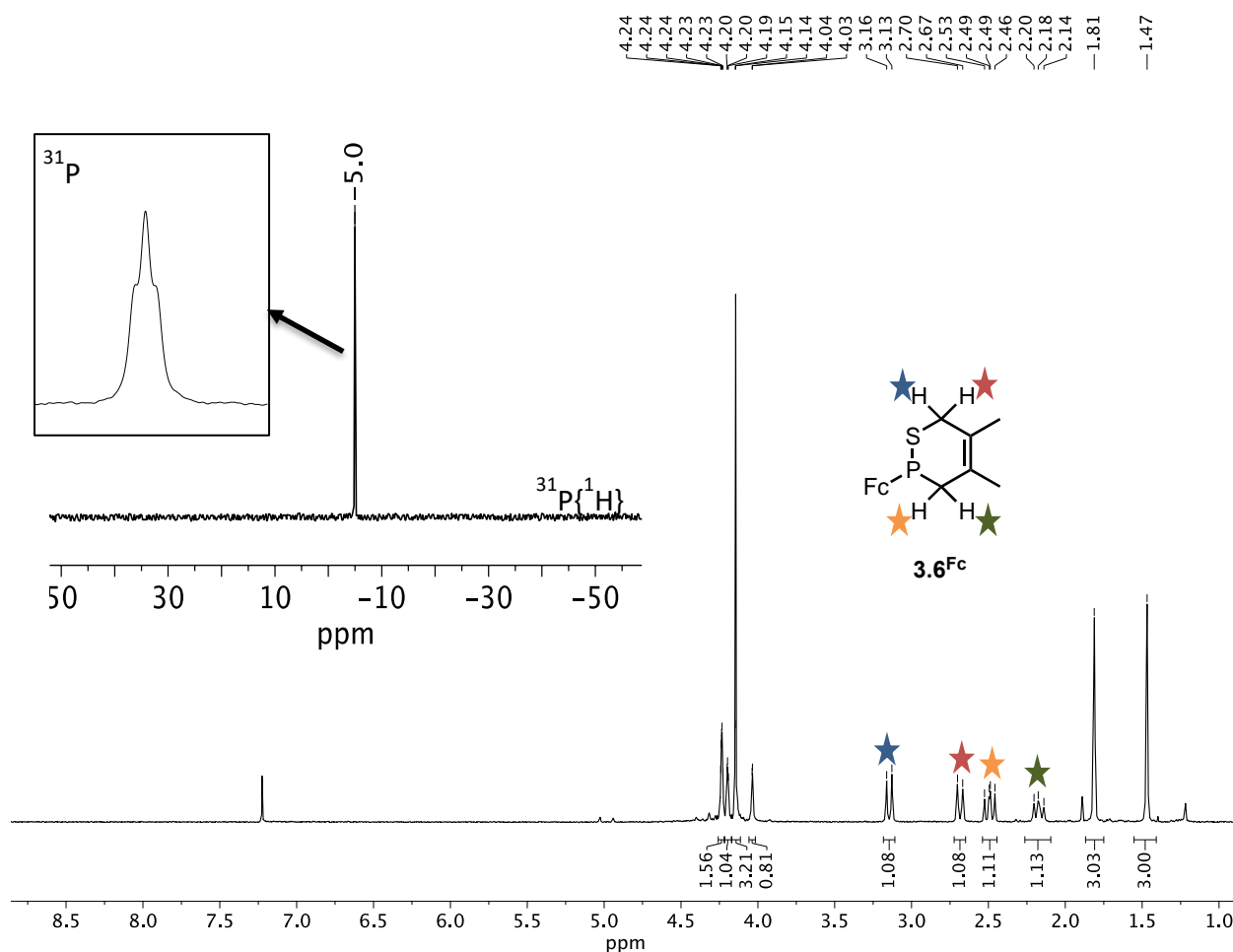


Figure 3-8. ^1H NMR spectrum of **3.6**^{Fc} with expansion of $^{31}\text{P}\{^1\text{H}\}$ and ^{31}P NMR spectra included. Ring protons have been assigned with star labels.

The analogous reaction performed with $^{\text{F}}\text{PhPCl}_2$ resulted in the appearance of one major signal in the $^{31}\text{P}\{^1\text{H}\}$ NMR spectrum at -4.7 ppm, assigned to compound **3.6**^{FPh}. The phosphorus chemical shifts of **3.6**^{Fc} and **3.6**^{FPh} are nearly identical despite a large difference in the electronic nature of the ligands bound to the phosphorus center (*ie.* Fc *versus* $^{\text{F}}\text{Ph}$). Interestingly, coupling to fluorine is not observed in the $^{31}\text{P}\{^1\text{H}\}$ NMR spectrum of **3.6**^{FPh}. The ^{31}P NMR spectrum displayed coupling from phosphorus to the allylic proton with a magnitude of 29.9 Hz. The $^{19}\text{F}\{^1\text{H}\}$ NMR spectrum contained three different resonances corresponding to *ortho*-, *meta*-, and *para*- positions of the phenyl ring ($\delta_{\text{F}} = -133.6, -153.4, -162.2$). The ^1H NMR spectrum contained signals corresponding to the two CH_3 groups on the diene portion of the [2+4] cycloadduct and 4 different

resonances corresponding to the methylene protons (Figure 3-9). The three different resonances resulted from the the diastereotopic protons adjacent to the chiral P(III) center, whereas the protons of the $-\text{CH}_2$ group adjacent to sulfur were overlapped. Compound **3.6^{FPh}** possessed higher symmetry than **3.6^{Fc}** based on the ^1H NMR spectra because each of the **3.6^{Fc}** methylene protons possessed a distinct signal. The multiplet at $\delta_{\text{H}} = 3.27$ contains a doublet corresponding to 29.9 Hz and coupling ($^2J_{\text{HH}} = 16$ Hz) to the proton on the same carbon, which had an upfield shift in comparison to the same proton on **3.6^{Fc}**. The ESI-MS spectrum of **3.6^{FPh}** contained a similar fragmentation pattern to **3.6^{Fc}**, with a base peak of 82.07 m/z corresponding to a dmbd fragment ($[\text{C}_6\text{H}_{10}]^+$) and a peak at 229.91 m/z corresponding to the phosphinidene sulfide fragment ($[\text{C}_6\text{F}_5\text{PS}]^+$). A molecular ion peak was also present at 311.99 m/z .

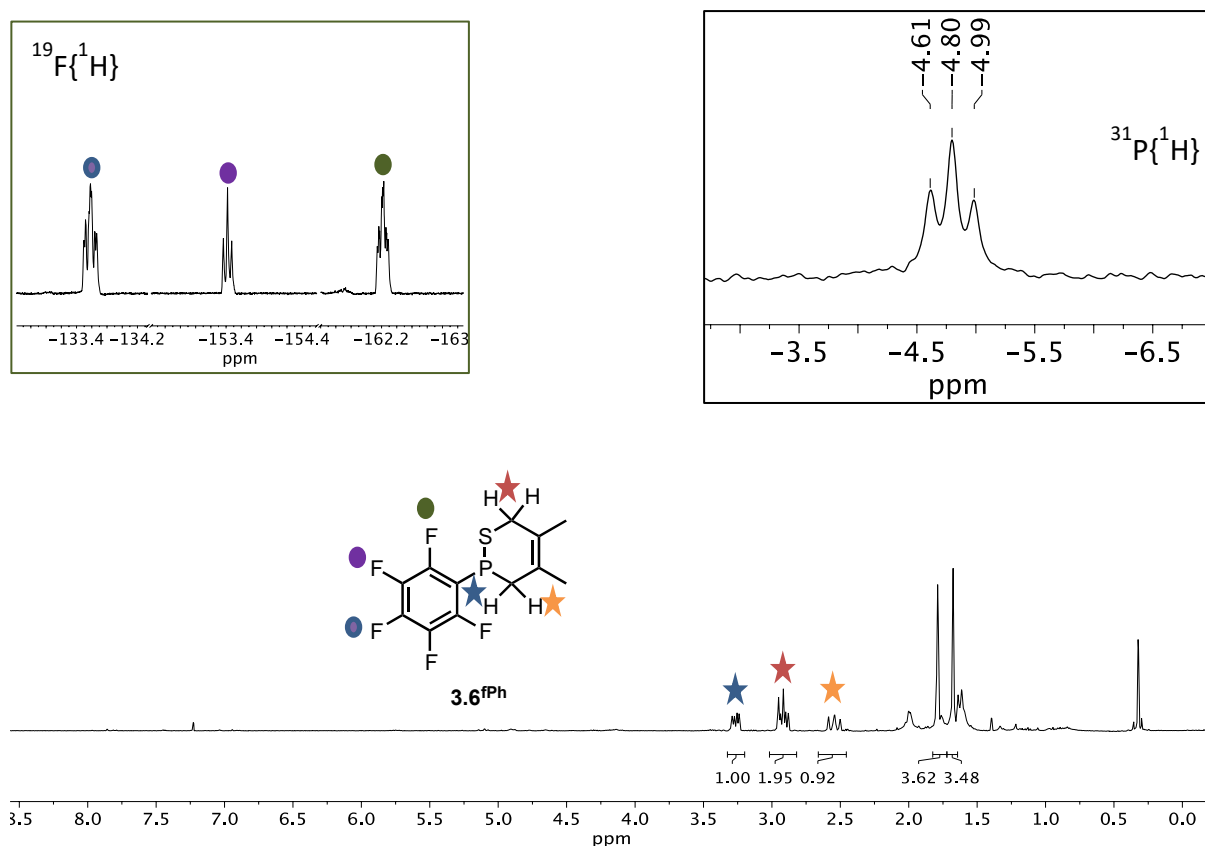


Figure 3-9. ^1H NMR spectrum of **3.6^{FPh}** with inset $^{19}\text{F}\{^1\text{H}\}$ and $^{31}\text{P}\{^1\text{H}\}$ NMR spectra expansions included. Proton assignments are denoted by coloured stars, whereas fluorine atom assignments are indicated by coloured circles. The unlabeled peak near 0 ppm corresponds to unreacted $\text{S}(\text{TMS})_2$.

The atom connectivity of compound **3.6^{FPh}** was confirmed by X-ray diffraction data obtained from single crystals grown from an impure oily sample allowed to rest at room temperature for a week. The high boiling point of S(TMS)₂ (163 °C) lead to difficulty in removal of S(TMS)₂ from compound **3.6^{FPh}**. Heating of the crude oil at temperatures greater than 40 °C in an effort to remove excess S(TMS)₂ lead to the decomposition of **3.6^{FPh}**, likely *via* a retro-Diels Alder mechanism. In the hopes of obtaining a crystalline substance to facilitate the removal of excess S(TMS)₂, modification of the P(III) center was targeted with a variety of different reaction partners with no success (*eg.* BCF, W(CO)₅THF, Mo(CO)₅THF, MeI, AuCl(THT)). The high solubility of compound **3.6^{FPh}** in common organic solvents made purification by solubility slow and challenging, and resulted in the poor isolated yield of **3.6^{FPh}** despite 100 % conversion to **3.6^{FPh}** by integration of the ³¹P{¹H} NMR spectrum (yield: 19%).

In contrast to the reactivity observed with FcPCL₂ and ^FPhPCL₂, dichlorophenylphosphine resulted in both olefinic and carbenic reactivity to yield [2+4] and [1+4] cycloadducts, respectively. This reaction proceeded at a slower rate in comparison to FcPCL₂ and ^FPhPCL₂, and required 3 days to reach full conversion from the PhPCL₂ signal to two new major signals in the ³¹P{¹H} NMR spectrum (**3.7**, δ_P = 45.5, ; **3.6^{Ph}**, δ_P = -0.1). The chemical shift of **3.6^{Ph}** corresponded well with those observed for **3.6^{Fc}** and **3.6^{FPh}**, although the shift is slightly downfield by comparison (Δδ_{P(avg)} = + 4.7). As such, the proposed structure was the [2+4] cycloadduct (**3.6^{Ph}**). Phospholene sulfide (**3.7**) was previously isolated and characterized.⁵¹ Dilution of the reaction mixture with toluene (5:1 toluene:dmbd) was found to favour the formation of **3.6^{Ph}** and allowed **3.6^{Ph}** to be isolated from **3.7** as a pentane-soluble oil (Figure 3-10). Previous attempts to separate an equal mixture of the two structural isomers on the basis of solubility proved to be unsuccessful. Column chromatography on silica gel under inert conditions resulted in the elution of only compound **3.7**. The ³¹P NMR spectrum of **3.7** displayed a broad triplet at 45.5 ppm with a coupling constant of 11.3 Hz, which corresponded well to the existing literature for this compound.⁵¹ The ¹H NMR spectrum obtained from a sample of isolated **3.6^{Ph}** contained a similar distribution of peaks corresponding to the dmbd portion of the [2+4] cycloadduct was noted in comparison to **3.6^{FPh}**. Peaks in the aromatic region which corresponded to the phenyl ring were also observed (Chapter 5.4, Figure 5-4).

Multiple attempts to remove residual $\text{S}(\text{TMS})_2$ by freeze-drying from benzene did not result in its complete removal from the oil, and the high solubility of $\mathbf{3.6^{Ph}}$ in common organic substances has hindered further purification. Compound $\mathbf{3.6^{Ph}}$ was found to be prone to decomposition within a week of its preparation and often resulted in a major peak with a chemical shift corresponding to $\mathbf{3.7}$ by $^{31}\text{P}\{^1\text{H}\}$ NMR spectroscopy. This posed an interesting mechanistic question which has not been addressed.

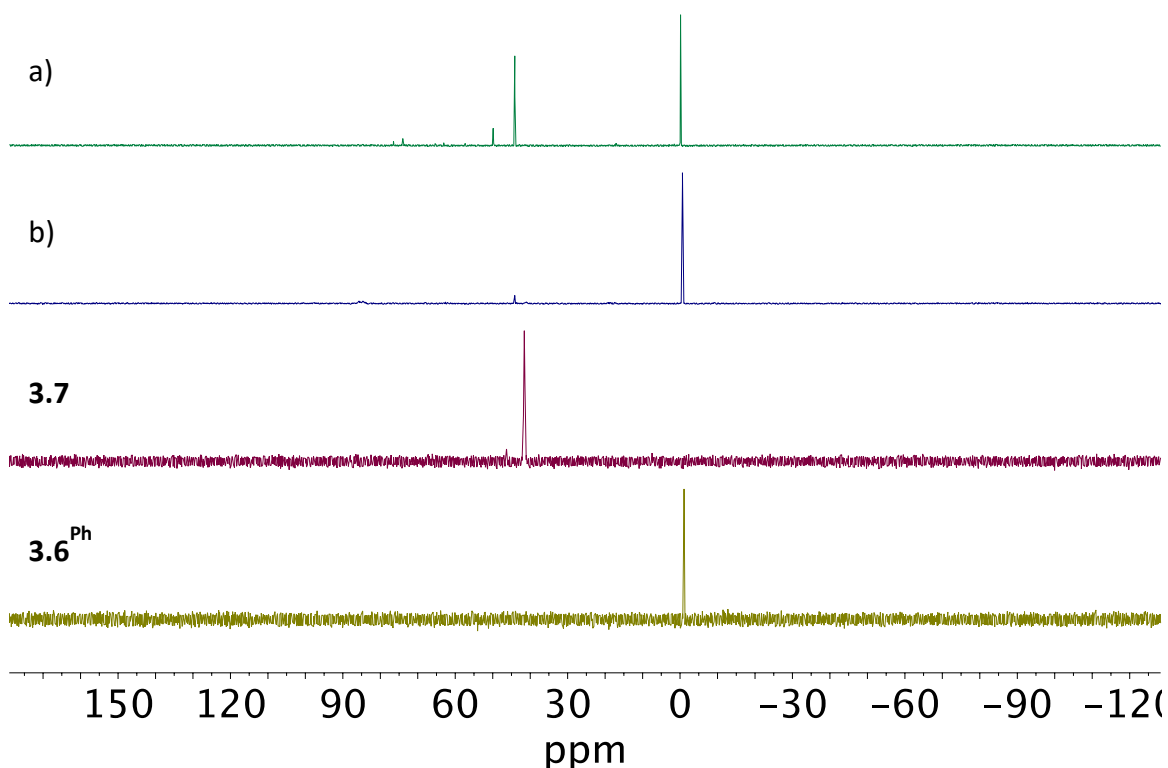


Figure 3-10. Stacked $^{31}\text{P}\{^1\text{H}\}$ NMR spectra. a) Crude reaction mixture in neat dmbd at 30 mg/mL. b) Crude reaction mixture in a 5:1 toluene:dmbd ratio, resulting in primarily olefinic reactivity. $^{31}\text{P}\{^1\text{H}\}$ NMR spectra of purified $\mathbf{3.6^{Ph}}$ and $\mathbf{3.7}$ have also been included.

Compound $\mathbf{3.7}$ was isolated *via* column chromatography; however, $\mathbf{3.6^{Ph}}$ did not elute. Modification of the P(III) center present in $\mathbf{3.6^{Ph}}$ was targeted through the addition of various reactive partners in an aim to significantly alter the solubility of the [2+4] adduct such that crystals suitable for X-ray crystallography could be obtained. Quaternization and metallation of the P(III) center were attempted; however, neither of

these strategies resulted in the disappearance of the signal corresponding to **3.6^{Ph}** by $^{31}\text{P}\{^1\text{H}\}$ NMR spectroscopy.

The metallation of **3.6^{Ph}** by AuCl(THT) was successful. A change in chemical shift from $\delta_{\text{P}} = -0.1$ to $\delta_{\text{P}} = 39.4$ was observed upon stirring a mixture of **3.6^{Ph}** and **3.7** with one stoichiometric equivalent of AuCl(THT) for 15 minutes in DCM. The signal originating from **3.7** remained at $\delta_{\text{P}} = 45.5$ as the P(V) center could not accommodate a Lewis acidic metal. Upon removal of volatiles *in vacuo* and washing the sticky white powder with pentane, compound **3.8^{Au}** was isolated as an insoluble white powder (yield: 82 %). The ^1H NMR spectrum obtained in CDCl_3 displayed characteristic broad peaks that resulted from the coordination between phosphorus and Au. Similar to **3.6^{Ph}**, three distinct signals corresponding to the methylene protons and 2 signals were present for the CH_3 groups on the dmbd portion of the [2+4] cycloadduct were present in the ^1H NMR spectrum (Figure 3-11). While the isolation of **3.8^{Au}** greatly aided in the characterization of **3.6^{Ph}**, the complex was exceptionally light and solution sensitive. After one day the formation of Au(0) was indicated by the deposition of a purple layer on the vial walls and the solution was turbid and dark red/brown. This inhibited the growth of single crystals and the collection of elemental analysis data to confirm the bulk composition, although sufficient NMR spectroscopic data were obtained to support the predicted structure.

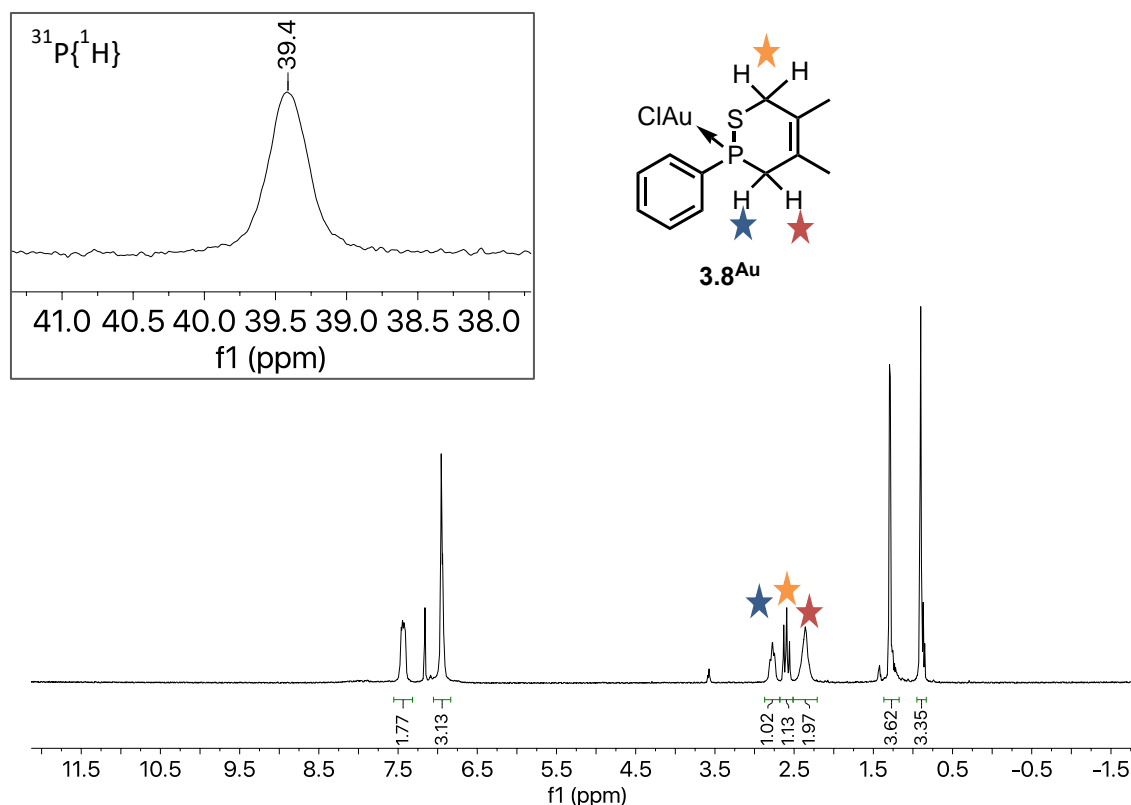
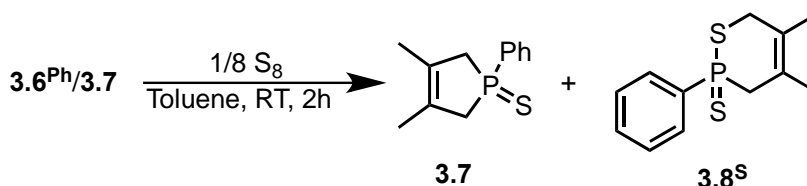


Figure 3-11. ^1H NMR spectrum of **3.8^{Au}**, where ring protons have been assigned with coloured star labels. An expansion of the $^{31}\text{P}\{^1\text{H}\}$ NMR spectrum has also been included.

Sulfurization of **3.6^{Ph}** was targeted as further evidence to support the formation of the [2+4] cycloadduct. One stoichiometric equivalent of elemental sulfur was added to a mixture of **3.6^{Ph}** and **3.7** in toluene at room temperature (Scheme 3-4). Over the course of 1 h, a new peak was observed in the $^{31}\text{P}\{^1\text{H}\}$ NMR spectrum ($\delta_{\text{P}} = 66.2$) and concurrent disappearance of the signal corresponding to **3.6^{Ph}** was also noted. Again, the peak corresponding to **3.7** remained at the same chemical shift as the phosphorus center was fully oxidized. Compound **3.8^S** was previously reported by the Mathey group as a result of similar cycloaddition chemistry with their 7-phosphanorbornadiene scaffolds, and $^{31}\text{P}\{^1\text{H}\}$ and ^1H NMR spectroscopic data obtained matched that of this initial report.²⁷ Separation of **3.7** and **3.8^S** was accomplished by column chromatography on silica gel with a 6:1 THF:Pentane eluent under inert conditions. Multinuclear NMR spectroscopic

data obtained for each fraction confirmed the hypothesized structures with respect to earlier reports (**3.7**, yield: 23 %. **3.8^S**, yield: 42 %).²⁷



Scheme 3-4. Preparation of **3.8^S** by the addition of elemental sulfur to a mixture of **3.6^{Ph}** and **3.7**

The reaction of freshly distilled PCl_3 and $\text{S}(\text{TMS})_2$ lead to the appearance of one major product in the $^{31}\text{P}\{^1\text{H}\}$ NMR spectrum ($\delta_{\text{P}} = 96.5$), along with other unidentified minor products (Figure 3-12). Washing the crude, colourless oil with pentane and Et_2O after removal of solvent *in vacuo* left $\delta_{\text{P}} = 96.5$ as the major product with two smaller flanking peaks ($\delta_{\text{P}} = 97.9$ and 95.3) integrating to 20 % each with respect to the main signal by $^{31}\text{P}\{^1\text{H}\}$ NMR spectroscopy. The differences in chemical shift from the central peak indicate that these are not the result of coupling to phosphorus, and are speculated to be structural variations of the parent peak in the spectrum at this time. ^{31}P NMR spectra indicated coupling to hydrogen for $\delta_{\text{P}} = 96.5$ as a broad multiplet similar to what was observed for **3.6^{Fc}**, and both flanking peaks are unique, complex multiplets. The ^1H NMR spectrum of the oil contained residual impurities, but had diagnostic chemical shifts and coupling constants corresponding to 3 different environments for the 4 methylene protons on a [2+4] cycloaddition product, hence the tentatively proposed structure of **3.6^{Cl}** (Section 5.4, Figure 5-5).

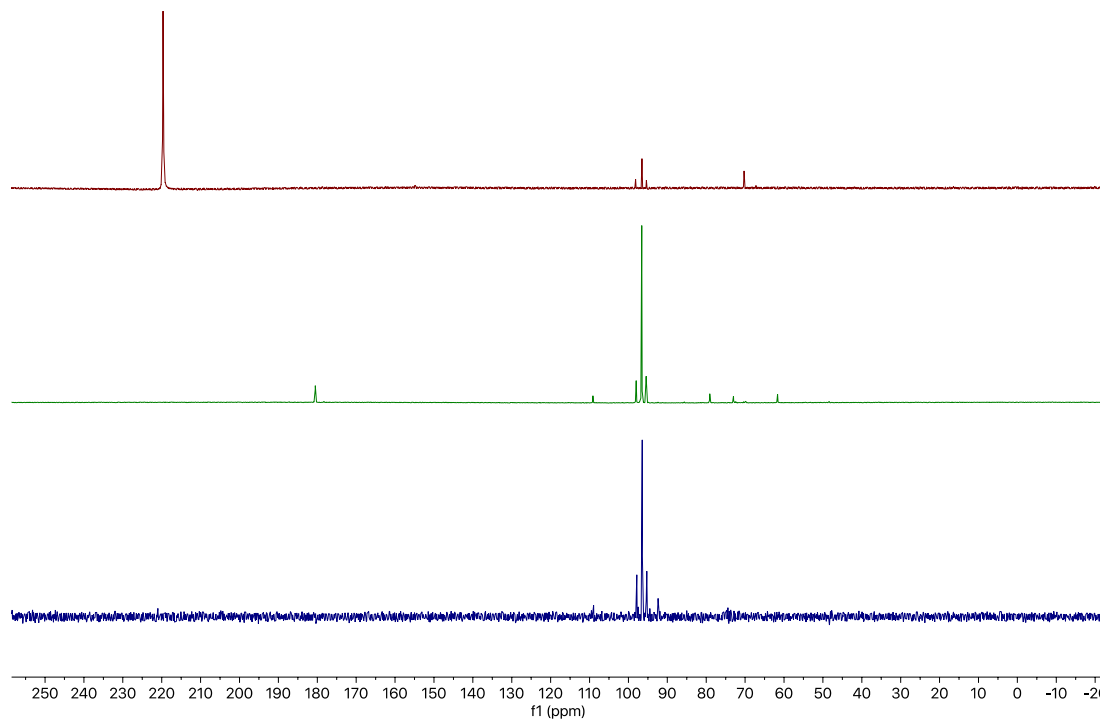


Figure 3-12. Stacked $^{31}\text{P}\{^1\text{H}\}$ NMR spectra for the reaction of PCl_3 and $\text{S}(\text{TMS})_2$ in neat dmbd to yield **3.6^{Cl}** at four hours (top), three days (middle) and after washing the crude oil with *n*-pentane (bottom)

Difficulties pertaining to the purification of **3.6^{Cl}** caused us to pursue modification of the hypothesized P(III) center; however, multiple attempts with MeI, BCF, $\text{W}(\text{CO})_5$, $\text{Mo}(\text{CO})_5$, $\text{AuCl}(\text{THT})$ and CuCl offered no promising results. Halide abstraction (with TMSOTf) and hydrolysis (with de-oxygenated H_2O and H_2O_2) of the hypothesized P-Cl bond in compound **3.6^{Cl}** was targeted. In both cases, the appearance of multiple new signals in the $^{31}\text{P}\{^1\text{H}\}$ NMR spectra were observed and could not be isolated. Performing the reaction in the presence of 1.1 stoichiometric equivalents of DMAP, to neutralize the HCl generated as a byproduct of the the hydrolysis, did not decrease the number of signals by $^{31}\text{P}\{^1\text{H}\}$ NMR spectroscopy. At this time, the composition of **3.6^{Cl}** has not been verified by bulk analysis or X-ray diffraction as a result of difficulty obtaining analytically pure sample, and derivitization attempts have so far been unsuccessful.

The preparation of **3.6^R** and **3.7** followed the same room temperature synthetic protocol, with the cycloaddition remarkably occurring at room temperature. Two alternative mechanisms were observed by $^{31}\text{P}\{^1\text{H}\}$ NMR spectroscopy for the syntheses

in this section. Aliquots of reaction mixtures were taken at various time intervals indicated that the reactions which lead to the formation of **3.6^{Cl}**, **3.6^{Fc}**, **3.6^{Ph}** and **3.7** proceeded without the appearance of any spectroscopic signals that could be assigned to a reaction intermediate. Computational studies have predicted that although the mechanism of their formation likely favoured the phosphonium intermediate, free $\text{RP}=\text{S}$ was also an energetically viable reaction intermediate.⁵⁰ The formation of **3.6^{FPh}** proceeded through an alternate mechanism which has not been previously observed.

When the dichlorophosphine is $^{\text{F}}\text{PhPCl}_2$, an aliquot of the reaction mixture taken after 1 h at room temperature displayed nearly full conversion to 2 peaks in the $^{31}\text{P}\{^1\text{H}\}$ NMR spectrum ($\delta_{\text{P}} = 66.5$ and -4.7 , Figure 3-13). The broad triplet observed at $\delta_{\text{P}} = 66.5$ ($^3J_{\text{PF}} = 35.9$ Hz) decreased in relative intensity with respect to $\delta_{\text{P}} = -4.7$, which saw an increase in peak intensity after 4 hours. After stirring 16 hours, only the product at $\delta_{\text{P}} = -4.7$ remained and there was no longer a signal at $\delta_{\text{P}} = 66.5$. Interested in the nature of the intermediate formed prior to **3.6^{FPh}**, the reaction was halted at the point when all $^{\text{F}}\text{PhPCl}_2$ was consumed – approximately 1 hour – when the product ratio was 5 % **3.6^{FPh}** and 95 % intermediate (**3.9**) by integration. An alternative synthesis to **3.9** was found to be the condensation of $^{\text{F}}\text{PhPCl}_2$ and $\text{S}(\text{TMS})_2$ in toluene at $60\text{ }^{\circ}\text{C}$, where complete conversion to a single peak with an identical chemical shift was observed in the $^{31}\text{P}\{^1\text{H}\}$ NMR spectrum ($\delta_{\text{P}} = 66.5$). Removal of solvent *in vacuo* left product of suitable purity to obtain crystals (yield: 53 %). X-ray diffraction studies on single crystals grown from a concentrated pentane solution kept at $-30\text{ }^{\circ}\text{C}$ for a week confirm the core connectivity of **3.9**; however, the poor diffraction present across all submitted crystal samples past $0.9\text{ }\text{\AA}$ precludes the ability to assess fine structural details with precision. Nevertheless, it revealed the core structure of **3.9**, which consisted of a P_4S_4 ring. The ESI-MS data obtained from crystals of **3.9** contained a base peak at $722.04\text{ }m/z$ corresponding to $[\text{C}_{18}\text{F}_{15}\text{P}_3\text{S}_4]^+$ and a molecular ion peak at $920.3\text{ }m/z$ corresponding to $[\text{C}_{24}\text{F}_{20}\text{P}_4\text{S}_4]^+$.

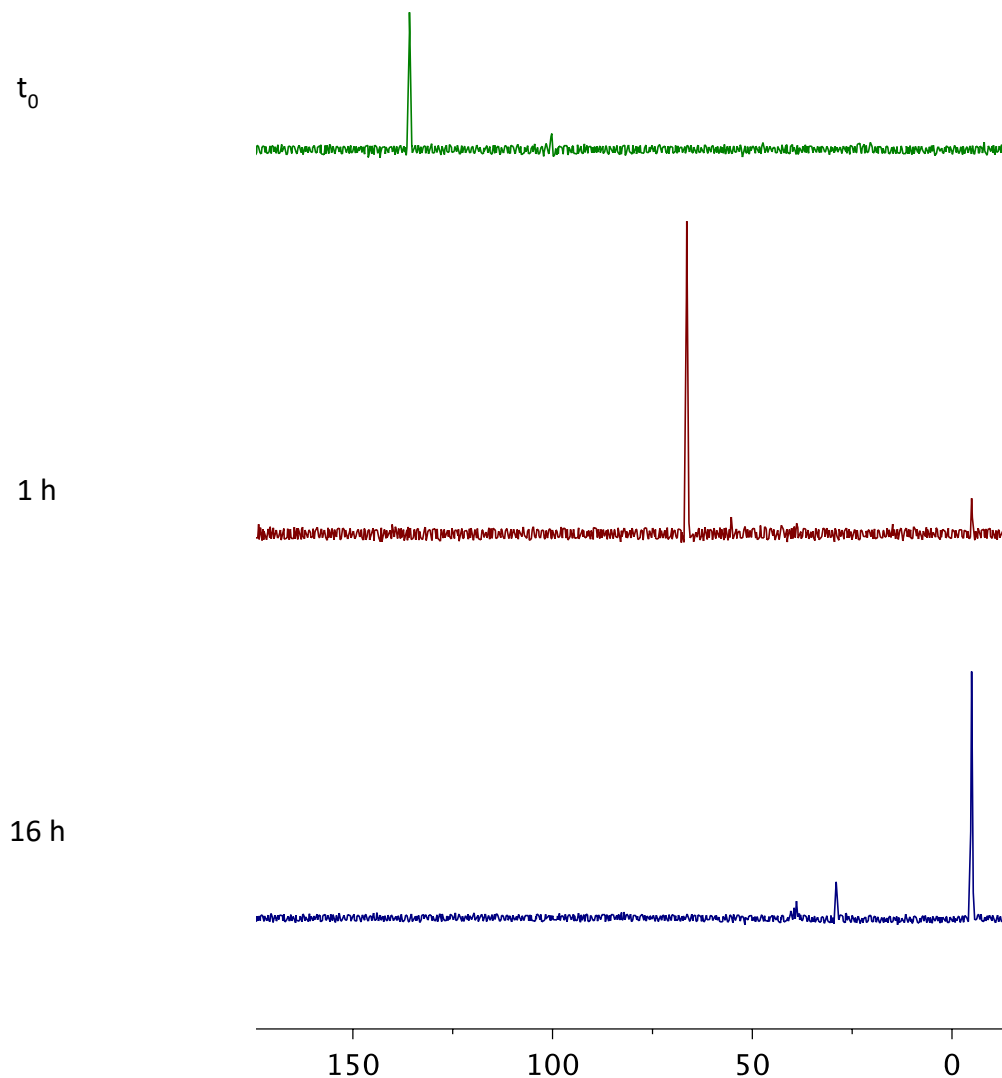


Figure 3-13. Stacked $^{31}\text{P}\{^1\text{H}\}$ NMR spectra taken from the reaction of $^{\text{F}}\text{PhPCl}_2$ with $\text{S}(\text{TMS})_2$ in neat dmbd. Conversion from the signal corresponding to **3.9** to a chemical shift of -4.7 ppm (**3.6^{FPh}**) was observed. The formation of compound **3.9** was quite rapid, in contrast to the slower formation of **3.6^{FPh}**.

This represented the first reported example of an 8-membered ring breaking into its constituent monomeric components to release phosphinidene sulfide in the presence of trapping agent, in this case dmbd. Remarkably the proposed breakdown of the 8-membered ring into its 4 constituent $^{\text{F}}\text{PhP}=\text{S}$ components took place at room temperature, particularly because ring strain in this case is not a driving force. The lysis of P,S-heterocycles has only been observed for our previously reported 4-membered P_2S_2 ring (**3.2**) upon the addition of heat, and has not been observed for P_xS_x heterocycles ($x = 3$ or

4). It is clear from $^{31}\text{P}\{^1\text{H}\}$ NMR spectra of aliquots taken over the course of the reaction to form **3.6^{FPh}** that there is a definite relationship between **3.9** and the resultant [2+4] cycloadduct. It is particularly remarkable that this transformation occurs at room temperature and without bulky aryl ligands, but with an electron withdrawing group on the phosphorus center.

3.2.4 Structural Confirmation of Cycloadducts by X-ray Diffraction

The solid state structure of **3.4^{IFc}** (Figure 3-14) represented the second known thiaphosphetene to be structurally characterized. It features a nearly planar PSC_2 ring with a $\text{C}=\text{C}$ double bond of 1.350(12) Å and a $\text{P}-\text{S}$ single bond of 2.176(3) Å. A slight elongation of the $\text{P}-\text{S}$ single bond and compression of internal ring bond angles was noted with respect to our previously prepared derivative.³⁷ Typical $\text{P}-\text{C}$ bond lengths were observed ($\text{P}(1)-\text{C}(1)$ 1.851(9) Å and $\text{P}(1)-\text{C}(25)$ 1.818(9) Å) with a distorted trigonal pyramidal geometry (sum of angles at phosphorus = 258.7(12)°).

Compound **3.3^{bisPh}** was found to contain a strained 3-membered PC_2 ring with $\text{P}-\text{C}_{(\text{avg})}$ bond distances of 1.749(2) Å with an exocyclic $\text{P}=\text{S}$ double bond of 1.9371(8) Å (Figure 3-14). The length of the $\text{P}=\text{S}$ double bond present in **3.3^{bisPh}** is comparable to other phosphirene sulfide derivatives prepared by our group.⁵⁰ Normal $\text{P}-\text{C}$, $\text{C}=\text{C}$ double and triple bond lengths were observed based on their Pykko & Atsumi bond radii (Figure 3-12).⁵² The sum of angles at phosphorus, excluding the $\text{P}=\text{S}$ double bond was 272.3(8)°, where the internal $\text{C}(1)-\text{P}(1)-\text{C}(2)$ bond angle was 44.36(10)°.

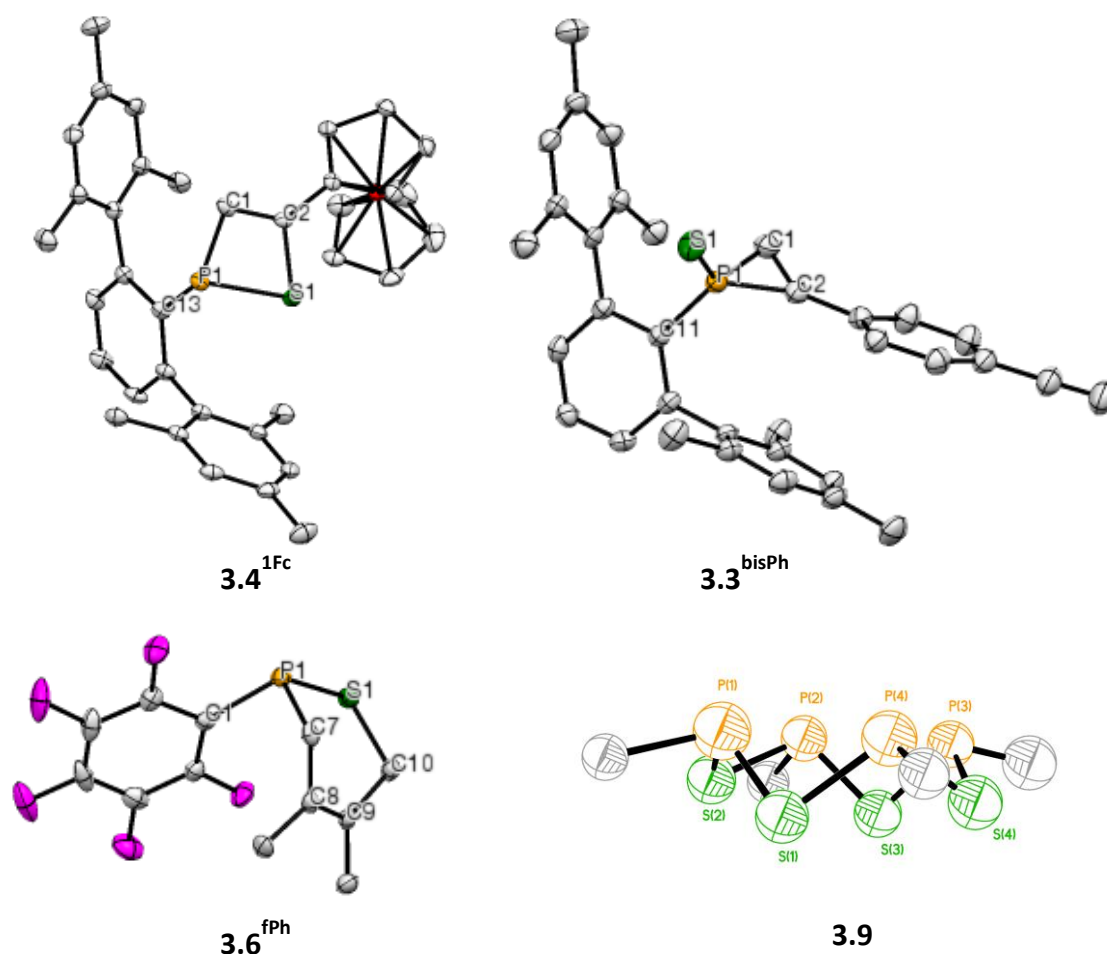


Figure 3-14. Solid state structures of **3.4**^{1Fc} (top left), **3.3**^{bisPh} (top right), **3.6**^{fPh} (bottom left) and **3.9** (bottom right) with thermal ellipsoids drawn at 50 % probability. Hydrogen atoms have been omitted for clarity. Selected bond lengths [Å] and angles [°]: **3.4**^{1Fc}: P(1)-S(1) 2.1729(11), P(1)-C(1) 1.823(2), P(1)-C(13) 1.850(2), S(1)-C(2) 1.781(2), C(1)-C(2) 1.350(3), C(1)-H(1) 0.9500, C(1)-P(1)-C(13) 105.37(10), C(1)-P(1)-S(1) 77.69(8), C(13)-P(1)-S(1) 102.41(8), C(2)-C(1)-P(1) 100.02(17), C(2)-S(1)-P(1) 75.84(8), C(2)-C(1)-H(1) 130.0, P(1)-C(1)-H(1) 130.0, C(1)-C(2)-S(1) 106.39(17). **3.3**^{bisPh}: P(1)-S(1) 1.9371(8), P(1)-C(1) 1.746(2), P(1)-C(2) 1.752(2), P(1)-C(11) 1.809(2), C(1)-C(2) 1.320(3), C(1)-H(1) 0.99(3), C(2)-C(3) 1.460(3), C(1)-P(1)-C(2) 44.36(10), C(1)-P(1)-C(11) 112.26(10), C(2)-P(1)-C(11) 115.68(10), C(1)-P(1)-S(1) 126.68(8), C(2)-P(1)-S(1) 123.69(8), C(11)-P(1)-S(1) 115.52(7), C(2)-C(1)-P(1) 68.06(14), C(2)-C(1)-H(1) 141.0(14), P(1)-C(1)-H(1) 149.2(14). **3.6**^{fPh}: P(1)-S(1) 2.0879(7), P(1)-C(1) 1.8705(18), P(1)-C(7) 1.8693(17), S(1)-C(10) 1.8613(18), C(7)-P(1)-C(1) 97.83(8), C(7)-P(1)-S(1) 98.26(5), C(10)-S(1)-P(1) 103.09(5), C(2)-C(1)-P(1) 114.39(12).

Although compound **3.6^{FPh}** was oily at room temperature, single crystals were obtained from a sample left to sit at room temperature for a week. Generally, compounds of this nature have required modification of the P(III) center in order to obtain crystals suitable for analysis by X-ray diffraction and this represents the first example where this was not required. The solid-state structure, shown in Figure 3-14, confirmed the hypothesized [2+4] cycloaddition product. A P-S bond length of 2.0879(7) Å was measured, which corresponded to a single bond between the two heteroatoms. Again, a distorted tetrahedral geometry is observed at the P(III) center (sum of angles at phosphorus = 310.5 °) with typical P-C and C=C bond lengths.⁵²

The data collected from multiple crystalline samples of compound **3.9** were sufficient to confirm the nature of the P₄S₄ core; however, the data in all cases was severely disordered. This disorder could be modeled such that the core P₄S₄ ring was confirmed, but disorder present in the ancillary ^FPh ligands could not be modeled (Figure 3-14). Growing single crystals of **3.9** across a variety of different conditions did not lead to an improvement in the quality of diffraction data. As such, the isotropic structure shown does not contain the ancillary ^FPh ligands and only serves as confirmation of the core ring structure. Bond lengths and angles have not been included for this reason. The composition of **3.9** was confirmed by ESI-MS, where the data also supported the proposed structure as previously discussed.

3.3 Conclusions

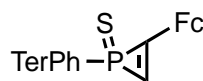
We have detailed the synthesis of a number of new thiaphosphetenes (**3.4ⁿ**), phosphirene sulfides (**3.3ⁿ**), and [2+4] cycloadducts (**3.6^R**, R = Fc, ^FPh, Ph, Cl) which have been characterized by multinuclear NMR spectroscopy, mass spectrometry, and X-ray crystallography (where possible). The condensation reaction of **3.1** and S(TMS)₂ generated R-P=S fragments *in situ* from a number of dichlorophosphines to yield **3.6^R** and **3.7**, which confirmed that both olefinic and carbenic reactivity pathways were accessible. We have shown the first example of an 8-membered P₄S₄ heterocycle (**3.9**) breaking into its constituent monomeric units to form a [2+4] cycloadduct with dmbd (**3.6^{FPh}**). The use of the condensation method instead of the thermolysis method resulted in improved NMR spectroscopic and isolated yields of cycloadducts **3.4^{IFc}** ([2+2]) and

3.3^{bisPh} ([1+2]). Structural characterization data was not obtained for many of the P(III) derivatives as they exist at oils at room temperature and were prone to decomposition shortly after their preparation. Characterization of the parent heterocycles was targeted through manipulation of the P(III) center with other organic substrates or metals (*ie.* **3.8^S**; AuCl(THT), **3.8^{Au}**). Further development of purification methods for the resulting cycloadducts has been ongoing in order to obtain analytically pure material for bulk compositional analysis. Should aryldichlorophosphines generally be amenable to *in situ* phosphinidene sulfide generation by condensation and transfer with S(TMS)₂, a large number of [1+4] and [2+4] P,S-containing heterocycles could be prepared, characterized and contrasted to deepen fundamental understanding of RP=S transfer and its potential application in synthesis.

3.4 Experimental Section

Please see Chapter 5 for general experimental and crystallographic details.

3.4.1 Synthesis of **3.3^{1Fc}**



A vial was charged with **3.2** (120 mg, 0.159 mmol) and ethynyl ferrocene (67 mg, 0.319 mmol) in the glovebox. 10 mL of toluene was added and this solution was transferred to a glass tube, which was sealed with grease. The mixture was heated for 16 h at 50 °C. At this time, all volatiles were removed *in vacuo* and the residual oil was washed three times with 3 mL of acetonitrile. Volatiles were removed from the soluble fraction under vacuum, leaving a dark red oil which was washed with pentane (3 x 5 mL) and then redissolved in a minimal amount of DCM. Pentane (1 mL) and ether (0.5 mL) were layered on top and the vial was placed at -30 °C for five days, resulting in a dark red oil, **3.7**. Yield 8 mg (9.9 %).

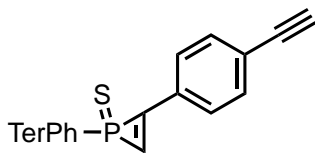
ESI-MS: 313.2 *m/z*, [C₂₄H₂₅]⁺, 587.2 *m/z* [C₃₆H₃₅FePS + H]⁺.

¹H NMR (C₆D₆, 400 MHz, δ): 2.02-2.03 (s, 12H, Mes CH₃), 2.27 (s, 6H, Mes CH₃), 3.96 (s, 5H, Fc CH), 3.97-4.07 (m, 4H, Fc CH), 4.60 (d, ²*J*_{HP} = 54.4 Hz, 1H, C_{sp2}H), 6.86-6.88 (s, 4H, TerPh CH), 6.96 (dd, ³*J*_{HH} = 7.6 Hz, ⁴*J*_{HP} = 2.4 Hz, 2H, Ph CH), 7.35 (t, ³*J*_{HH} = 7.6 Hz, *para* CH).

$^{13}\text{C}\{^1\text{H}\}$ NMR (CDCl_3 , 150.8 MHz, δ): 20.3, 20.8, 21.3, 21.4, 22.4, 34.2, 63.9, 68.7, 69.9 (d, $^2J_{\text{CP}} = 5.7$ Hz), 70.1, 70.6, 70.9, 71.5, 72.0, 112.5, 128.0, 129.0, 129.2 (d, $^1J_{\text{CP}} = 25.2$ Hz), 129.3 (d, $^2J_{\text{CP}} = 18.1$ Hz), 131.2 (d, $^3J_{\text{CP}} = 3.9$ Hz), 132.0, 135.4 (d, $^2J_{\text{CP}} = 20.9$ Hz), 136.7, 137.1, 137.2 (d, $^2J_{\text{CP}} = 8.3$ Hz), 137.5, 142.7 (d, $^2J_{\text{CP}} = 18.1$ Hz), 156.1 (d, $^2J_{\text{CP}} = 7.2$ Hz).

^{31}P NMR (C_6D_6 , 161.8 Hz, δ): -86.0 (m).

3.4.2 Synthesis of **3.3^{bisPh}**



A vial was charged with **3.2** (90 mg, 0.120 mmol) and 1,4-ethynylbenzene (100 mg, 0.793 mmol). 10 mL of toluene was added and this solution was transferred to a glass tube, and sealed with grease. The mixture was heated at 40 °C for 12 h. At this time, all volatiles were removed *in vacuo* and the residual yellow sticky powder was washed with 3 mL of pentane. The pentane soluble portion of the reaction mixture was concentrated and yielded crystals suitable for X-ray diffraction after one night at -30 °C. Yield: 20 mg (33 %). Alternatively, **3.3^{bisPh}** was obtained by charging a vial with **3.1** (60 mg, 0.144 mmol) and 1,4-ethynylbenzene (280 mg, 2.220 mmol). Neat $\text{S}(\text{TMS})_2$ (0.064 mL, 0.311 mmol) was added after the addition of 5 mL of toluene. This solution was kept at room temperature for 15 days, yielding **3.3^{bisPh}** as the sole product. Yield: 30 mg (49 %).

mp (nitrogen sealed capillary): 72.5-74 °C

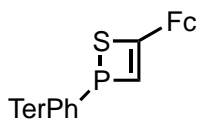
ESI-MS: 313.2 m/z [$\text{C}_{24}\text{H}_{25}$] $^+$, 525.2 m/z [$\text{C}_{34}\text{H}_{32}\text{PS} + \text{Na} - \text{H}$] $^+$, 1027.4 m/z [$2(\text{C}_{34}\text{H}_{32}\text{PS}) - \text{Na}$] $^+$.

^1H NMR (C_6D_6 , 400 MHz, δ): 2.00 (s, 1H, CCH), 2.22 (s, 12H, Mes CH_3), 2.74 (s, 6H, Mes CH_3), 6.64-6.66 (s, 2H, Mes CH), 6.82 (d, $^3J_{\text{HH}} = 7.6$ Hz, 2H, Ph CH), 6.91 (s, 2H, Mes CH), 7.11 (t, $^3J_{\text{HH}} = 7.6$ Hz, 1H, Ph *para*-CH), 7.18 (s, 2H, Mes CH), 7.24 (d, $^3J_{\text{HH}} = 8.0$ Hz, 2H, Ph CH), 7.43 (d, $^3J_{\text{HP}} = 10.4$ Hz, Ph CH)

$^{13}\text{C}\{^1\text{H}\}$ NMR (CDCl_3 , 150.8 MHz, δ): 21.2 (d, $^2J_{\text{CP}} = 11.3$ Hz), 21.3, 29.4, 29.7, 31.2, 31.9, 79.1, 122.5, 124.2, 128.2, 128.3 (d, $^2J_{\text{CP}} = 12.2$ Hz), 128.9, 129.3 (d, $^1J_{\text{CP}} = 18.5$ Hz), 131.5 (d, $^3J_{\text{CP}} = 4.4$ Hz), 131.8, 132.0, 136.6, 136.7, 136.8, 136.9 (d, $^1J_{\text{CP}} = 29.5$ Hz), 137.7, 142.8 (d, $^2J_{\text{CP}} = 18.4$ Hz), 144.6 (d, $^3J_{\text{CP}} = 3.5$ Hz).

^{31}P NMR (C_6D_6 , 161.8 Hz, δ): -84.1 (br m).

3.4.3 Synthesis of **3.4**^{1Fc}



A vial was charged with **3.2** (120 mg, 0.159 mmol) and ethynyl ferrocene (67 mg, 0.319 mmol) in the glovebox. To this, 10 mL of toluene was added and this solution was transferred to a glass tube, which was sealed with grease. The mixture was heated for 16 h at 50 °C. After this time, all volatiles were removed *in vacuo* and the residual oil was washed three times with 3 mL of acetonitrile. **3.4**^{1Fc} was isolated as an MeCN insoluble orange powder. Crystals suitable for X-ray crystallographic analysis were grown from a concentrated solution of **3.4**^{1Fc} in pentane kept at -30 °C for two nights. Yield 50 mg (62 %). Alternatively, **3.6** was obtained by charging a vial with **3.1** (70 mg, 0.169 mmol) and ethynyl ferrocene (106 mg, 0.505 mmol) and dissolving in 5 mL of toluene. Neat S(TMS)₂ (0.053 mL, 0.252 mmol) was added and the mixture was heated for 16 h at 50 °C to yield **3.6** as the only product when solvent was removed *in vacuo*. Yield 70 mg (82 %).

m.p. (nitrogen sealed capillary): 189.4 – 191.1 °C

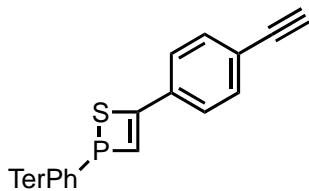
ESI-MS: 586.29 *m/z* [C₃₆H₄₉FePS]⁺, 339.21 *m/z* [C₂₄H₂₅ + Na + H]⁺

¹H NMR (C₆D₆, 400 MHz, δ): 2.20 (s, 6H, Mes CH₃), 2.26-2.28 (s, 12H, Mes CH₃), 3.85 (s, 2H, Fc CH), 3.94 (s, 5H, Fc CH), 4.16 (d, ²J_{HP} = 21.7 Hz, 1H, olefinic CH), 4.18 (s, 1H, Fc CH), 6.88-6.94 (m, 6H, Mes CH), 7.18 (t, ³J_{HH} = 5.2 Hz, 1H, *para* CH).

¹³C{¹H} NMR (CDCl₃, 150.8 MHz, δ): 20.8, 20.86, 20.9, 21.0, 22.4, 65.6, 66.0, 68.8, 68.9, 69.7, 71.4, 81.9, 114.8 (d, ¹J_{CP} = 11.3 Hz), 127.6, 127.8, 128.4, 128.7 (d, ²J_{CP} = 6.6 Hz), 129.3, 136.1, 136.3, 137.1, 138.1, 138.2 (d, ²J_{CP} = 2.6 Hz), 138.6, 143.7 (d, ¹J_{CP} = 18.4 Hz), 146.9 (d, ¹J_{CP} = 32.0 Hz).

³¹P NMR (C₆D₆, 161.8 Hz, δ): 47.8 (d, ²J_{PH} = 21.7 Hz)

3.4.4 Synthesis of **3.4**^{bisPh}



A vial was charged with **3.2** (90 mg, 0.120 mmol) and 1,4-ethynylbenzene (100 mg, 0.793 mmol). 10 mL of toluene was added and this solution was transferred to a glass tube, and sealed with grease. The mixture was heated at 40 °C for 12 h. At this time, all volatiles were removed *in vacuo* and the residual yellow sticky powder

was washed with 3 mL of pentane. From there, 12 consecutive crystallizations were required to isolate modestly pure material as follows: (1-3) From 10 mg/mL and 2 x 20 mg/mL pentane at -30 °C to remove excess 1,4-ethynylbenzene and some **3.5**. (4-6) Reverse vapor diffusion of 5 and 15 mg/mL pentane solutions into toluene at room temperature, removing **3.3^{bisPh}**. (8-11) Reverse vapor diffusion of 5-15 mg/mL pentane solutions into MeCN at -30 °C, removing **3.3^{bisPh}** (12) Concentrated pentane solution at -30 °C overnight. Yield: 5 mg (5.9 %).

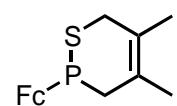
ESI-MS: 525.2 m/z [$C_{34}H_{31}PS + Na$]⁺, 343.2 m/z [$C_{24}H_{25}$]⁺

¹H NMR (C_6D_6 , 400 MHz, δ): 1.82 (s, 1H, $C_{sp^3}H$), 2.05-2.10 (2 s, 12 H, Mes CH_3), 2.37 (s, 6H, Mes CH_3), 4.64 (d, $^2J_{HP} = 32.0$ Hz), 6.93-7.09 (9 H, Mes/Ph CH), 7.24 (3H, Ph CH), 7.47 (t, $^3J_{HH} = 8$ Hz, Ph *para*-CH).

¹³C{¹H} NMR ($CDCl_3$, 150.8 MHz, δ): 20.8 (d, $^2J_{CP} = 7.5$ Hz), 21.0 (d, $^2J_{CP} = 3.0$ Hz), 21.2 (s), 29.7 (s), 31.2 (s), 31.9 (s), 38.2 (s), 77.2 (s), 117.4 (d, $^2J_{CP} = 12.0$ Hz), 123.4 (s), 128.1 (d, $^1J_{CP} = 13.6$ Hz), 128.4 (s), 128.7 (s), 129.7 (s), 135.4 (s), 136.4 (s), 136.7 (s), 137.5 (s), 138.0 (d, $^2J_{CP} = 4.5$ Hz), 143.9 (d, $^1J_{CP} = 19.6$ Hz).

³¹P NMR (C_6D_6 , 161.8 Hz, δ): 38.2 (d, $^2J_{PH} = 32.0$ Hz).

3.4.5 Synthesis of **3.6^{Fc}**

 Dichloroferrocenylphosphine ($FcPCL_2$) was prepared according to a known literature procedure.⁵⁵ $FcPCL_2$ (140 mg, 0.606 mmol) was then dissolved in a minimum amount of toluene (~0.8 mL) and 2.0 mL of 2,3-dimethyl-1,3-butadiene was added. To this solution, neat $S(TMS)_2$ (0.128 mL, 0.616 mmol) was added dropwise and the solution was allowed to stir for two days at room temperature. All volatiles were removed *in vacuo*, followed by 3 x 5 mL washes with pentane, keeping the sample under vacuum for 2 h between washes to remove excess liquid reagents. The orange oil was redissolved in benzene and placed in the freezer until the solution was frozen, then placed under vacuum until an orange powder remained. NMR spectroscopic data obtained from samples of this powder confirmed the predicted structure of **3.6^{Fc}**. Yield: 160 mg (80 %).

m.p. (nitrogen sealed capillary): 124.0 – 125.3 °C

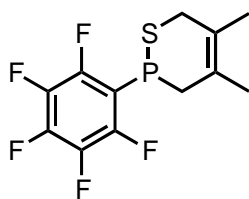
ESI-MS: 330.05 m/z $[\text{C}_{16}\text{H}_{19}\text{FePS}]^+$, 247.95 m/z $[\text{C}_{10}\text{H}_9\text{FePS}]^+$, 82.08 m/z $[\text{C}_6\text{H}_{10}]^+$.

^1H NMR (C_6D_6 , 400 MHz, δ): 1.51 (s, 3H, CH_3), 1.85 (s, 3H, CH_3), 2.21 (br m, 1H, CH_2), 2.53 (dd, $^2J_{\text{HH}} = 12.0$ Hz, $^2J_{\text{HP}} = 15.2$ Hz, 1H, CH_2), 2.72 (d, $^2J_{\text{HH}} = 13.6$ Hz, 1H, CH_2), 3.18 (d, $^2J_{\text{HH}} = 13.6$ Hz, 1H, CH_2), 4.07 (s, 1H, Fc CH), 4.18-4.24 (s, 5H, Fc CH), 4.26 (m, 1H, Fc CH), 4.27 (m, 2H, Fc CH).

$^{13}\text{C}\{^1\text{H}\}$ NMR (CDCl_3 , 150.8 MHz, δ): 20.6 (s), 21.8 (s), 30.9 (s), 34.0 (s), 68.9 (s), 69.5 (d, $^1J_{\text{CP}} = 24.9$ Hz), 69.7 (d, $^2J_{\text{CP}} = 3.5$ Hz), 70.6 (s), 71.5 (d, $^1J_{\text{CP}} = 11.8$ Hz), 71.8 (s), 72.0 (s), 126.2 (d, $^2J_{\text{CP}} = 8.7$ Hz), 126.9 (s).

^{31}P NMR (C_6D_6 , 161.8 Hz, δ): -4.9 (br m).

3.4.6 Synthesis of **3.6^{fPh}**



Dichloro(pentafluorophenyl)phosphine (90.0 mg, 0.335 mmol) was dissolved in 0.8 mL of 2,3-dimethyl-1,3-butadiene. To this solution, neat $\text{S}(\text{TMS})_2$ (0.105 mL, 0.503 mmol) was added at room temperature. After being allowed to sit at room temperature for 18

h, a single product was observed in the $^{31}\text{P}\{^1\text{H}\}$ NMR spectrum. At this point, all volatiles were removed *in vacuo*, yielding a pale yellow oil, which was dissolved in 3 mL of pentane and then subjected to high vacuum until no traces of dmbd or $\text{S}(\text{TMS})_2$ remained in the ^1H NMR spectrum. Crystals suitable for X-ray crystallography were obtained by allowing the crude oil to sit at room temperature for 7 days. Yield: 20 mg (19 %).

ESI-MS: 311.99 m/z $\text{C}_{12}\text{H}_{10}\text{F}_5\text{PS} [\text{M}]^+$, 229.91 $[\text{C}_6\text{F}_5\text{PS}]^+$, 82.07 $[\text{M} - \text{C}_6\text{F}_5\text{PS}]^+$.

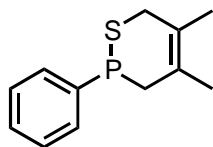
^1H NMR (C_6D_6 , 400 MHz, δ): 1.68 (s, 3H, CH_3), 1.79 (s, 3H, CH_3), 2.55 (dd, 1H, $^2J_{\text{HH}} = 16.0$ Hz, $^2J_{\text{HP}} = 29.9$ Hz, 1H, CH_2), 2.88-2.95 (2H, S- CH_2), 3.27 (dd, $^2J_{\text{HH}} = 16.0$ Hz, $^2J_{\text{HP}} = 29.9$ Hz, 1H, P- CH_2).

$^{13}\text{C}\{^1\text{H}\}$ NMR (CDCl_3 , 150.8 MHz, δ): 21.6 (s), 31.2 (d, $^2J_{\text{CP}} = 6.0$ Hz), 33.7 (s), 33.9 (s), 126.2 (d, $^2J_{\text{CP}} = 9.0$ Hz), 128.4 (s), 129.1 (s), 131.0 (s), 138.1 (d, $^1J_{\text{CP}} = 57.3$ Hz).

^{19}F NMR (C_6D_6 , 376.3 MHz, δ): 162.2 (m, *ortho*- F), -153.4 (t, $^3J_{\text{FF}} = 20.7$ Hz, *para*- F), -133.6 (m, *meta*- F)

^{31}P NMR (C_6D_6 , 161.8 Hz, δ): -4.7 (t, $^3J_{\text{PF}} = 29.9$ Hz).

3.4.7 Synthesis of **3.6^{Ph}**



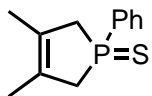
Dichlorophenylphosphine (90.0 mg, 0.502 mmol) was dissolved in 2 mL of neat dmbd and transferred to a glass tube. To this, 8 mL of toluene and 1.2 stoichiometric equivalents of S(TMS)₂ (0.158 mL, 0.753 mmol) were added and the solution was allowed to stir at room temperature for 3 days. All volatiles were removed *in vacuo* and the resulting thick white oil was washed with 2 mL of pentane (3-5 times) and lyophilized from 2 mL of benzene to remove excess S(TMS)₂. Compound **3.6^{Ph}** readily decomposed to **3.7** and other ³¹P-containing products in 24 h, which inhibited further characterization. Mixture yield: 45 mg (42 %).

¹H NMR (C₆D₆, 400 MHz, δ): 1.28 (s, 3H, CH₃), 1.85 (s, 3H, CH₃), 2.25 (dd, ²J_{HP} = 24.1 Hz, ²J_{HH} = 8 Hz, 1H, P–CH₂), 2.76 (m, 2H, S–CH₂), 3.30 (d, ²J_{HH} = 8 Hz, 1H, P–CH₂), 7.23-7.36 (3H, Ph CH), 7.46 (m, 2H, Ph CH).

¹³C{¹H} NMR (CDCl₃, 150.8 MHz, δ): 21.6, 22.4, 31.2 (d, ²J_{CP} = 4.0 Hz), 33.7 (d, ¹J_{CP} = 27.0 Hz), 125.4, 126.2 (d, ²J_{CP} = 9.0 Hz), 126.8 (d, ³J_{CP} = 1.5 Hz), 127.9 (d, ²J_{CP} = 7.5 Hz), 128.4, 130.8, 131.0, 138.1 (d, ¹J_{CP} = 40.0 Hz).

³¹P NMR (C₆D₆, 161.8 MHz, δ): -1.0 (m).

3.4.8 Synthesis of **3.7**

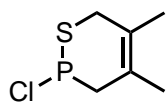


Dichlorophenylphosphine (90 mg, 0.502 mmol) was dissolved in 2 mL of neat 2,3-dimethyl-1,3-butadiene and transferred to a glass tube. To this, 1.2 stoichiometric equivalents of S(TMS)₂ (0.158 mL, 0.753 mmol) were added and the solution was allowed to stir at room temperature for 3 days. All volatiles were removed *in vacuo* and the resulting thick white oil was washed with 2 mL of pentane (3-5 times) and the pentane insoluble portion was found to contain **3.7**, based on the ¹H and ³¹P NMR spectroscopic data in comparison to previous literature.⁵³ Yield: 25 mg (23 %).

¹H NMR (C₆D₆, 400 MHz, δ): 1.84 (s, 6H, CH₃), 3.25 (d, ²J_{HP} = 12 Hz, 4H, CH₂), 7.56 (m, 4H, Ph CH), 7.87 (dd, ⁵J_{HP} = 4 Hz, ³J_{HH} = 12 Hz, 1H, Ph *para*-CH).

³¹P NMR (C₆D₆, 161.8 MHz, δ): 45.5 (br m, ²J_{PH} = 11.7 Hz).

3.4.9 Synthesis of **3.6^{Cl}**

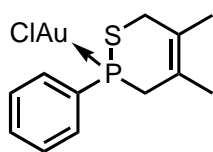


Freshly distilled trichlorophosphine (50 mg, 0.364 mmol) was dissolved in 5 mL of neat dmbd and transferred to a glass tube. To this, 1.2 stoichiometric equivalents of S(TMS)₂ (0.091 mL, 0.437 mmol) were added and the tube was sealed with grease. This was allowed to stir at room temperature for three days, at which point volatiles were removed *in vacuo*. The resulting cloudy oil was lyophilized from 3 mL of benzene six times to remove excess S(TMS)₂, although this strategy did not remove 100 % of the impurity. Further development of the purification method for this compound is necessary.

¹H NMR (C₆D₆, 400 MHz, δ): 0.32 (s, resid. S(TMS)₂), 1.67 (s, 3H, CH₃), 1.79 (s, 3H, CH₃), 2.54 (m, 1H, P–CH₂), 2.91 (m, 2H, S–CH₂), 3.26 (dd, ²*J*_{HH} = 6.4 Hz, ²*J*_{HP} = 16 Hz).

³¹P NMR (C₆D₆, 161.8 Hz, δ): 100.5 (br m).

3.4.10 Synthesis of **3.8^{Au}**



A mixture of **3.6^{Ph}/3.7** (30 mg, 0.135 mmol wrt **3.6^{Ph}**) was dissolved in 2 mL of DCM. To this, a solution of AuCl(THT) (43 mg, 0.135 mmol) in 0.5 mL of DCM was added with stirring. An immediate colour change was observed from colourless to yellow, and after 15 min of stirring, all volatiles were removed *in vacuo* to yield a yellow oil. This powder was washed with pentane and the pentane soluble portion was discarded, leaving a yellow powder after residual pentane was removed *in vacuo*. Yield: 50 mg (82 %).

m.p. (nitrogen sealed capillary): 151 °C (pale yellow to dark orange), 189-190 °C (melt)

¹H NMR (C₆D₆, 400 MHz, δ): 0.90 (s, 3H, CH₃), 1.29 (d, ⁴*J*_{HH} = 8 Hz, 3H, CH₃), 2.36 (br s, 2H, CH₂), 1.13 (dd, ²*J*_{HP} = 16 Hz, 1H, CH₂), 2.77 (dd, ²*J*_{HP} = 12 Hz, 1H, CH₂), 6.96 (m, 3H, Ph CH), 7.44 (dd, ⁵*J*_{HP} = 12 Hz, ⁴*J*_{HH} = 8 Hz, 2H, Ph CH).

¹³C{¹H} NMR (CDCl₃, 150.8 MHz, δ): 21.2 (d, ²*J*_{CP} = 4.5 Hz), 22.3, 33.2 (d, ²*J*_{CP} = 9.0 Hz), 36.2, 125.5 (d, ²*J*_{CP} = 6.6 Hz), 128.9 (d, ¹*J*_{CP} = 18.1 Hz), 130.5, 130.9, 131.0, 132.2, 132.4, 135.3 (d, ¹*J*_{CP} = 39.2 Hz).

³¹P NMR (C₆D₆, 161.8 Hz, δ): 39.4 (br).

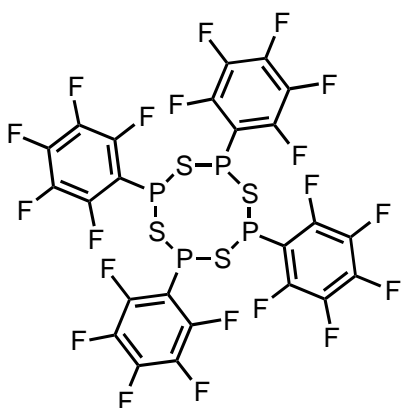
3.4.11 Synthesis of **3.8**^S

To a mixture of **3.6**^{Ph}/**3.7** (100 mg, 0.450 mmol wrt **3.6**^{Ph}) in 7.5 mL of toluene, one stoichiometric equivalent of elemental sulfur was added. The solution was allowed to stir vigorously overnight, at which point volatiles were removed *in vacuo* and left an off-white oil in the vial. Compound **3.8** was the first compound to elute from a 6:1 THF:pentane silica gel column performed under inert conditions. This compound has been previously isolated and characterized.⁵¹ Yield 30 mg (31 %).

¹H NMR (C₆D₆, 400 MHz, δ): 0.32 (s, resid. S(TMS)₂), 1.67 (s, 3H, CH₃), 1.79 (s, 3H, CH₃), 2.54 (m, 1H, P-CH₂), 2.91 (m, 2H, S-CH₂), 3.26 (dd, ²*J*_{HH} = 6.4 Hz, ²*J*_{HP} = 16 Hz).

³¹P NMR (C₆D₆, 161.8 Hz, δ): 66.2 (br m)

3.4.12 Synthesis of **3.9**



Dichloro(pentafluorophenyl)phosphine (50 mg, 0.186 mmol) was dissolved in 1 mL toluene and added to an NMR tube. Neat S(TMS)₂ was added to this and the solution was allowed to sit at 60 °C for half an hour. Upon complete consumption of starting phosphine, volatiles were removed *in vacuo* to yield a colourless oil. Crystals suitable for X-ray diffraction were grown from a concentrated pentane solution kept at -30 °C for

a week. Yield: 90 mg (53 %).

m.p. (nitrogen sealed capillary): 126.2 – 128.0 °C

ESI-MS: 920.28 *m/z* [C₂₄F₂₀P₄S₄]⁺, 722.04 *m/z* [C₁₈F₁₅P₃S₄]⁺

¹⁹F NMR (C₆D₆, 376 Hz, δ): -124.5 (m, *ortho*- F), -145.7 (tt, ³*J*_{FF} = 6.0 Hz, ⁴*J*_{FF} = 2.0 Hz, *para*-F), -158.1 (tdd, ³*J*_{FF} = 6.0 Hz, ⁴*J*_{FF} = 2.0 Hz, ⁴*J*_{FP} = 1.5 Hz, *meta*-F).

¹³C{¹H} NMR (CDCl₃, 150.8 MHz, δ): 111.2 (m), 127.8 (m), 136.5 (m), 139.0 (m), 145.0 (br s), 147.5 (br s).

³¹P NMR (C₆D₆, 161.8 Hz, δ): 66.5 (t, ³*J*_{PF} = 35.9 Hz).

3.4.13 Special Considerations for X-ray Crystallography

For compound **3.9**, severe disorder was present among the $-\text{C}_6\text{F}_5$ ligands bound to phosphorus. Several attempts were made to model this disorder; however, no chemically sensible solution could be obtained. For this reason, the structure was only solved isotropically and only serves as complimentary information to mass spectrometric data towards the confirmation of the P_4S_4 core.

Table 3-1. Summary of X-ray diffraction collection and refinement details for the compounds reported in Chapter 3

	3.3^{bisPh}	3.4^{1Fc}	3.6^{fPh}
CCDC Ref #			
Formula	$\text{C}_{34}\text{H}_{31}\text{PS}$	$\text{C}_{36}\text{H}_{35}\text{FePS}$	$\text{C}_{12}\text{H}_{10}\text{F}_5\text{PS}$
MW	502.62	586.52	312.23
Crystal system	monoclinic	orthorhombic	monoclinic
Space Group	$\text{P } 2_1/\text{c}$	$\text{P } 2_1 2_1 2_1$	$\text{P } 2_1/\text{c}$
<i>T</i> (K)	110	110	110
<i>a</i> (Å)	18.142(3)	7.684(3)	13.417(5)
<i>b</i> (Å)	9.1441(20)	18.479(6)	7.549(3)
<i>c</i> (Å)	16.666(2)	20.797(7)	12.544(3)
	90	90	90
	91.998(8)	90	101.246(8)
	90	90	90
<i>V</i> (Å³)	2763.1(9)	2953.1(17)	1246.0(7)
<i>Z</i>	4	4	4
<i>F</i> (000)	1064	1232	632
(g cm⁻¹)	1.208	1.319	1.664
Wavelength (Å)	0.71073	0.71073	0.71073
<i>Mu</i> (cm⁻¹)	0.196	0.659	0.431
Measured fraction of data	0.998	0.998	1.000
<i>R</i>_{merge}	0.0841	0.0726	0.0680
<i>R</i>₁, <i>wR</i>₂	0.0435, 0.1093	0.0342, 0.0705	0.0401, 0.0856
<i>R</i>₁ (all data)	0.0586	0.0487	0.0599
<i>wR</i>₂ (all data)	0.1167	0.0769	0.0922
GOF	1.084	1.014	1.077

3.5 References

- (1) Heal, H. G. *The inorganic heterocyclic chemistry of sulphur, nitrogen, and phosphorus*; Academic Press, **1980**.
- (2) He, G.; Shynkaruk, O.; Lui, M. W.; Rivard, E. *Chem. Rev.* **2014**, *114*, 7815–7880.
- (3) Wang, L.; Ganguly, R. *Organometallics*. **2014**, *4*, 14–17.
- (4) Van Eis, M. J.; Zappey, H.; De Kanter, F. J. J.; De Wolf, W. H.; Lammertsma, K.; Bickelhaupt, F. J. *Am. Chem. Soc.* **2000**, *122*, 3386–3390.
- (5) Santini, C. C.; Fischer, J.; Mathey, F.; Mitschler, A. *J. Am. Chem. Soc.* **1980**, *102*, 5809–5815.
- (6) Price, A. N.; Nichol, G. S.; Cowley, M. J. *Angew. Chem. - Int. Ed.* **2017**, *56*, 9953–9957.
- (7) Li, X.; Lei, D.; Chiang, M. Y.; Gaspar, P. P. *J. Am. Chem. Soc.* **1992**, *114*, 8526–8531.
- (8) Hung, J.; Yang, S.; Chand, P.; Gray, G. M. *J. Am. Chem. Soc.* **1994**, *10*, 10966–10971.
- (9) Frenking, G.; Bertrand, G. *Science*. **2012**, *337*, 1526–1529.
- (10) Dielmann, F.; Bertrand, G. *Chem. Eur. J.* **2015**, *21*, 191–198.
- (11) Chitnis, S. S.; Sparkes, H. A.; Annibale, V. T.; Pridmore, N. E.; Oliver, A. M.; Manners, I. *Angew. Chem. - Int. Ed.* **2017**, *56*, 9536–9540.
- (12) Gaspar, P. P.; Qian, H.; Beatty, A. M.; André D'Avignon, D.; Kao, J. L. F.; Watt, J. C.; Rath, N. P. *Tetrahedron*. **2000**, *56*, 105–119.
- (13) Henne, F. D.; Watt, F. A.; Schwedtmann, K.; Hennersdorf, F.; Kokoschka, M.; Weigand, J. J. *Chem. Comm.* **2016**, *52*, 2023–2026.
- (14) Liu, L.; Ruiz, D. A.; Munz, D.; Bertrand, G. *Chem.* **2016**, *1*, 147–153.
- (15) Mathey, F. *Angew. Chem. - Int. Ed.* **1987**, *26* (4), 275–286.
- (16) Schwedtmann, K.; Hennersdorf, F.; Bauz, A.; Frontera, A.; Fischer, R.; Weigand, J. J. *Angew. Chem. - Int. Ed.* **2017**, *3*, 6218–6222.
- (17) Waterman, R. *Chem.* **2016**, *1*, 27–29.
- (18) Marinetti, A.; Mathey, F.; Fischer, J.; Mitschler, A. *J. Am. Chem. Soc.* **1982**, *104*, 4484–4485.
- (19) Fruhauf, H. *Chem. Rev.* **1997**, *97*, 523–596.

- (20) Fischer, J.; Marinetti, A.; Charrier, C.; Mathey, F. *Organometallics*. **1985**, *4*, 2134–2138.
- (21) Breunig, J. M.; Hu, A.; Bolte, M.; Wagner, M.; Lerner, H. *Organometallics*. **2013**, *32*, 6792–6799.
- (22) Aktas, H.; Slootweg, J. C.; Ehlers, A. W.; Lutz, M.; Spek, A. L.; Lammertsma, K. *Organometallics*. **2009**, *28*, 5166–5172.
- (23) Caputo, C. A.; Koivistoinen, J.; Moilanen, J.; Boynton, J. N.; Tuononen, H. M.; Power, P. P. *J. Am. Chem. Soc.* **2013**, *135*, 1952–1960.
- (24) Foreman, M. R. S. J.; Slawin, A. M. Z.; Woollins, J. D. *J. Chem. Soc. Dalt. Trans.* **1999**, *3*, 1175–1184.
- (25) Lammertsma, K. *Top. Curr. Chem.* **2003**, *229*, 95–119.
- (26) Transue, W. J.; Velian, A.; Nava, M.; Garc, C.; Temprado, M.; Cummins, C. C. *J. Am. Chem. Soc.* **2017**, *139*, 10822–10831.
- (27) Compain, C.; Donnadieu, B.; Mathey, F. *Organometallics*. **2005**, *24*, 1762–1765.
- (28) Folkins, P. L.; Vincent, B. R.; Harpp, D. N. *Tetrahedron Lett.* **1991**, *32*, 7009–7012.
- (29) Foreman, M. R. S. J.; Slawin, A. M. Z.; Woollins, J. D. *Chem. Comm.* **1997**, *7*, 855–856.
- (30) Kalinina, I.; Donnadieu, B.; Mathey, F. *Organometallics*. **2005**, *24*, 696–699.
- (31) Kyri, A. W.; Schnakenburg, G.; Streubel, R. *Chem. Comm.* **2016**, *52*, 8593–8595.
- (32) Majhi, P. K.; Koner, A.; Schnakenburg, G.; Kelemen, Z.; Nyulászi, L.; Streubel, R. *Eur. J. Inorg. Chem.* **2016**, *22*, 3559–3573.
- (33) Marinetti, A.; Mathey, F. *J. Am. Chem. Soc.* **1985**, *107*, 4700–4706.
- (34) Nakayama, S.; Yoshifuji, M.; Okazaki, R.; Inamoto, N. *Chem. Comm.* **1971**, *113*, 1186–1187.
- (35) Nakayama, S., Yoshifuji, M., Okazaki, R., Inamoto, N. *Chem. Comm.* **1971**, 546–548.
- (36) Wit, J. B. M.; Eijkel, G. T. Van; Franciscus, J. J.; Kanter, D.; Schakel, M.; Ehlers, A. W.; Spek, A. L.; Lammertsma, K. *Angew. Chem. - Int. Ed.* **1999**, *2*, 2596–2599.
- (37) Wit, J. B. M.; De Jong, G. B.; Schakel, M.; Lutz, M.; Ehlers, A. W.; Slootweg, J. C.; Lammertsma, K. *Organometallics*. **2016**, *35*, 1170–1176.

- (38) Graham, C. M. E.; Valjus, J.; Pritchard, T. E.; Boyle, P. D.; Tuononen, H. M.; Ragogna, P. J. *Inorg. Chem.* **2017**, *15*, 13500-13509.
- (39) Graham, C. M. E.; Pritchard, T. E.; Boyle, P. D.; Valjus, J.; Tuononen, H. M.; Ragogna, P. J. *Angew. Chem. - Int. Ed.* **2017**, *129*, 6332–6336.
- (40) Charles, M. U. H.; Caughlan, N.; Ramirez, F.; Pilot, J. F.; Smith, C. P. *J. Am. Chem. Soc.* **1971**, *93*, 5229–5235.
- (41) Kawashima, T.; Okazaki, R.; Okazaki, R. *Chem. Comm.* **1997**, *109*, 2500–2502.
- (42) Kawashima, T.; Okazaki, R.; Takami, H. *J. Am. Chem. Soc.* **1994**, *116*, 4509–4510.
- (43) Kawashima, T.; Kato, K. *Angew. Chem. - Int. Ed.* **1993**, *32*, 869–870.
- (44) Kyri, A. W.; Brehm, P.; Schnakenburg, G.; Streubel, R. *Dalt. Trans.* **2017**, *46*, 2904–2909.
- (45) Kyri, A. W.; Schnakenburg, G.; Streubel, R. *Organometallics*. **2016**, *35*, 563–568.
- (46) Foreman, M. R. S. J.; Slawin, A. M. Z.; Woollins, J. D. *Phosphorus, Sulfur, Silicon Relat. Elem.* **1997**, *124*, 469–472.
- (47) Puke, C.; Erker, G.; Aust, N. C.; Würthwein, E. U.; Fröhlich, R. *J. Am. Chem. Soc.* **1998**, *120*, 4863–4864.
- (48) Wilker, S.; Laurent, C.; Sarter, C.; Puke, C.; Erker, G. *J. Am. Chem. Soc.* **1995**, *117*, 7293–7294.
- (49) Kawashima, T.; Iijima, T.; Kikuchi, H.; Okazaki, R. *Phosphorus, Sulfur, Silicon Relat. Elem.* **2008**, *6507*, 2–6.
- (50) Graham, C. M. E.; Macdonald, C.; Boyle, P.; Wisner, J.; Ragogna, P. J.; *Chem. Eur. J.* **2017**, *28*, 743-749.
- (51) Apitz, J.; Grobe, J.; Le Van, D. Z. *Naturforsch.* **1988**, *43*, 257–260.
- (52) Pyykkö, P.; Atsumi, M. *Chem. Eur. J.* **2009**, *33*, 186–197.
- (53) Holand, S.; Mathey, F. *J. Org. Chem.* **1981**, *46*, 4386–4389.

Chapter 4

4 Conclusions and Future Outlook

4.1 Conclusions

This thesis encompasses the synthesis and characterization of a number of novel P,S-heterocycles and asymmetric phosphines. Despite the high interest in Groups 15 and 16, phosphinidene chalcogenides have remained elusive species and their reactivity is poorly understood. Literature examples do exist for oxygen and sulfur derivatives of this system, with recent achievements highlighting the transfer of $RP=S$ from the thermolysis of P_2S_2 heterocycles and transfer from 7-phosphanorbornadienes to unsaturated organic moieties.¹⁻⁴ Particularly exciting about this work is the successful transfer of $RP=S$ by simple salt metathesis at room temperature without the need for metal stabilization or bulky ligand design, and often without requiring solvent to yield novel [2+4] cycloadducts.¹ Two mechanisms have been proposed for these transformations, most notable being the transfer of $RP=S$ from an 8-membered ring discussed in Chapter 3.

Asymmetric phosphines (**2.2-2.4**) were prepared by metathesis reactions performed utilizing compound **2.1** as a precursor. These phosphines contained a bulky *m*-terphenyl substituent in addition to two unique functional groups (*eg.* $N(Et)_2$, Cl, H, TMS). The potential to use these asymmetric phosphines as stoichiometric reagents for the generation of P-P single bonds was probed, although no promising results were obtained which indicated the successful formation of a P-P single bond. Nevertheless, compounds **2.2-2.4** were characterized to the fullest extent and can be envisioned to act as monodentate ligands for transition metals or as reagents in various other chemical transformations. The formation of a single P-P bond was achieved without the need for transition metals by the reduction of diphosphene (**2.5**) to diphosphane (**2.6**). Terphenyldiphosphane was structurally characterized for the first time. The utility of compound **2.6** as a reagent was probed by targeting dehydrohalogenation with S_2Cl_2 and base, with no reproducible results. Monophosphanysulfane (**2.7**) and diphosphanyselane (**2.8**) were obtained by the condensation reaction of **2.2** with $S(TMS)_2$ and $Se(TMS)_2$,

respectively, and belong to a class of underrepresented compounds in literature. They see potential use as precursors for the synthesis of phosphorus chalcogen heterocycles as well.

Monomeric $\text{RP}=\text{S}$ was accessed from the parent dimer **3.2** with gentle heat to result in the formation of novel phosphirene sulfides (**3.3ⁿ**) and thiaphosphetenes (**3.4ⁿ**) in the presence of alkynes. The thermolysis of the parent ring successfully transferred $\text{RP}=\text{S}$ to electron-rich and aryl-substituted alkynes; however, alkynes which possessed TMS functional groups did not result in the formation of heterocyclic compounds. When the thermolysis was performed with an electron-rich alkyne (*ie.* ethynylferrocene), olefinic reactivity was dominant and resulted in the formation of **3.4^{IFc}** as the major product. This was a contrast to the formation of **3.3^{bisPh}** as the major product as result of carbenic reactivity when 1,4-ethynylbenzene was used as the trapping agent during the thermolysis reaction. Allowing **3.1** and $\text{S}(\text{TMS})_2$ to stir in a saturated solution of ethynylferrocene or 1,4-ethynylbenzene resulted in the successful transfer of $\text{RP}=\text{S}$ to yield **3.4^{IFc}** and **3.3^{bisPh}** as the sole products, respectively. At this time the reason as to why one reactivity pathway was favoured over the other is not fully understood, but was largely dependent on the trapping agent used.

Monomeric $\text{RP}=\text{S}$ was generated from the condensation reaction of various dichlorophosphines which did not possess steric bulk and $\text{S}(\text{TMS})_2$. Performing these reactions in neat dmbd lead to the formation of [2+4] and [1+4] cycloadducts (**3.6^R** and **3.7**, respectively). This marked the first successful transfer of a phosphinidene sulfide to a diene without a norbornadiene scaffold, Lewis acidic metal, or bulky aryl substituent. Performing the condensation reaction with FcPCl_2 , $^{\text{F}}\text{PhPCl}_2$, and PCl_3 resulted in only olefinic reactivity and yielded [2+4] cycloadducts with dmbd. Interestingly, when PhPCl_2 was used both olefinic (**3.6^{Ph}**) and carbenic (**3.7**) products were isolated. The synthesis of these P(III) heterocycles is an exciting feat for this field, as derivitization has been required to isolate these compounds in most cases.⁵⁻⁸ That being said, the resultant cycloadducts were prone to decomposition in a short time period and their oily nature has largely inhibited structural analysis by X-ray diffraction. Attempts to derivitize the P(III) center of these compounds to obtain crystalline sample have not resulted in the successful formation of product across many reaction partners, perhaps because of intrinsic

instability of the cycloaddition products. No ^{31}P -containing spectroscopic signal which could be assigned as an intermediate was observed for most of these reactions; however, in the case where $^{\text{F}}\text{PhPCl}_2$ was used, a different reaction mechanism was observed. The intermediate in this case was an 8-membered P_4S_4 ring, which was proposed to degrade into monomeric $\text{RP}=\text{S}$ fragments at room temperature that subsequently underwent a [2+4] cycloaddition in the presence of dmdb. The lysis of an 8-membered P_xS_x ($x = 3, 4$) ring into its phosphinidene sulfide monomeric units is unprecedented in the literature.

The work detailed in this thesis described not only the synthesis and characterization of novel asymmetric phosphines and cycloaddition products, but development of a method whereby various dichlorophosphines were utilized as reliable sources of $\text{RP}=\text{S}$ when used in reactions with $\text{S}(\text{TMS})_2$ and dmdb. This exciting finding demonstrated that intricate ligand design and transition metals are not a requirement for the transfer of low-coordinate phosphorus species to organic units of unsaturation, and the reaction remarkably takes place at room temperature. Although further development pertaining to the purification of these compounds for bulk compositional analysis is required, this finding was an exciting addition to the known methods for $\text{RP}=\text{S}$ transfer. These results contribute to the vast understanding of phosphorus-sulfur chemistry and are aimed to motivate discussion regarding the true electronic nature of phosphinidene sulfides and what factors govern their preference to react in either an olefinic or carbenic fashion. It would be particularly exciting if the condensation method described here could be performed with other heteroatoms as well, potentially broadening the scope of $\text{RP}=\text{E}$ transfer reactions ($\text{E} = \text{N}, \text{Se}, \text{Te}$).

4.2 Future Work

4.2.1 Additional Work Pertaining to Chapter 3

Although many of the compounds described in Chapter 3 have been successfully isolated, difficulty has persisted in obtaining analytically pure bulk samples of [2+4] cycloadducts for elemental analysis prior to their decomposition. To confirm the composition of these oily compounds, for which analysis by X-ray diffraction has not been possible, elemental analysis data are required. For this reason, further development

of purification methods for these cycloadducts is necessary – especially as it pertains to residual S(TMS)₂ removal from the oils. Modification of the P(III) center was attempted with a variety of reaction partners, although no promising results have been obtained thus far. In an attempt to circumvent the high boiling point of S(TMS)₂, Na₂S and Li₂S were employed as the source of sulfide but did not result in the formation of the desired products.

Throughout the optimization of the condensation method across the differing dichlorophosphines, it was found that olefinic reactivity was favoured by performing the reaction at low concentrations. Increasing the dilution of the reaction mixture lead to increased formation of olefinic reactivity products and decreased formation of other minor products. The formation of **3.6^{Ph}** was favoured over **3.7** (< 5 % by integration) when the reaction mixture was diluted 1:4 with toluene. Performing this same reaction at higher concentrations (50 mg/ mL in neat dmbd) lead to an almost equal distribution of **3.6^{Ph}** and **3.7** by integration of the ³¹P{¹H} NMR spectrum. A similar dependence on concentration was observed for the thermolysis method, whereby increased dilution favoured the formation of olefinic products. Further studies to assess the nature of this concentration dependence are encouraged, as the ability to bias the formation of [2+2] over [1+2] cycloadducts would circumvent the need for the time-consuming purification methods described above.

A mechanistic study focusing on the lysis of the 8-membered ring (**3.9**) to release reactive RP=S in solution at room temperature is also warranted. This mechanism has not been observed by researchers in the field previously for 6- and 8-membered P,S-heterocycles. Our early work has defined a definite relationship between **3.9** and the resultant [2+4] cycloadduct, **3.6^{FPh}**. In order to better understand what occurred here, kinetic studies are imperative. In doing so, the role of the various reaction partners can be ascertained such that the role of the trapping agent and R group on phosphorus are better understood.

4.2.2 Bulky Ligands to Stabilize RP=S

We have previously demonstrated that the bulk of the *m*-terphenyl ligand is sufficient to stabilize the P(III) center in RP=S dimer **3.2** from degradation, but not bulky enough to inhibit dimerization of monomer RP=S. Increasing the steric bulk at phosphorus has enabled us to observe a free phosphinidene sulfide by $^{31}\text{P}\{^1\text{H}\}$ NMR spectroscopy through the condensation reaction of TripPCl_2 and $\text{S}(\text{TMS})_2$ (Trip = 2,6-Mes* $_2\text{C}_6\text{H}_3$, Mes* = 2,4,6-triisopropylphenyl). Dimerization did still occur and compound **4.1** has been isolated and structurally characterized as a product of this reaction (Figure 4-1).

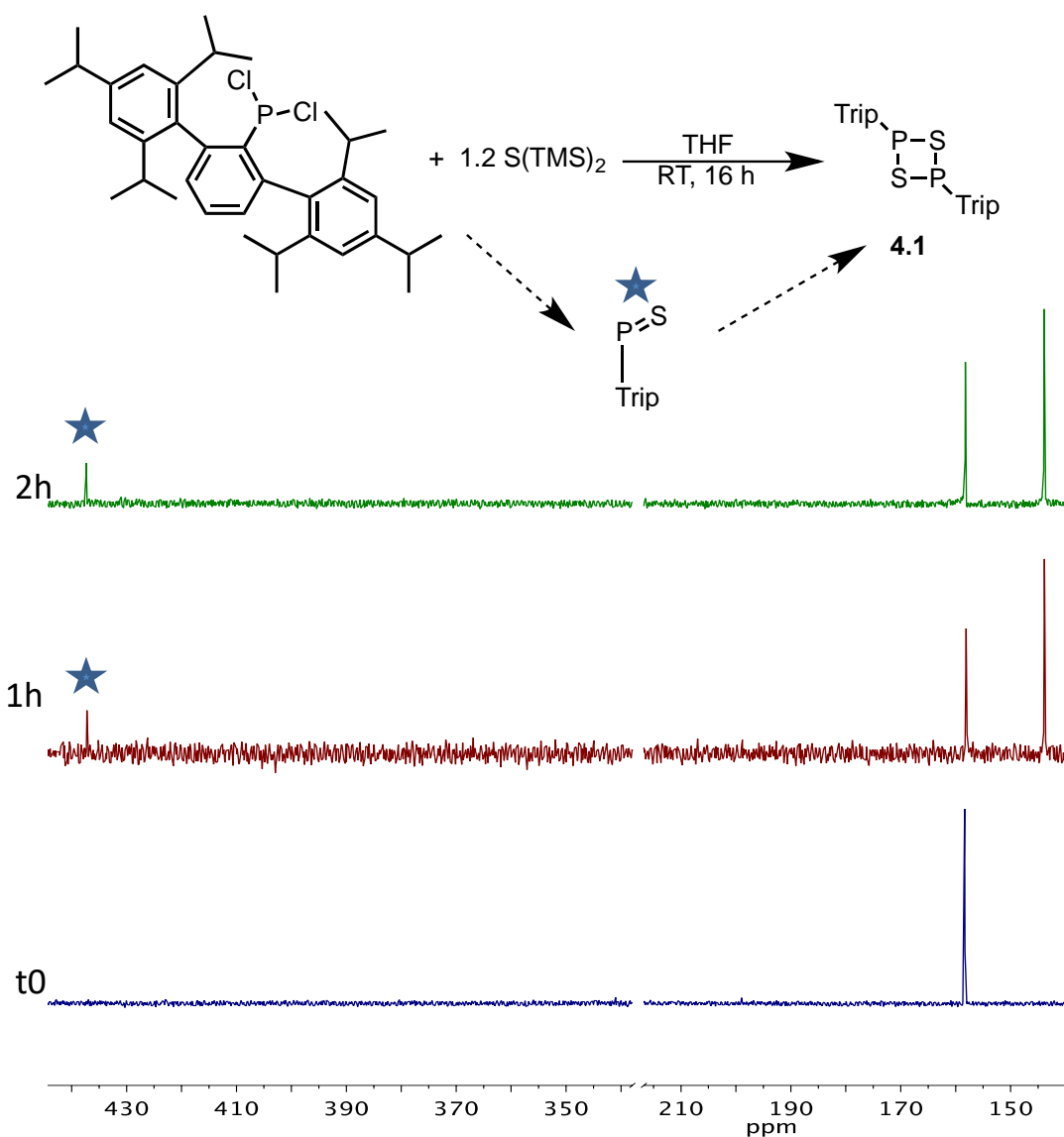


Figure 4-1. Reaction of TripPCl_2 with $\text{S}(\text{TMS})_2$ to form $\text{RP}=\text{S}$ dimer **4.1**. Stacked $^{31}\text{P}\{^1\text{H}\}$ NMR spectra taken at various time points are included to show the hypothesized formation of free $\text{RP}=\text{S}$ (denoted with a star) at 438 ppm. Dimer **4.1** has a phosphorus chemical shift of 143 ppm.

When the reaction was performed in toluene, compound **4.1** readily crystallized from the reaction mixture and crystals were submitted for analysis by X-ray diffraction which confirmed the structure of the dimer (Figure 4-2). Compound **4.1** crystallized with 2 molecules in the asymmetric unit and a single toluene molecule. In comparison to compound **3.2** which was previously characterized by our group, there was an increase in bond lengths and angles which was attributed to the added strain imparted by the bulkier Trip ligand.² The ¹H NMR spectrum contained a single set of Trip resonances, where each of the Me groups corresponding to the ⁱPr portion of the ligand have distinct chemical shifts – another indication of ring strain given that the compound contains high

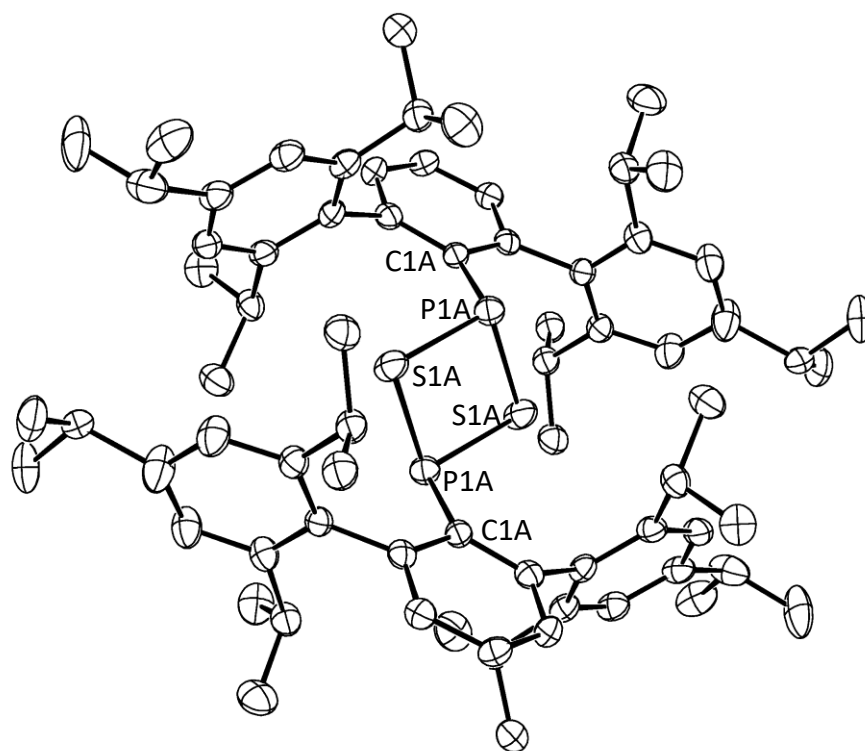
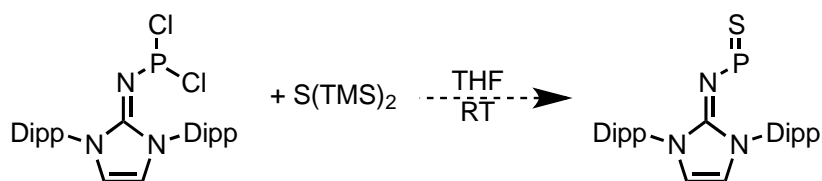


Figure 4-2. Solid state structure of **4.1** as determined by X-ray diffraction. The crystal contains two molecules in the asymmetric unit, although only one has been shown here for clarity. Pertinent bond lengths (Å) and angles (°) are as follows: S(1A)-P(1A) 2.1388(14), S(1A)-P(1A)¹ 2.1460(12), P(1A)-C(1A) 1.845(3), P(1A)-S(1A)-P(1A)¹ 90.58(5), C(1A)-P(1A)-S(1A)¹ 103.72(10), C(1A)-P(1A)-S(1A) 107.23(11), S(1A)-P(1A)-S(1A)¹ 89.42(5), C(2A)-C(1A)-P(1A) 119.0(3), C(6A)-C(1A)-P(1A) 123.7(2).

symmetry. Interestingly, despite 3 separate environments for the methyl groups, only two multiplets were observed corresponding to the central C-H bond of the ⁱPr group (³J_{HH} = 8 Hz).

A further increase in the steric bulk at phosphorus could allow for the isolation of a phosphinidene sulfide. Bulky amido ligands developed by Jones and coworkers offer a similar reactivity profile in comparison to the terphenyl ligands used by Power, but have not yet resulted in the formation of phosphinidene sulfides.^{9,10} Through collaboration with the Rivard group a potential remedy to this issue has been offered by using the bulky ligand shown in Scheme 4-2.



Scheme 4-1. Hypothesized reaction between an NHC-based dichlorophosphine and $\text{S}(\text{TMS})_2$ to yield an isolable phosphinidene sulfide

Early experiments performing the condensation reaction with this dichlorophosphine have resulted in the formation of a product with a chemical shift of $\delta_{\text{P}} = 488$. This downfield chemical shift was indicative of $\text{RP}=\text{S}$ formation although further work is required to ascertain the true structure of the product. Should the dichlorophosphine provided by the Rivard group allow to the isolation of $\text{RP}=\text{S}$, it would be quite interesting to explore this chemistry with heavier main group elements as well (*eg.* As, Sb, Se, Te).

4.2.3 Cycloaddition Chemistry: Expanding the scope of trapping reagents

Both thermolysis and condensation methods have proven to be successful for the *in situ* generation of $\text{RP}=\text{S}$ and its subsequent transfer to trapping reagents, such as alkynes and dmbd. It would be of both fundamental and synthetic interest to expand this reactivity beyond unsaturated C-C bonds to those which include other heteroatoms (*eg.* C=O, C=N). Early experiments have been performed which have used the thermolysis

method to assess RP=S transfer to a number of various trapping reagents with mixed results.

Heating a sample of **3.2** in a saturated solution of ferrocenecarboxaldehyde resulted in the formation of one new peak in the $^{31}\text{P}\{^1\text{H}\}$ NMR spectrum at -5 ppm (Figure 4-3). Unreacted ferrocenecarboxaldehyde proved to be exceptionally difficult to remove from the crude dark red oil – with both solubility and sublimation being unsuccessful. The tentatively proposed structure is compound **4.2**, where a [2+2] cycloaddition occurred between the RP=S double bond and the C=O double bond of the aldehyde. The peak assigned to **4.2** was a broad multiplet in the ^{31}P NMR spectrum. While further characterization of this compound is required, the formation of one major isolable product was encouraging. It would be of interest to perform the analogous reaction by the condensation method to see if the selectivity for the product at -5 ppm is maintained. At this time, further work is necessitated to fully understand this transformation.

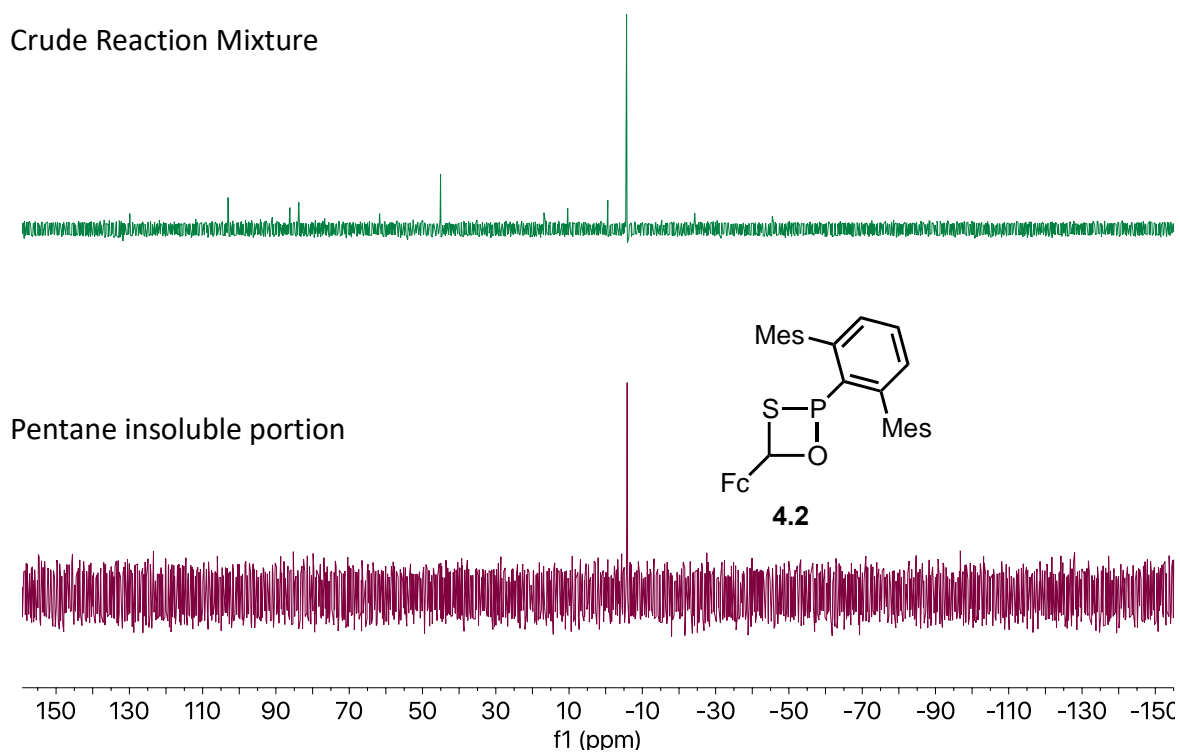


Figure 4-3. Stacked $^{31}\text{P}\{^1\text{H}\}$ NMR spectra which show the crude reaction mixture following the thermolysis of **3.2** in a saturated toluene solution of ferrocenecarboxaldehyde (top) and the pentane insoluble portion (bottom)

A number of other trapping agents were used as reaction partners by the thermolysis methodology. Generally, these reactions consisted of gently heating a toluene solution of **3.2** in a solution of 5 stoichiometric equivalents of trapping reagent. It was observed that performing the reaction without a great excess of trapping agent leads to poor conversion and decreased selectivity by $^{31}\text{P}\{^1\text{H}\}$ NMR spectroscopy. While the aldehydes tested indicated that a reaction with $\text{RP}=\text{S}$ readily occurred, benzophenone and acetone did not result in the formation of product. When azobenzene or diphosphene (**2.5**) were used as reaction partners, a large number of unidentifiable peaks were observed in the $^{31}\text{P}\{^1\text{H}\}$ NMR spectra. Performing the reaction with MeCN lead to the appearance of 5 new signals in the crude $^{31}\text{P}\{^1\text{H}\}$ NMR spectrum; however, the analogous reaction with phenylnitrile did not result in the disappearance of **3.2** by $^{31}\text{P}\{^1\text{H}\}$ NMR spectroscopy. The thermolysis of **3.2** in the presence of various diaza-esters, provided in collaboration with the Workentin Group, also resulted in the formation of 1 or 2 major products by $^{31}\text{P}\{^1\text{H}\}$ NMR spectroscopy, although major difficulty in the separation of the resulting products was an issue.

Performing this reactivity assay has indicated to us that $\text{RP}=\text{S}$ transfer can be accomplished with unsaturated functional groups outside of C-C double and triple bonds using the thermolysis methodology. These reactions have often resulted in the formation of numerous products in contrast to the more selective reactivity observed with alkynes and dmbd. It remains a question as to whether the number of products formed would decrease should the condensation method be employed for these transformations. Expanding the reactivity assay study to include 1,3-dipoles (*eg.* isocyanates) offers an interesting opportunity to expand on the cycloaddition chemistry we have observed thus far.

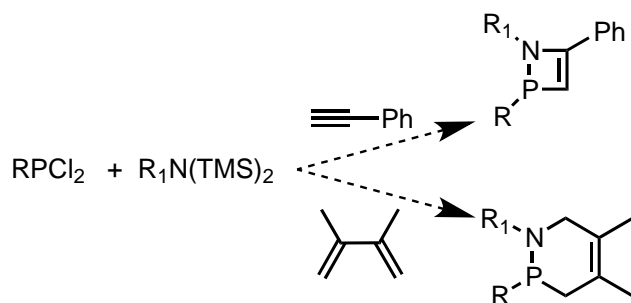
4.2.4 Cycloaddition Chemistry: Alkynes with β -Hydrogens

As part of the reactivity assay performed to asses the versatility of the thermolysis method, a number of alkynes with β -hydrogens (*eg.* 2-butyne) were employed as trapping reagents. The resultant crude $^{31}\text{P}\{^1\text{H}\}$ NMR spectra contained new signals which did not correspond to what we had previously observed for thiaphosphetenes or phosphirene sulfides. Instead, the major products were found to contain P-H coupling constants which

would typically be assigned as $^1J_{\text{PH}}$. We have not yet fully characterized the products of these reactions; however, similar product distributions were observed when bromo-3-propyne and (trimethylsilyl)-3-propyne were used as the trapping reagent. It was hypothesized that a rearrangement could take place because of the presence of β -hydrogen atoms. Complete characterization of these products would give insight into the nature of this transformation.

4.2.5 The Condensation Method: Can we transfer other $\text{RP}=\text{E}$?

This work has demonstrated the versatility of both the thermolysis and condensation methods of *in situ* $\text{RP}=\text{S}$ transfer with gentle heat and at room temperature, respectively. With these results in mind, it is reasonable to entertain that other $\text{Ch}(\text{TMS})_2$ reagents may also be amenable to subsequent $\text{RP}=\text{Ch}$ transfer in a similar fashion. Test reactions performed with $\text{Se}(\text{TMS})_2$ lead to the appearance of spectroscopic signals which had similar chemical shifts to their respective [1+2], [2+2], and [2+4] derivatives. While this was promising, the inherent instability of the heavier chalcogen congener resulted in uncontrolled reactivity and many signals in the $^{31}\text{P}\{^1\text{H}\}$ NMR spectrum. This had not been pursued further, but presents an opportunity to transfer $\text{RP}=\text{Ch}$ with heavier chalcogen atoms, an area absent in current literature. Others working in the area of phosphinidene transfer have shown the successful transfer of $\text{RP}=\text{E}$ fragments by extrusion from 7-phosphanorbornadiene scaffolds ($\text{E} = \text{B}, \text{N}, \text{P}, \text{S}, \text{W}(\text{CO})_5$).^{5,7,8,11–14} It would be interesting to explore whether $\text{RE}(\text{TMS})_2$ reagents would result in similar reactivity as $\text{S}(\text{TMS})_2$ and result in the formation of cycladducts such as the ones proposed in Figure 4-4 ($\text{R} = \text{alkyl}, \text{aryl}$). This would offer a superior method to what is currently available in literature for $\text{RP}=\text{NR}$ transfer to trapping reagents such as dmbd and alkynes. Ideally, a library of 3-6-membered rings could be synthesized as the result of reactivity of a variety of two-coordinate phosphidenes with alkenes, dienes and alkynes. These could then be characterized to develop a firm understanding of the structure and bonding in products formed as a result of the condensation method of *in situ* phosphinide generation.



Scheme 4-2. Proposed $\text{RP}=\text{NR}_1$ to phenylacetylene or dmbd upon the condensation of a dichlorophosphine with $\text{R}_1\text{N}(\text{TMS})_2$ to yield 4- and 6-membered rings respectively. R is an alkyl or aryl group for each case.

4.3 Synthesis of 4.1

TripPCl_2 was prepared according to a method developed by the Ragogna Group for the synthesis of bulky dichlorophosphines.² TripPCl_2 (60 mg, ___ mmol) was dissolved in 1 mL toluene and added to an NMR tube. Neat $\text{S}(\text{TMS})_2$ was added to this and the solution was allowed to sit at room temperature overnight. The colourless solution becomes a peach colour over this time, although the powder is off-white upon removal of volatiles *in vacuo*. Crystals suitable for X-ray diffraction grew from the reaction mixture at room temperature over the course of the reaction. Yield: 50 mg (___ %).

m.p. (nitrogen sealed capillary): 126.2 – 128.0 °C

ESI-MS: 577.3 m/z [$\text{C}_{36}\text{H}_{49}\text{PS}_2$]⁺, 1089.6 [$\text{C}_{72}\text{H}_{98}\text{P}_2\text{S}_2$]⁺.

^1H NMR (CDCl_3 , 400 MHz, δ): 1.09 (d, $^3J_{\text{HH}} = 8.0$ Hz, 12H, Mes* *ortho*-CH₃), 1.22 (d, $^3J_{\text{HH}} = 8.0$ Hz, 12H, Mes* *ortho*-CH₃), 1.32 (d, $^3J_{\text{HH}} = 8.0$ Hz, 12H, Mes* *para*-CH₃), 2.53 (sept, $^3J_{\text{HH}} = 8.0$ Hz, 4H, Mes* *ortho*-CH), 2.96 (sept, $^3J_{\text{HH}} = 8.0$ Hz, 2H, Mes* *para*-CH), 7.06 (s, 4H, Mes* C_{sp2}H), 7.14-7.16 (s, 2H, Ph CH), 7.39 (t, $^3J_{\text{HH}} = 7.2$ Hz, 1H, Ph CH)

$^{13}\text{C}\{^1\text{H}\}$ NMR (CDCl_3 , 150.8 MHz, δ): 14.1 (s), 22.3 (s), 23.0 (s), 24.0 (s), 25.6 (s), 30.9 (s), 33.9 (s), 34.1 (s), 67.9 (s), 120.6 (s), 127.7 (s), 131.4 (s), 134.9 (s), 143.2 (s), 146.3 (s), 147.8 (s).

^{31}P NMR (C_6D_6 , 161.8 Hz, δ): 143.0 (s)

4.4 References

- (1) Ragogna, P. J.; Graham, C.; Macdonald, C.; Boyle, P.; Wisner, J. *Chem. A Eur. J.* **2017**, *24*, 743-749.
- (2) Graham, C. M. E.; Pritchard, T. E.; Boyle, P. D.; Valjus, J.; Tuononen, H. M.; Ragogna, P. J. *Angew. Chem. - Int. Ed.* **2017**, *129*, 6332–6336.
- (3) Byrne, P. A.; Gilheany, D. G. *Chem. Soc. Rev.* **2013**, *42*, 6670.
- (4) Mathey, F. *Angew. Chem. - Int. Ed.* **2003**, *42*, 1578–1604.
- (5) Compain, C.; Donnadiou, B.; Mathey, F. *Organometallics*. **2005**, *24*, 1762–1765.
- (6) Mathey, F. *Dalton Trans.* **2007**, *42*, 1861–1868.
- (7) Transue, W. J.; Velian, A.; Nava, M.; Garc, C.; Temprado, M.; Cummins, C. C. *J. Am. Chem. Soc.* **2017**, *139*, 10822–10831.
- (8) Wang, L.; Ganguly, R. *Organometallics*. **2014**, *33*, 5614–5617.
- (9) Rodrigues, R. R. *et al. Chem. Comm.* **2014**, *50*, 162–164.
- (10) Bockfeld, A. D.; Bannenberg, T.; Jones, P. G.; Bockfeld, D.; Bannenberg, T.; Jones, G.; Tamm, M. *Eur. J. Inorg. Chem.* **2017**, *28*, 3452-3458.
- (11) Mathey, F. *Angew. Chem. - Int. Ed.* **1987**, *26*, 275–286.
- (12) Frenking, G.; Bertrand, G. *Science*. **2012**, *337*, 1526–1529.
- (13) Liu, L.; Ruiz, D. A.; Munz, D.; Bertrand, G. *Chem.* **2016**, *1*, 147–153.
- (14) Rivard, E.; Merrill, W. A.; Fettingner, J. C.; Wolf, R.; Spikes, G. H.; Power, P. P. *Inorg. Chem.* **2007**, *46*, 2971–2978.

Chapter 5

5 Appendices

5.1 Experimental Methods

5.1.1 General Experimental Details

All manipulations were performed under inert atmosphere either in a nitrogen-filled MBraun Labmaster 130 Glovebox or on a Schlenk line. Solvents were obtained from Caledon and dried using an MBraun Solvent Purification System or by distillation from CaH_2 (HMDSO, CDCl_3). Dried solvents were collected under vacuum in a flame dried Straus flask and stored over 4 Å molecular sieves. Solvents for NMR spectroscopy (CDCl_3 , C_6D_6) were stored in the drybox over 4 Å molecular sieves. Solvent used for CV (MeCN) was freshly distilled from CaH_2 .

5.1.2 General Instrumentation

Solution ^1H , $^{13}\text{C}\{^1\text{H}\}$, $^{19}\text{F}\{^1\text{H}\}$, and $^{31}\text{P}\{^1\text{H}\}$ Nuclear Magnetic Resonance (NMR) spectra was recorded on a Varian INOVA 400 MHz spectrometer (^1H 400.09 MHz, ^{31}P 161.8 MHz, ^{19}F 377 MHz, $^{13}\text{C}\{^1\text{H}\}$ 100.5 MHz) unless otherwise noted. Some $^{13}\text{C}\{^1\text{H}\}$ spectra were recorded on a Varian INOVA 600 MHz spectrometer (^{13}C 150.8 MHz) and referenced to the ^{13}C signal of the solvent relative to tetramethylsilane (CDCl_3 ; $\delta_{\text{C}} = 77.1$, C_6D_6 ; $\delta_{\text{C}} = 128.06$). All samples for ^1H NMR spectroscopy were referenced to the residual protons in the deuterated solvent relative to tetramethylsilane (CDCl_3 ; ^1H $\delta = 7.26$, C_6D_6 ; ^1H $\delta = 7.16$). The chemical shifts for $^{31}\text{P}\{^1\text{H}\}$ (85% H_3PO_4 ; $\delta_{\text{P}} = 0.0$) and $^{19}\text{F}\{^1\text{H}\}$ (CF_3COOH ; $\delta = -63.9$) NMR spectroscopy were referenced using an external standard. FT-IR spectroscopy was performed on samples as KBr pellets using a Bruker Tensor 27 FT-IR spectrometer, with a 4 cm^{-1} resolution. Mass spectrometry was recorded in house in positive- and negative-ion modes using electrospray ionization Micromass LCT spectrometer. Melting or decomposition points were determined by flame-sealing the sample in nitrogen-filled capillaries and heating using a Gallenkamp Variable Heater.

Elemental analysis was performed at the University of Montreal and is reported as an average of two samples weighed under air and combusted immediately thereafter.

5.1.3 General Crystallographic Methods

Single crystal X-ray diffraction studies were performed at the Western University X-ray Facility. Crystals were selected under Paratone(N) oil, mounted on a MiTeGen polyimide micromount, and immediately put under a cold stream of nitrogen for data to be collected on a Bruker and Nonius Apex II detectors using Mo-K α radiation ($\lambda = 0.71073 \text{ \AA}$) or Cu-K α radiation ($\lambda = 1.54178 \text{ \AA}$). The Bruker and Nonius instruments operate Bruker's Apex2 software. The data collection strategy was a number of ϕ and ω scans which collected data up to 2θ . The frame integration was performed using SAINT. The resulting raw data was scaled and absorption corrected using a multi-scan averaging of symmetry equivalent data using SADABS. The structure was solved by using a dual space methodology using the SHELXT program. All non-hydrogen atoms were obtained from the initial solution. The hydrogen atoms were introduced at idealized positions and were allowed to ride on the parent atom. The structural model was fit to the data using full matrix least-squares based on F^2 . The calculated structure factors included corrections for anomalous dispersion from the usual tabulation. The structures were refined using the SHELXL program from the SHELXTL suite of crystallographic software. The majority of solid-state structures reported were well refined and converged to one single solution, where restraints were not necessary. In the situations where special refinement cycles were necessary, these details have been included in the experimental section in their corresponding chapter.

5.2 Supplementary Information for Chapter 2

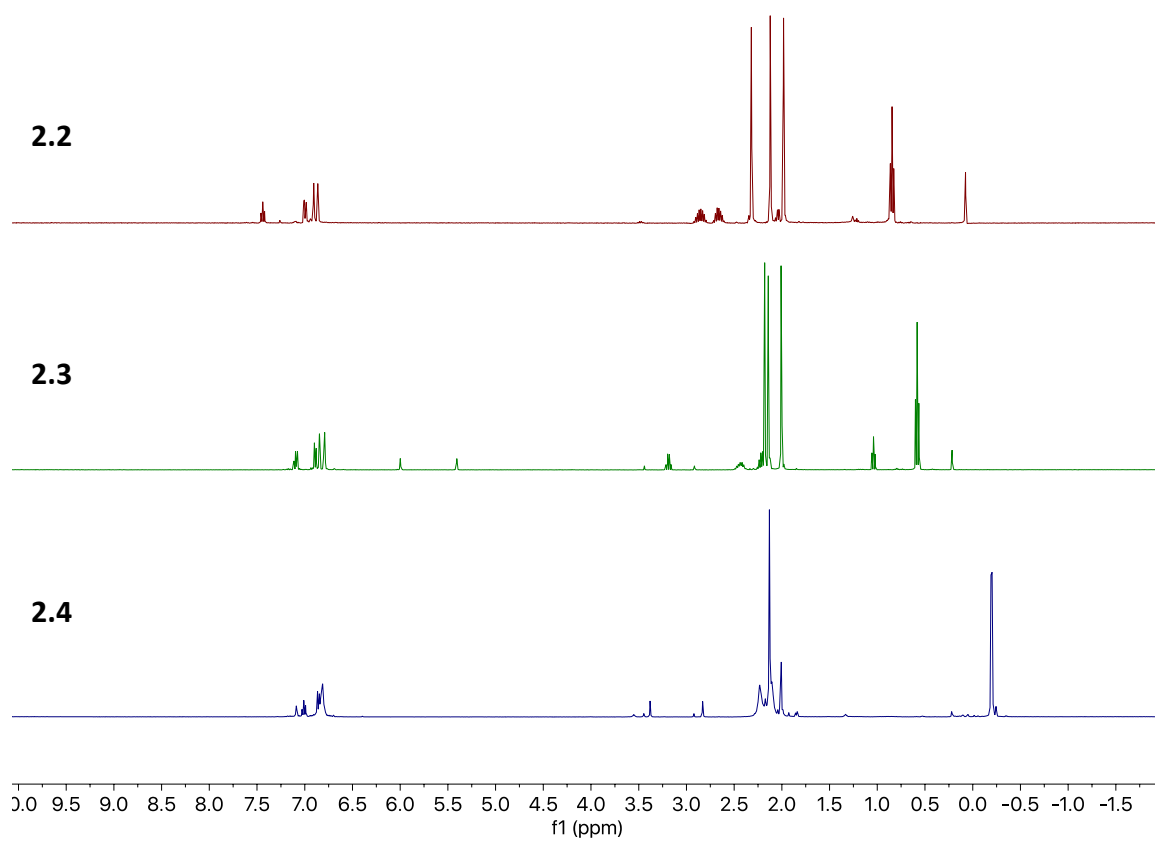


Figure 5-1. Stacked ^1H NMR spectra of asymmetric phosphines in CDCl_3

5.3 Supplementary Information for Chapter 3

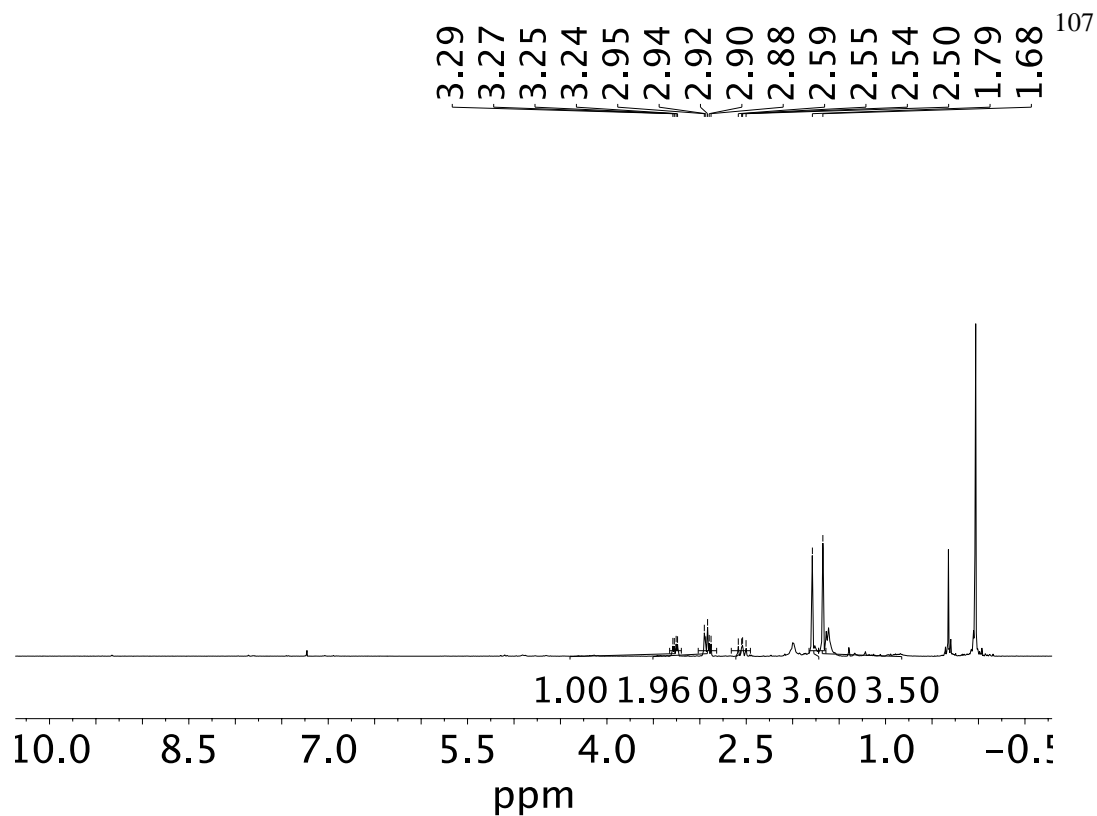


Figure 5-3. ^1H NMR spectrum of **3.6^{Cl}** in CDCl_3 . Residual $\text{S}(\text{TMS})_2$ and pentane were present in the sample.

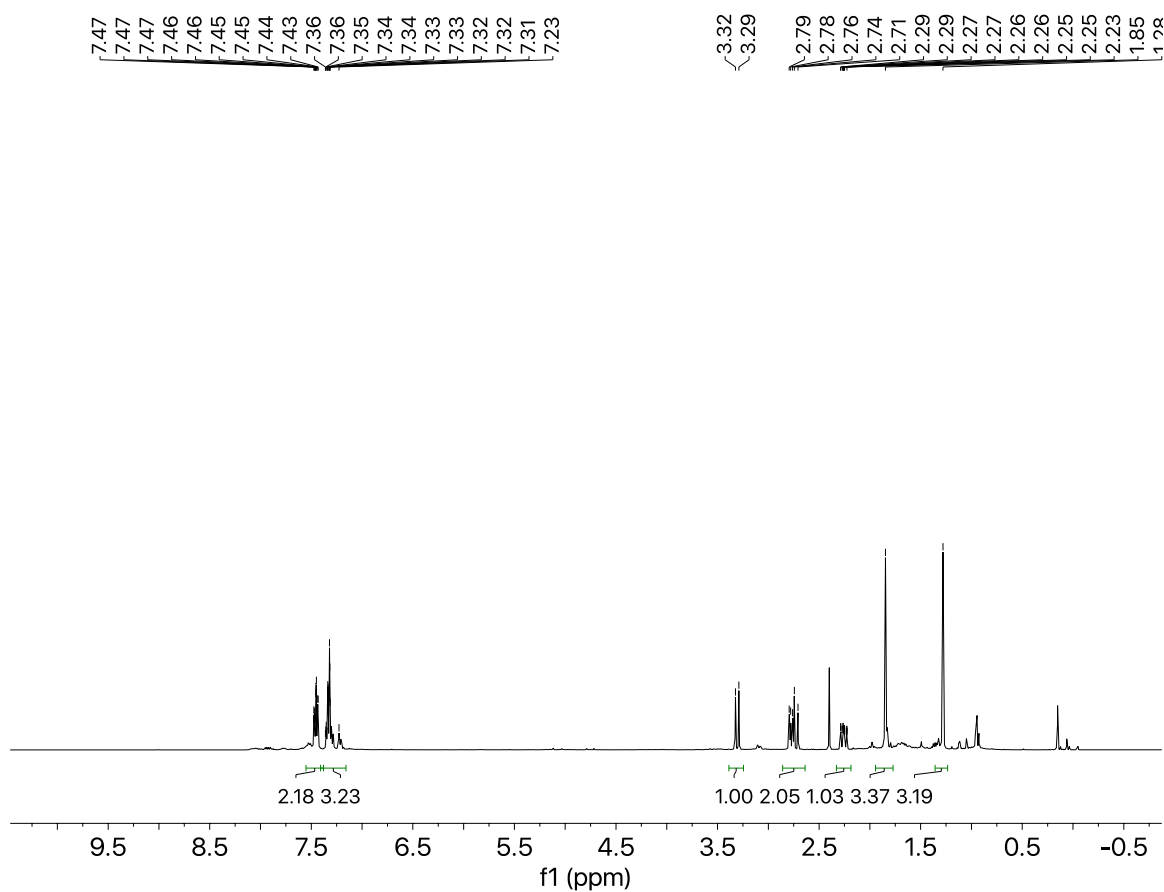


Figure 5-2. ^1H NMR spectrum of **3.6^{Ph}** in CDCl_3

Taylor Pritchard

Department of Chemistry
Western University

Academic Background

- ❖ Master's of Science in Inorganic Chemistry | Western University, London, ON
 - *Masters Thesis*: Exploring the Chemistry of Phosphinidene Sulfides
 - Completion: August 31, 2018
- ❖ Bachelor's of Science Honours | Western University, London, ON
 - June 2016

Publications

1. Graham, C. M. E., Pritchard, T. E., Valjus, J., Tuononen, H. M., Ragogna, P. J. *Angew. Chem. Int. Ed.* **2017**, 56, 6236-6240.
2. Graham, C. M. E., Valjus, J., Pritchard, T. E., Boyle, P. Tuononen, H. M., Ragogna, P. J. *Inorg. Chem.* [Manuscript Submitted].
3. Pritchard, T. E., Graham, C. M. E., Thakur, D., Ragogna, P. J. *Can. J. Chem.* 2018. [Manuscript in progress].
4. Pritchard, T. E., Graham, C. M. E., Boyle, P.D., Ragogna, P. J. *Chem. Comm.* 2018. [Manuscript in progress].

Research Experience

- ❖ Graduate Research Assistant | Dr. Paul Ragogna, Western University, London, ON
 - September 2016 – Present
 - Inorganic synthesis using low coordinate phosphorus centers and strained main group heterocycles. Development of metal-free, solvent-free, and room temperature method for RP=S generation and practical transfer.
 - Incorporation of main group elements into organic frameworks
 - Responsible for management, maintenance, and repair of MBraun Glovebox, high vacuum pump, solvent purification system, Schlenk line
 - Use of 400/600 MHz NMR spectrometers, FT-IR
 - Use of MBraun Glovebox and high vacuum/liquid nitrogen and N₂/Ar schlenk line
- ❖ Undergraduate Research Assistant | Dr. Paul Ragogna, Western University, London, ON
 - April 2015 – April 2016
 - Investigate the synthesis of novel, sugar-containing phosphines for polymerization and anti-bacterial applications
 - Inorganic synthesis of novel main group heterocycles and investigation of coordination behaviour with various metals

Presentation Experience

- ❖ Canadian Society of Chemistry Conference 2018 | Edmonton, AB
 - Oral presentation titled - Exploring the Reactivity of Phosphinidene Sulfides: Cycloadditions

Teaching Experience

- ❖ Teaching Assistant
 - Lab 2213A – Organic Chemistry I for Life Sciences
 - Resource Room TA – Fall 2016
 - Lab 2223B – Organic Chemistry II for Life Sciences
 - Wet Lab TA – Winter 2016, Spring 2017
 - Lab 2213A – Organic Chemistry I for Life Sciences
 - Wet Lab TA – Spring 2017
 - Lab 3371A – Transition Metal Chemistry
 - Wet Lab TA – Fall 2017

Courses

- ❖ 9503 – Advanced NMR Spectroscopy – Grade: 95%
- ❖ 9651 – Organometallic Bond Activation – Grade: 91%
- ❖ 9653 – Polymers: Synthesis to Function – Grade: 91%
- ❖ 9663 – Polymers: Self-Assembly and Application – Grade: 92%